UNIVERSITY OF CALIFORNIA

SANTA CRUZ

SHOREFACE MORPHODYNAMICS, BACK BEACH VARIABILITY, AND IMPLICATIONS OF FUTURE SEA-LEVEL RISE FOR CALIFORNIA'S SANDY SHORELINES

A dissertation submitted in partial satisfaction
of the requirements for the degree of

DOCTOR OF PHILOSOPHY

in

EARTH SCIENCES

by

E. Lynne Harden

June 2012

The Dissertation of E. Lynne Harden
is approved:

_____
Professor Gary B. Griggs, Chair

_____
Professor Andrew Fisher

_____
Dr. Curt D. Storlazzi

_____
Tyrus Miller
Vice Provost and Dean of Graduate Studies

Table of Contents

List of Figures and Tables

Abstract

Shoreface Morphodynamics, Back Beach Variability, and Implications of Future Sea-Level Rise for California's Sandy Shorelines

E. Lynne Harden

California's sandy shorelines are important resources in terms of ecological habitat, recreation and tourism, and aesthetic beauty. They also serve as important natural buffers, often protecting back-beach development and infrastructure from wave attack. Encroachment or fixing of the back beach in conjunction with sea-level rise will reduce the accommodation space of beaches and subsequently increase the vulnerability of the back beach to extreme water level events associated with storms. Understanding the present state of California's sandy shorelines in terms of landward migration potential, vulnerability to extreme water events, and local morphodynamic variability is important for coastal policymakers and managers to make informed decisions regarding the future of the California coastline. In this study, the landward migration potential of California's beaches was assessed through a statewide cataloging and classification of all sandy shorelines in the context of back beach immobility and restrictions to landward migration. Beach inundation vulnerability from increased frequency of high water events with rising sea level was determined with extreme water level exceedance distributions from historic tide gauge records and sea-level rise projections of 18 cm, 79 cm, and 140 cm by 2100. Finally, alongshore variability and the influence of high wave events and berm overtopping on beach profile morphodynamics were analyzed through seasonal beach surveying of a coastal lagoon pocket beach. Fifty-eight percent of the total length of sandy shoreline in California is restricted in the back beach from landward migration. This is primarily due (in Central and Southern California) to anthropogenic coastal development and infrastructure. Beach

inundation potential from extreme high water events is highly variable and is a function of berm height and backshore morphology. Backshore morphology influences foreshore and berm morphodynamics by modifying swash sediment transport. The growth and persistence of a berm on a bar-built coastal lagoon beach is dependent on berm overtopping; however, overtopping beyond a threshold frequency becomes destructive and can lead to berm erosion. While statewide more than half of California's sandy shorelines are being threatened by reduced accommodation space through terrestrial and marine encroachment, understanding local variability is essential for determining the future of these highly valued resources.

Dedication and Acknowledgments

I am so grateful for all of the support, mentorship, advice, wisdom, and encouragement that I have received throughout my graduate career that have made this dissertation possible. I'd like to thank my advisor, Gary Griggs, and my committee members, Andy Fisher and Curt Storlazzi for exceptional guidance. I'd also like to acknowledge Conrad Neumann and Tony Rodriguez, my undergraduate mentors who encouraged me to challenge myself and pursue my goals. Thanks to everyone who helped me in the field, especially Tom Reiss. To Doug, your dedication to making the world a better place through science, reason, and knowledge is awesome and inspiring, and I thank you for your unwavering support, patience, and humor. Thanks to Nonie, Max, my family, and my friends for your love and enthusiasm.

This dissertation is dedicated to my parents, Meg and Rick Harden, for all of your love, support, and encouragement. You believed in me from day one, and I am forever grateful.

ELH

CHAPTER 1

Back Beach Variability, Landward Migration Potential, and Historic Shoreline Change Rates for California's Sandy Shorelines

1.1 Introduction and Background

Coastal squeeze, also known as foreshore narrowing, or foreshore steepening, is a result of marine encroachment, such as sea level rise or increased wave energy and erosion in the presence of a back-beach barrier, and terrestrial encroachment such as coastal development. With increasing concerns regarding projections of future sea level rise and steadily growing coastal populations, coastal squeeze is being addressed by coastal managers and policymakers globally.

1.1.1 Beach Formation and Persistence in California

A beach will form along the coast where there is sufficient accommodation space, a sediment supply of appropriately sized grains, shelter from waves, and wave approach perpendicular to the shoreline or at a slight oblique angle. Perennial Southern California sandy beaches and modern littoral cells formed during Holocene sea-level rise between 9000-5000 years ago as river mouths were drowned and embayments, or regions of dissipated wave energy ideal for sediment deposition, were created. There is evidence that the primary factors controlling Holocene beach accretion and erosion in Central and Southern California were El Niño controls on the wave climate and sediment flux (Storlazzi and Griggs, 2000; Masters, 2006). El Niño events are associated with wet periods in California, and thus increased discharge and sediment load from rivers and streams. As fluvial sediments enter littoral cells, wave energy and littoral drift transport beach-sized sand alongshore and deposit it in coves or updrift of shore-perpendicular barriers such as headlands. Although the appearance of beaches along the California coast during the Holocene is evidence that

beaches can build up even with a rising sea level, this is highly dependent on availability of sediment supply. Given the current state of sediment impoundment by dams and flood control measures in California, it is highly unlikely that beaches will not narrow with future sea-level rise. Back-beach development, coastal armoring, and even natural resistant sea cliffs could also prevent landward migration of beaches with rising seas. With decreased sediment supplies and barriers to migration, the options for preserving and maintaining many beaches in California in the future are artificial nourishment, increased numbers of coastal engineering structures, the retreat of existing back beach development, or a combination of the three.

1.1.2 California Coastal Development

The period between about 1940 to the late 1970s was characterized by a cool phase of the Pacific Decadal Oscillation, a 20-30 year El Niño-like climate oscillation centered over the Pacific Ocean that has an effect on interdecadal climate variability in North America. In California, a cool phase PDO triggers persistent La Niña-like climate conditions along the coast, resulting in below average sea-surface temperatures and below average precipitation (Mantua and Hare, 2002). Before the establishment of the California Coastal Commission in 1972 and the implementation of the California Coastal Act in 1976, there were few regulations on the use of the coastal zone in California. The California coastline was intensely developed during the 1950s, 1960s, and 1970s during cool phase PDO mild climate conditions when many regions that have undergone significant changes due to El Niño events in recent decades were seemingly stable. A 1971 inventory of the California shoreline (bluffs + sandy shoreline) classified nearly 86% of the California coast as “critically eroding,” or areas where structures and utilities were being threatened by erosion (U.S. Army Corps of Engineers, 1971), while subsequent similar analyses in 1978 (Habel and Armstrong, 1978) and 1985 (Griggs and Savoy, 1985) classified about half to two-thirds of the coastline as “hazardous” due to erosion.

At the time that the California Coastal Commission was established and the Coastal Initiative passed in 1976, coastal retreat, setbacks, and potential coastal damage from storms were overshadowed by environmental and ecological issues. Today coastal policies in California still reflect this, and as a result much coastal development has continued in the face of known coastal hazards. Between 1980 and 2003, coastal population in the United States increased by 10%, or about 33 million people, and between 1999 and 2003, 51% of the country's total multi-family housing building permits were issued in coastal counties (Crossett et al., 2004). In California alone, the permanent coastal population between 1980 and 2003 increased by 47%, or almost 10 million people. In addition, Southern California beaches on average attract nearly 130 million beachgoers each year (Dwight et al., 2007). Beaches in California alone provide tens of billions of dollars annually to the national economy and to federal tax revenues, and provide hundreds of thousands of jobs across the U.S. (King, 1999).

1.1.3 Anthropogenic Impacts on Sediment Supply and Potential for Landward Migration

More than half of the California sandy beach coast has experienced erosion over the last ~50 years. The net average rate of sandy shoreline change between about 1970 to 2002 for the entire coast of California was -0.2±0.4 m/yr, with 66% of sandy beaches showing erosional trends (Hapke et al., 2006). During this period, short-term accretion rates and overall magnitudes of shoreline change were highest in Northern California (Oregon border to Bodega Bay), whereas the lowest erosion and accretion rates, or most stable sandy beaches, were in Central California (Bodega Bay to northern Santa Barbara county).

Analyzing shoreline change along the California coast is complicated by anthropogenic activities that can induce high rates of erosion or accretion that might not otherwise occur under natural conditions. Coastal engineering structures such as groins, jetties, and breakwaters have artificially widened many beaches along the California coast,

particularly in Southern California, while at the same time contributing to the erosion of beaches downcoast that subsequently receive a decreased longshore sediment supply (Fig. 1.1).

Fig. 1.1: Entrance to the Channel Islands Harbor entrance showing the east and west jetties. The beach has widened updrift of the west jetty and narrowed leeward of the east jetty as a result of the disruption and retainment of littoral drift sediment by the west jetty, resulting in a decreased sediment supply to beaches down drift (photo by Kenneth and Gabrielle Adelman)

Opportunistic and intentional artificial beach nourishment over the past century has succeeded in widening beaches such as Santa Monica and Venice Beaches, although it is not always a successful venture. Localized artificial nourishment projects have significantly decreased or in some cases ceased altogether within the past 10-20 years, which could be partially responsible for apparent increases in erosion rates in particular areas (Flick, 1993, Wiegel, 1994). Seawalls and rip-rap emplaced on beaches to protect back-beach structures or prevent sea cliff erosion have caused beach placement loss and passive erosion, or the

gradual loss of beach fronting a back-beach barrier (e.g. seawall) as the shoreline migrates landward (Fig. 1.2).

Fig. 1.2: The Best Western Hotel Beach Resort and seawall in Monterey showing passive erosion and severe placement loss of the beach (photo by Kenneth and Gabrielle Adelman)

Finally, the damming and in some cases concrete channelization of rivers and streams in California that flow to the coast have resulted in significant reductions in fluvial sediment supply to littoral cells and thus sandy beaches. While the pre-dam fluvial sand flux has been reduced by about 5% in Northern California due to sand impoundment, in Central and Southern California fluvial sand supplies have been reduced by 31% and 50%, respectively (Slagel and Griggs, 2008). In Southern California, dam and debris basin impoundment of sand has been equated to a potential deprivation of beach sand of ~3 m^3/yr per m of shoreline (Sherman et al., 2002).

Approximately 14% of the California coast from Marin County to the Mexican border is artificially armored (Runyan and Griggs, 2003), more than half of which protects back-beach developments or low-lying dynamic regions like harbors and dunes. Artificial armoring includes seawalls and retaining walls, rip-rap, bulkheads and revetments, sandbags, and soil nail walls. Many popular beaches, such as those in Southern California (including Santa Monica and Venice beach) that do not have back-beach armoring are still restricted in the back beach by infrastructure such as hotels and beachfront vacation homes, amusement parks, parking lots, and roadways. In some cases, this infrastructure is protected by a low seawall (e.g. Main Beach in Santa Cruz and Mission Beach, San Diego) where destructive waves can reach the back beach during ENSO events or strong storms, especially in conjunction with high tide (Storlazzi and Griggs, 1998). It is not uncommon for the type and scale of shore protection projects to undergo a predictable progression through time, including increased size and heft as structures are rebuilt, often repeatedly, after failing (Pilkey, 1981).

1.1.4 California Coastal Datasets

Characterization of the California coast and analyses of changes through time are made possible by maps, photographs, and critical data sets, such as the California Coastal Records Project oblique aerial photo archives (www.CaliforniaCoastline.org), high-resolution lidar data (NOAA Coastal Services Center, CSC), satellite imagery (Landsat, QuickBird), and databases of various coastal features. There are publically available catalogs of artificial coastal armoring and coastal engineering structures along the California coast (Dare, 2005; Kinsman and Griggs, 2010) and reports on and catalogs of coastal vulnerability (Thieler and Hammar-Klose, 2000; Boruff et al., 2005; Pendleton et al., 2006; Heberger et al., 2009; Griggs and Russell, 2012; and others) based on such criteria as shoreline slope, geomorphology, erosion rates, tide range, wave height, and in some cases taking into account coastal infrastructure and population. Continued collection and creation of important

coastal zone datasets are, and will continue to be, imperative for coastal policy and coastal management decisions in the state of California and nationwide, particularly with respect to adaptation and mitigation plans related to climate change and sea-level rise.

1.2 Objectives

The purpose of this study is to create a comprehensive catalog of sandy beaches along the California coast from the California-Oregon border to the U.S.-Mexico border classified by the presence or absence of a back-beach barrier. This catalog is unique in that it is not a database of coastal sea-level rise vulnerability based on data such as coastal elevations, but rather a catalog of detailed information about the degree to which individual sandy beaches along the California coast are restricted from landward migration either due to natural barriers like coastal bluffs or anthropogenic development and infrastructure. Beaches characterized by the presence of a back-beach barrier will additionally be classified by the nature of the barrier in terms of the effectiveness of the barrier at preventing landward migration of the back beach, or 'degree of immobility.' Statistical analyses will be conducted on the catalog to calculate the proportion of beaches that are publically owned (state/county beach, wildlife refuge, military base, etc.) within each class, to collect information on geographic variability (Northern vs. Central vs. Southern California) in back beach classification, and to determine the extent of anthropogenic influence on back beach immobility. The dataset will also be compared with historic shoreline change results from the U.S. Geological Survey National Assessment of Shoreline Change report for the sandy shorelines of the California coast to test the null hypothesis that beaches with variable degrees of back-beach barriers (immobility) have similar average erosion rates compared with unrestricted beaches.

1.3 Methods

The California sandy beach catalog was populated using Google Earth, oblique angle aerial photos from the California Coastal Records Project as well as high-resolution oblique angle and orthophotos from various sources, and ESRI Geographic Information System (GIS) software (ArcMap, ArcCatalog). Polylines denoting sandy beaches were initially drawn and annotated in Google Earth and then transformed from kml file formats to shapefiles for additional processing in an ArcGIS platform.

1.3.1 Google Earth

Google Earth is a powerful virtual geographic information tool that enables a user to explore and analyze the globe at various resolutions, angles, and in several places in three dimensions. Google Earth provides a complete map of the earth's surface by superimposing satellite imagery with aerial orthophotos from various providers. The spatial resolution of the images varies between 15 cm and 15 m based largely on areas of interest and popularity. Google Earth is used for a plethora of scientific applications such as climate change, natural disaster mapping (Morton et al., 2011; Nourbakhsh et al., 2006), environmental and geologic mapping, weather forecasting (Lakshmanan et al., 2007), and public health (Butler, 2006). The potential that this technology has to bridge the gap between scientific research and discovery and the baseline scientific education of the public is unprecedented.

1.3.2 California Coastal Records Project

The California Coastal Records Project (www.californiacoastline.org), created by Gabrielle and Kenneth Adelman, is an online image bank consisting of over 66,000 georeferenced oblique angle and orthonormal aerial photos of the California coast from the Oregon border to the U.S.-Mexico border (excluding the restricted coastline of the Vandenberg Air Force Base) taken between 1972 and 2010. The project has provided

invaluable insight into not only the geographic variability of the California coastline, but also changes in the nature and shape of the coastline through time as a result of natural forcings or anthropogenic activities. The resources provided by the California Coastal Records Project have been utilized by federal and California state and local governments, universities and other educational institutions, and various environmental and conservation groups.

1.3.3 California Sandy Shoreline Catalog: Back Beach Classifications

For beaches along the California coast to be included in the California sandy shoreline catalog, they must satisfy two main conditions:

1. The beach must be composed primarily of sand (63 μm to 2 mm). Beaches composed of greater than about 30% gravel as identified in aerial photos and satellite imagery are not included in the catalog. Gravel beaches in California are mainly found in the northern region close to the California-Oregon border, and tend to have a distinctly darker color (Fig. 1.3).

Fig. 1.3: Gravel beach near Point St. George in Del Norte County, Northern California (photo by Kenneth and Gabrielle Adelman)

2. If a beach is narrow, it must have a clear and identifiable wet-dry line in the aerial photos and satellite imagery. Multiple imagery sources were consulted in the case of ambiguity. Narrow beaches with insufficient subaerial beach area and pocket beaches with less than 50 m of shoreline length are not included in the catalog. Subtidal 'beaches' are common features often fronting steep or vertical bluffs or armored infrastructure (Fig. 1.4), but are often either infrequently exposed or inaccessible.

Fig. 1.4: Sea cliff in Ventura County: An example of a subtidal sandy beach that is not included in the sandy shoreline catalog (photo by Kenneth and Gabrielle Adelman)

Sandy beaches that are not too narrow are classified in the catalog primarily based on the presence or absence of a back-beach barrier, and secondarily on the effectiveness of the barrier at preventing landward migration of the beach if a barrier is in fact present. The classifications are as follows:

Class 0: Almost complete back beach mobility for at least one beach width of landward migration due to no back-beach barrier or a distantly landward back-beach barrier (Fig. 1.5):

Fig. 1.5: Example of Class 0 sandy shoreline: Limantour State Reserve, Marin County (photo by Kenneth and Gabrielle Adelman)

Class I: Low degree of back beach immobility due to a relatively flat back-beach, road/walkway/esplanade/golf course or sparse infrastructure (Fig. 1.6):

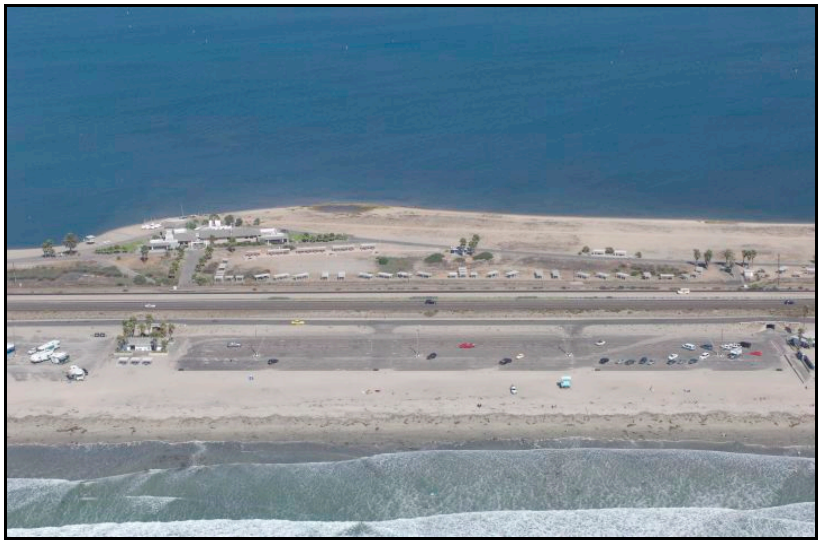

Fig. 1.6: Example of Class I sandy shoreline: Silver Strand, San Diego County (photo by Kenneth and Gabrielle Adelman)

Class II: Moderately low degree of back beach immobility due to a relatively flat back beach with sparse infrastructure and/or rip rap or low seawall (Figs. 1.7 and 1.8):

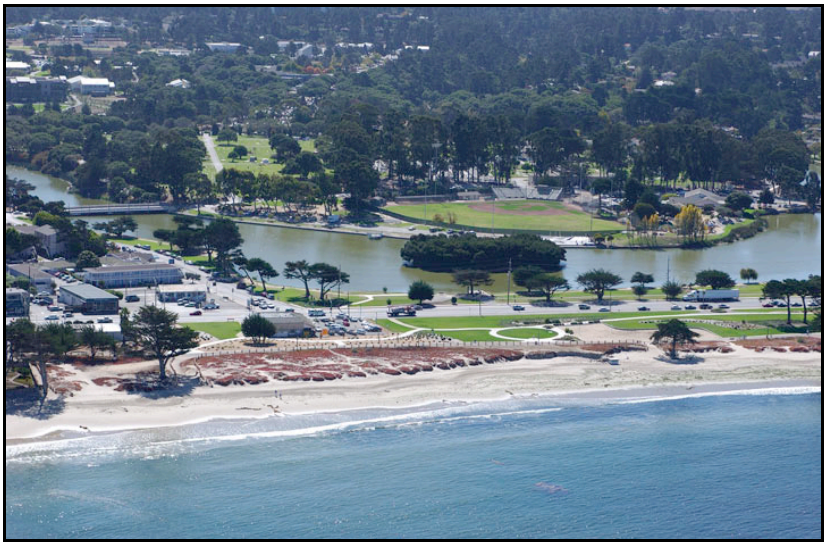

Fig. 1.7: Example of Class II sandy shoreline: Monterey State Beach, Monterey County (photo by Kenneth and Gabrielle Adelman)

Fig. 1.8: Example of Class II sandy shoreline: Near Ventura Harbor, Ventura County (photo by Kenneth and Gabrielle Adelman)

Class III: Moderate degree of back beach immobility due to low bluffs or moderate infrastructure with relatively wide beach fronting (Figs. 1.9 and 1.10):

Fig. 1.9: Example of Class III sandy shoreline: Near Ventura Harbor, Ventura County (photo by Kenneth and Gabrielle Adelman)

Fig. 1.10: Example of Class III sandy shoreline: Año Nuevo, San Mateo County (photo by Kenneth and Gabrielle Adelman)

Class IV: Moderately high degree of back beach immobility due to high cliffs or bluffs with relatively narrow beach fronting or dense infrastructure (Figs. 1.11 and 1.12):

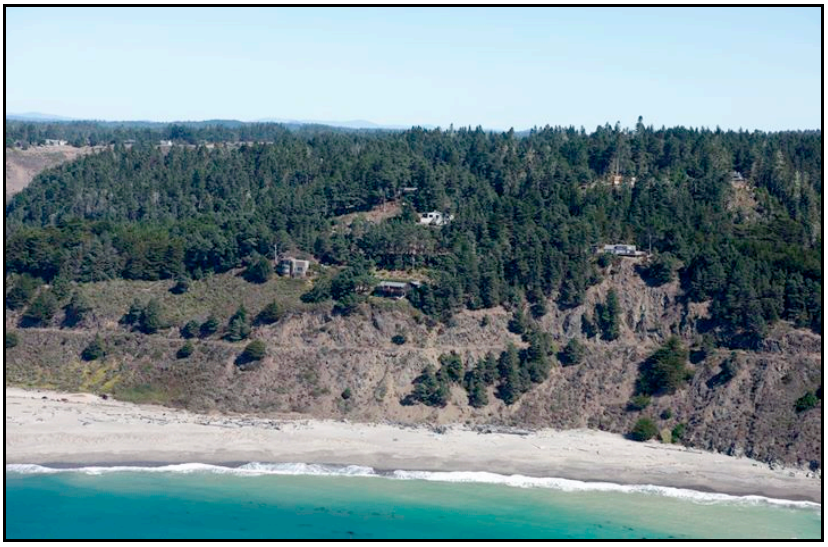

Fig. 1.11: Example of Class IV sandy shoreline: Near Navarro River Mouth, Mendocino County **(**photo by Kenneth and Gabrielle Adelman)

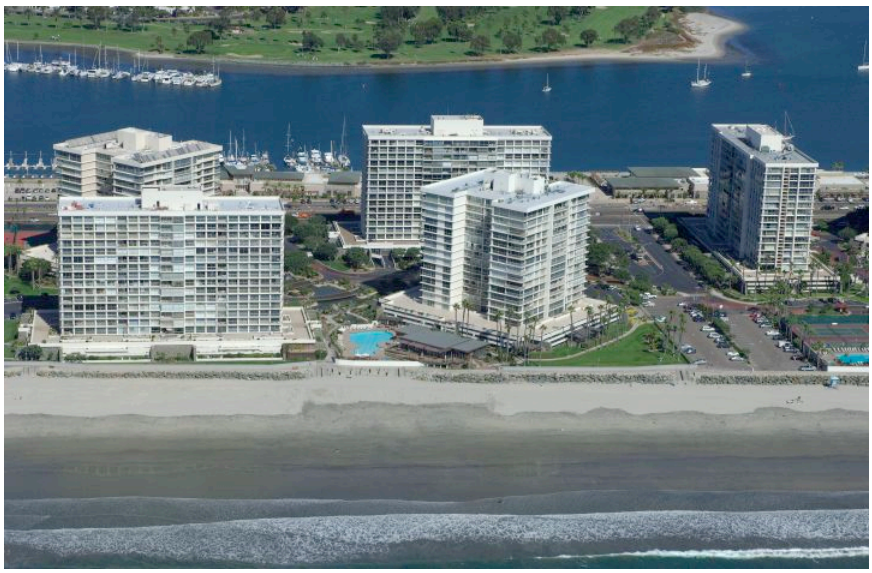

Fig. 1.12: Example of Class IV sandy shoreline: Coronado, San Diego County (photo by Kenneth and Gabrielle Adelman)

Class V: Very high degree of back beach immobility due to dense infrastructure/seawall with bluffs, narrow beach, and existing coastal armoring (Figs. 1.13 and 1.14):

Fig. 1.13: Example of Class V sandy shoreline: Near New Brighton State Beach, Santa Cruz County **(**photo by Kenneth and Gabrielle Adelman)

Fig. 1.14: Example of Class V sandy shoreline: Pearl Beach, Orange County **(**photo by Kenneth and Gabrielle Adelman)

Natural bluffs are back-beach barriers in that they act as a physical topographical barrier to landward beach migration. However, where bluffs are weak and unconsolidated, they can be a source of sediment for the fronting beach. Some of the undeveloped bluffs along the California coast may be able to migrate landward (erode) at high enough rates to continually provide new back-beach accommodation space. Because of this, undeveloped or sparsely developed low bluffs (5-10 m) are considered moderate barriers to landward beach migration (Class III), and undeveloped or sparsely developed high bluffs (15+ m) are considered as a slightly higher barrier to landward migration (Class IV). Class V beaches are those backed by medium-to-high bluffs with infrastructure either on the fronting beach and/or atop the bluffs and with evidence of attempts at coastal armoring, such as seawalls or rip-rap at the bluff toe. The presence of seawalls or rip-rap indicates that measures are being taken and will likely continue to be taken in the future to prevent or retard bluff erosion. Where sea walls or rip rap are protecting a relatively flat and undeveloped regions landward of the back beach, accommodation space for landward migration is more easily achieved, and thus beaches with such back-barrier conditions are classified as 'II'. Finally, Class I shorelines indicate that landward migration would be most feasible, but with some minor costs. Sandy shorelines of any class that are publically owned (state or county parks, wildlife refuges or reserves, military bases) were labeled as such in the catalog for comparison with beaches that are not state parks or otherwise publically owned.

1.3.4 Classification Comparisons with Historic Shoreline Change Rates

California sandy shoreline classifications were compared with historic rates of shoreline change data to determine what, if any, are the relationships between historic shoreline change rates and the degree of back beach immobility. Rate of change data was obtained from the National Assessment of Shoreline Change Report for the sandy shorelines of coastal California (Hapke et al., 2006) conducted by the U.S. Geological Survey to assess short and long-term shoreline change and land loss associated with California's beaches.

Long-term change rates were calculated using four shorelines from different time periods and data sources: 1800s, 1920s-1930s, and 1950s-1970s shorelines from maps (topographic sheets), and a 1998-2002 shoreline from coastal lidar surveys. Short-term change rates were calculated in GIS using only the 1950s-1970s and 1998-2002 shorelines, and represent sandy shoreline erosion or accretion along the California coast during a period characterized not only by high coastal development, but also by the establishment of the California Coastal Commission and implementation of the Coastal Zone Management Act. Short-term rates were calculated using a straightforward endpoint rate method where the spatial and temporal differences between two shoreline intersection points of a shore-normal transect were used to calculate the rate of change, while long-term rates were calculated between more than two shorelines using a linear regression method for all shoreline dates (Fig. 1.15).

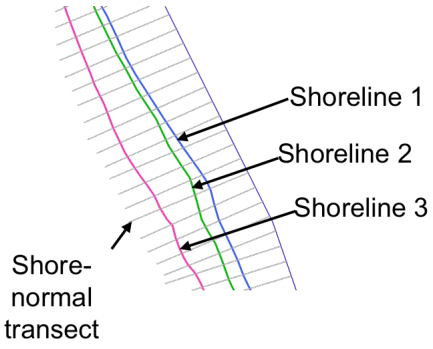

Fig. 1.15: Example of the methodology used in the National Assessment of Shoreline Change report. Shoreline change rates are calculated based on the spatial and temporal differences between shorelines as determined by the intersections of shore-normal transects with each shoreline.

For the purposes of this study, short-term shoreline change data from the National Assessment of Shoreline Change study (Hapke and Reid, 2006) were compared with back-beach barrier classifications, as classifications in the sandy beach catalog are heavily influenced by back-beach anthropogenic development and infrastructure, much of which was constructed during the time periods used for the short-term analysis. Numbers reported are

based only on transects that intersect sandy shorelines defined in the catalog. The Shoreline Change study reports that short-term change rates were calculated for 44% of the total California coastline, or approximately 4% more sandy shoreline than was cataloged in this study. As sandy shorelines without significant subaerial surface area were discarded from the catalog, most, but not all, transects correspond to a cataloged beach. National Assessment of Shoreline Change transect data and cataloged sandy shoreline classification data were merged into a single database using ESRI ArcGIS software, and statistics were calculated using Matlab (The Mathworks, Inc.).

1.3.5 Statistical Hypothesis Testing

The Mann-Whitney U-test, or rank-sum test (Mann and Whitney, 1947), is a hypothesis test of the null hypothesis that two independent and random samples of observations are drawn from the same distributions. The Mann-Whitney U-test is used in place of a two-sample t-test for distributions that are not normally distributed. It is a comparison of the medians of two distributions, which should be equal if the samples are from identical populations. The U-test does not require the distributions to have the same number of observations. To calculate U-statistics, data is arranged in order from smallest to largest values, and given an associated rank based on this order. Identical observations are given a rank that is the average of the position of the scores within the ordered sequence. The U-test statistic is then calculated for each sample as:

$$U_1 = R_1 - \frac{n_1(n_1+1)}{2} \tag{1.1}$$

and

$$U_2 = R_2 - \frac{n_2(n_2+1)}{2} \tag{1.2}$$

where U_1 and U_2 are the U-statistics for samples 1 and 2, respectively; n_1 and n_2 are the sizes of samples 1 and 2, respectively; and R_1 and R_2 are the sums of the ranks of samples 1 and 2, respectively. Calculated U-statistics are compared to a critical U-value at the desired significance level, and the null hypothesis is rejected if the smallest test statistic is below the critical U-value.

Initial tests for normality (e.g., Lilliefors) have been applied to shoreline change rate distributions separated by class (these distributions are introduced in Results). As the null hypothesis of normally distributed data was rejected in favor of the alternative hypothesis that the distributions are not normally distributed for a large proportion of the change rate class distributions, the Mann-Whitney U-test was used for all hypothesis tests for consistency. U-testing was conducted to compare each of the Class I-V shoreline change rate distributions for each region individually with the Class 0 distributions to determine if there is a statistically significant difference between the median shoreline change rate of beaches with various degrees of back-beach immobility (I-V) versus beaches with no back-beach barrier (0). Statistically significant differences in median shoreline change rates do not necessarily indicate a direct cause-and-effect relationship between the nature of the back beach and erosion or accretion.

1.4 Classification Results

1.4.1 Statewide Shoreline Classifications

The California Sandy Shoreline catalog is available as both an ESRI GIS polyline shapefile in North American Datum 1983 (NAD83) UTM zone 10N, and as a Google Earth kml file. The GIS shapefile attribute table contains fields for the 'ObjectID' (a default ESRI field of consecutive integer numbers), 'Name' (a user defined identification number), 'Class' (0, I, II, III, IV, or V), 'County', 'Publically Owned' (name of beach if it is a state or county park, reserve, military base, etc.), 'Back Barrier' (brief description of the back-beach barrier), and

'CCRP Link', which contains a hyperlink to one of a possible series of aerial photographs in the California Coastal Records Project archives.

The sandy beach catalog encompasses about 600 kilometers, or approximately 40% of the total length of coastline of California from the Oregon border to the U.S.-Mexico border. Approximately 42% of the total length of sandy shoreline is Class 0 with no back-beach barrier, equal to 17% of the total California coastline. Of the sandy shoreline with a back-beach barrier (Classes I-V), 37% lies within Classes III and IV (moderate to high degree of back beach immobility), whereas only 4% is Class V (very high degree of back beach immobility) (Table 1.1).

Table 1.1: Sandy shoreline classification statistics for the entire California coast showing the percent of total length of sandy shoreline and total length of the entire coastline (sandy shoreline + bluffs/cliffs) represented by each class

Class	Percent of total length of statewide sandy shoreline	Percent of total length of California coastline
0	42%	17%
I	11%	4%
II	6%	2%
III	21%	8%
IV	16%	7%
V	4%	1%

The highest proportion (42%) of the total length of Class 0 shoreline along the entire California coast and lowest proportion of the total length of Class V shoreline are both within the Northern California region (Table 1.2).

Table 1.2: Percent of the total statewide length of each sandy shoreline class represented in Northern, Central and Southern California

Class	Northern CA: Percent of Statewide Class	Central CA: Percent of Statewide Class	Southern CA: Percent of Statewide Class
0	47%	41%	12%
I	9%	29%	62%
II	7%	46%	46%
III	10%	42%	47%
IV	20%	42%	39%
V	3%	69%	28%

1.4.2 Northern California: Del Norte to Sonoma County

The Northern California coastline makes up about 30% of the total California coastline and includes Del Norte, Humboldt, Mendocino, and Sonoma counties. The morphology of the coast is in part a result of the Mendocino triple junction near Cape Mendocino where the Pacific plate, North American plate, and Gorda plate intersect and separate a region dominated by subduction processes in the north to right-lateral strike-slip movement to the south. The triple junction is a region of rapid Holocene uplift and deformation (Merritts, 1996), creating a Northern California coastline characterized by rocky cliffs and bluffs with sparse sand and gravel pocket beaches, or high steep cliffs fronted by narrow beaches. Due to the tectonic setting, relative sea level along parts of the Northern California coast such as Crescent City is falling where uplift rates exceed sea-level rise rates (NOAA NOS/CO-OPS).

The Northern California coast and mountains are sparsely populated, with only about 14 people per square mile compared to about 8,000 people per square mile in Los Angeles

(U.S. Census Bureau). South of Eureka is one of the longest stretches of undeveloped coastline in the U.S. (excluding Alaska), called the Lost Coast because of its remoteness and steep, almost inaccessible terrain. There are significant stretches of sandy shoreline (often in the form of long sandy spits) along the Northern California coast around major river mouths such as Klamath River (Fig. 1.16). About 34% of the coastline in Northern California is sandy beach, the vast majority (74%) of which is Class 0 with no back-beach barrier. Twelve percent of the sandy shoreline is Class IV, largely due to the high, steep coastal terrain and often comparably narrow beaches, although less than 1% of the sandy shoreline is Class V (Table 1.3; Fig. 1.17).

Fig. 1.16: Long, narrow sand spit fronting the Klamath River mouth in Northern California (photo by Kenneth and Gabrielle Adelman)

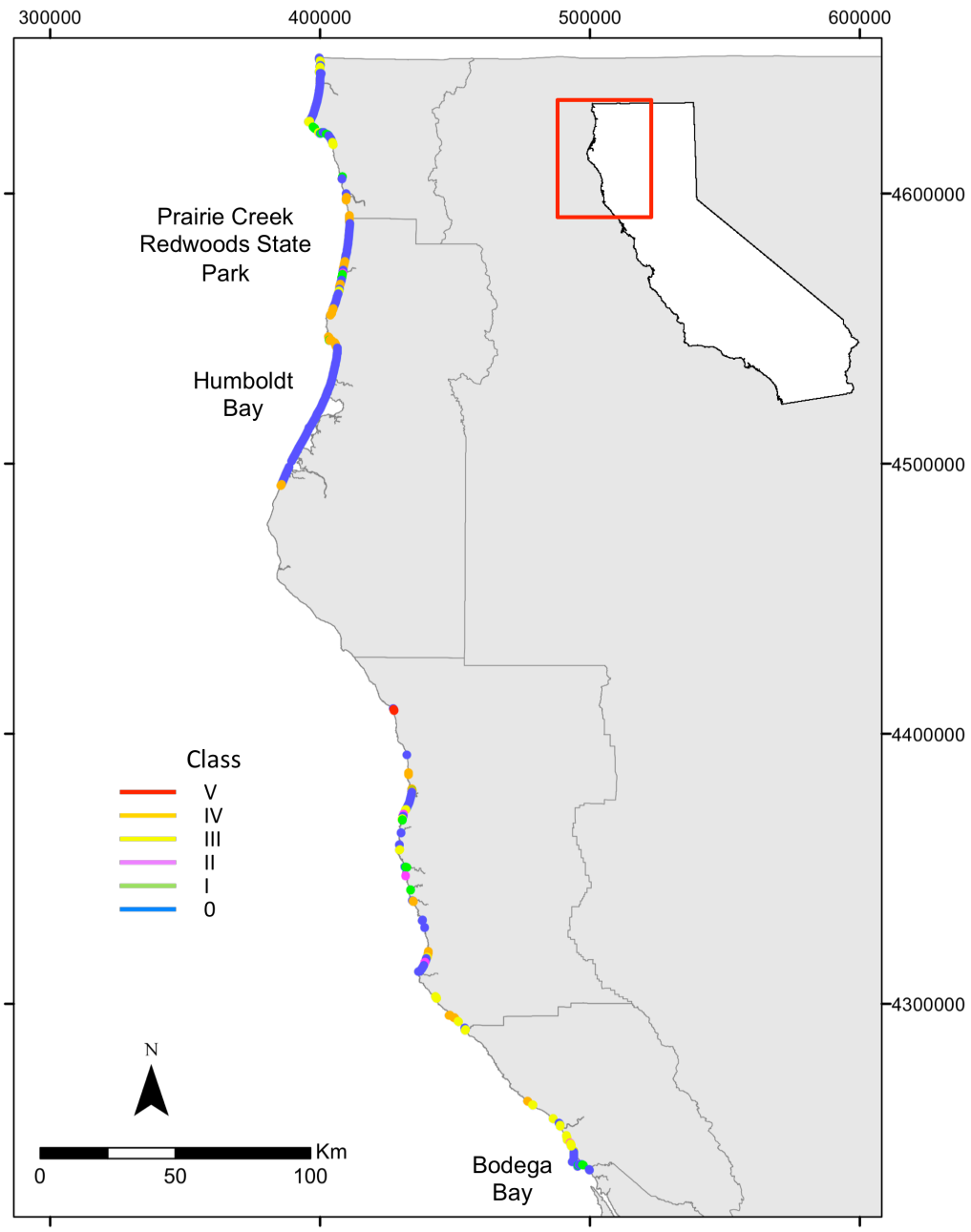

Fig. 1.17: Sandy shoreline classifications for the Northern California coast (Del Norte County to Sonoma County)

Table 1.3: Percent of the total regional and statewide sandy shoreline represented in each class for Northern California

Class	Percent of total regional sandy shoreline	Percent of total statewide sandy shoreline
0	74%	20%
I	3%	1%
II	2%	0.5%
III	8%	2%
IV	12%	3%
V	0.4%	0.1%
	TOTAL:	27%

Nearly half of the total length of sandy shoreline in Northern California is publically owned. Sixty-eight percent of the total length of publically owned shoreline in Northern California is Class 0, whereas an additional 26% is Class III-IV (Table 1.4). Northern California has the highest proportion of sandy beach that is publically owned compared with Central and Southern California.

Table 1.4: Percent of the total length of publically owned regional and statewide sandy shoreline represented in each class for Northern California

Class	Percent of total regional publically owned sandy shoreline	Percent of total statewide publically owned sandy shoreline
0	68%	24%
I	5%	2%
II	1%	0.5%
III	20%	7%
IV	6%	2%
V	0%	0%
	TOTAL:	35%

1.4.3 Central California: Marin to Santa Barbara County

The Central California coastline makes up about 46% of the total California coastline and includes Marin, San Francisco, San Mateo, Santa Cruz, Monterey, San Luis Obispo, and Santa Barbara counties. The coastal morphology of Central California is diverse, ranging from vast sand fields in the north at Point Reyes and in the south within Vandenberg Air Force Base, high rocky cliffs and coastal mountains in Big Sur, and vertical bluffs interspersed with sandy pocket beaches and preserved coastal marine terraces between San Francisco Bay and Monterey Bay. The Monterey Bay is characterized by long stretches of continuous sandy beach backed by infrastructure, steep bluffs, dunes, and agricultural fields.

Thirty-six percent of the Central California coastline is sandy shoreline, 43% of which is Class 0 with no back-beach barrier. An additional 37% is Class III-IV, while only 6% of the Central California sandy shoreline is Class V (Fig. 1.18; Table 1.5). The Central California sandy shoreline comprises about 42% of the total length of sandy shoreline along the entire California coast.

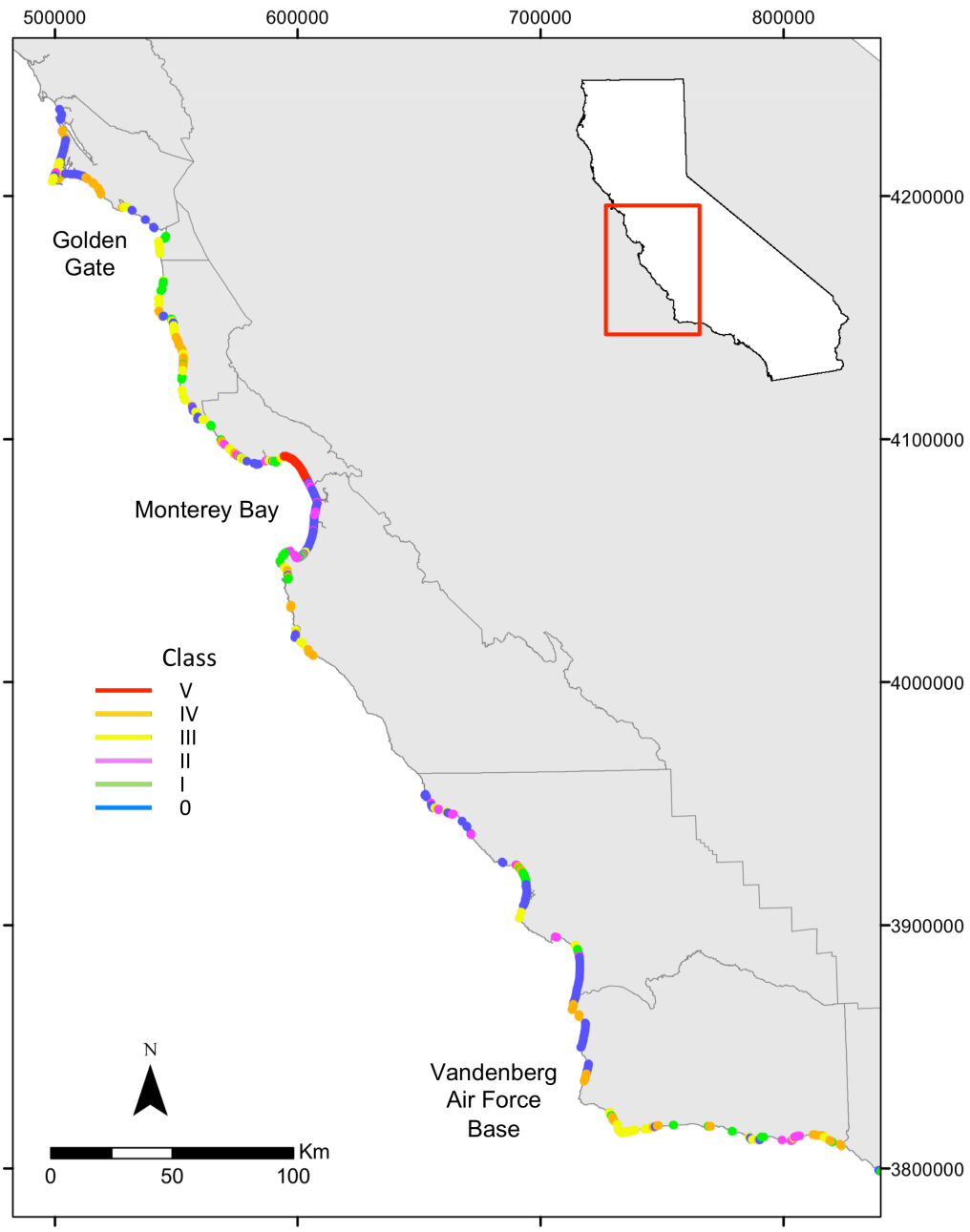

Fig. 1.18: Sandy shoreline classifications for the Central California coast (Marin County to Santa Barbara County)

Table 1.5: Percent of the total regional and statewide sandy shoreline represented in each class for Central California

Class	Percent of total regional sandy shoreline	Percent of total statewide sandy shoreline
0	42%	17%
I	7%	3%
II	7%	3%
III	21%	9%
IV	16%	7%
V	6%	3%
	TOTAL:	42%

Forty-two percent of the total length of sandy shoreline along the Central California coast is publically owned beach. Twenty-three percent of the Central California publically owned sandy shoreline is Class 0 with no back-beach barrier, while an additional 28% and 29% are Class I and III, respectively. Only 1% of the publically owned sandy shore is Class V (Table 1.6). The high proportion of publically owned sandy shoreline in Central California is largely due to the Point Reyes National Seashore in Marin county, which comprises nearly 50 km of the Central California open ocean coastline, much of which is unrestricted Class 0 beach backed by extensive dunes (Fig. 1.19). Also, a large fraction of the southern Central California coast is undeveloped and 'protected' due to the location of Vandenberg Air Force Base in Santa Barbara County, which spans approximately 56 km of coastline from Point Sal south to Point Arguello.

Table 1.6: Percent of the total length of publically owned regional and statewide sandy shoreline represented in each class for Central California

Class	Percent of total regional publically owned sandy shoreline	Percent of total statewide publically owned sandy shoreline
0	23%	11%
I	28%	13%
II	14%	7%
III	29%	14%
IV	4%	2%
V	1%	1%
	TOTAL:	47%

Fig. 1.19: Extensive Class 0 sandy shoreline of Point Reyes National Seashore in Central California (photo by Kenneth and Gabrielle Adelman)

1.4.4 Southern California: Ventura to San Diego County

The Southern California coastline, including Ventura, Los Angeles, Orange, and San Diego counties, comprises about 23% of the total coastline of California, but contains a third of the total sandy beach shoreline. On a regional scale, Southern California has the highest ratio of sandy shoreline to total coastline, with sandy beaches comprising 55% of the Southern California coastline versus 35% in Central California and 34% in Northern California (Fig. 1.20). Thirty-one percent of the sandy shoreline in Southern California is Class III, while only 16% is Class 0 with no back-beach barrier (Table 1.7). Southern California also has the highest total percentage of Class III or higher sandy shoreline at 54%, compared with 43% in Central California, and only 20% in Northern California.

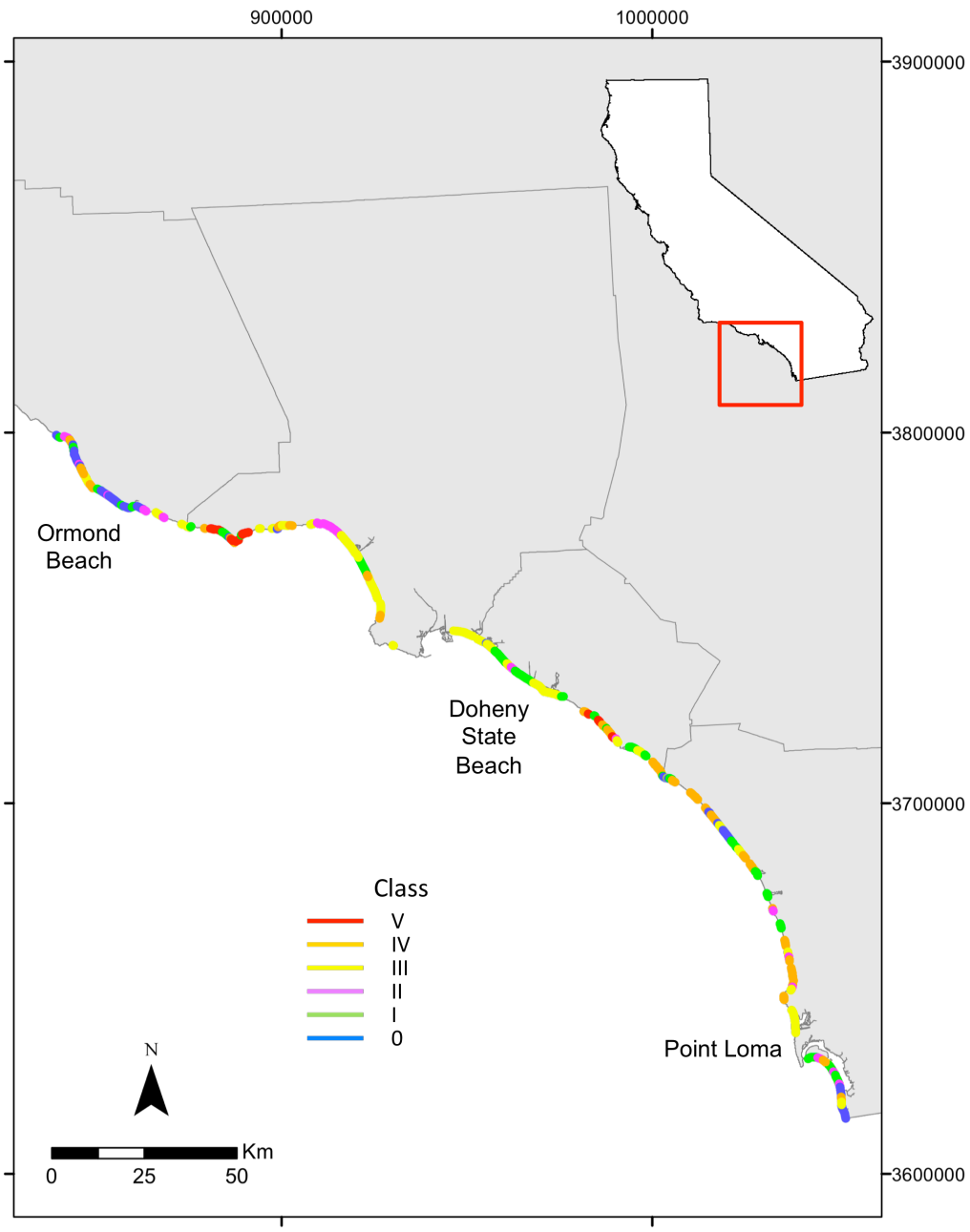

Fig. 1.20: Sandy shoreline classifications for the Southern California coast (Ventura County to San Diego County)

Table 1.7: Percent of the total regional and statewide sandy shoreline represented in each class for Southern California

Class	Percent of total regional sandy shoreline	Percent of total statewide sandy shoreline
0	16%	5%
I	21%	7%
II	9%	3%
III	31%	10%
IV	20%	6%
V	3%	1%
	TOTAL:	32%

Forty-two percent of the total length of sandy shoreline in Southern California is publically owned, with a fairly even spread between Classes 0-IV (Table 1.8) ranging from 14% for Class IV sandy shoreline to 25% for Class I. Southern California has the highest regional proportion of Class V publically owned sandy shoreline at 6%.

Table 1.8: Percent of the total length of publically owned regional and statewide sandy shoreline represented in each class for Southern California

Class	Percent of total regional publically owned sandy shoreline	Percent of total statewide publically owned sandy shoreline
0	20%	4%
I	25%	5%
II	14%	3%
III	17%	3%
IV	18%	3%
V	6%	1%
	TOTAL:	19%

1.5 Back Beach Classifications and Historic Shoreline Change Rates

1.5.1 Northern California

The average short-term shoreline change rates for the Northern California coast are accretional and range from 0.0 m/yr to +0.4 m/yr. The highest short-term accretion rate (+7.3 m/yr) for both the Northern California coast and the entire state occurred along the Prairie Creek Redwoods State Park coastline (see Fig. 1.17), while the highest short-term erosion rate for Northern California of -2.7 m/yr occurred on the North Spit of Humboldt Bay, north of the Humboldt Bay jetty. The highest short-term accretion and erosion rates both correspond to a Class 0 sandy shoreline (Fig. 1.21 a, b), which, as mentioned previously, is the dominant shoreline classification along the Northern California coast. The distributions of shoreline change rates for each sandy shoreline classification reflect the high percentage of Class 0 shoreline along the Northern California coast (Fig. 1.22).

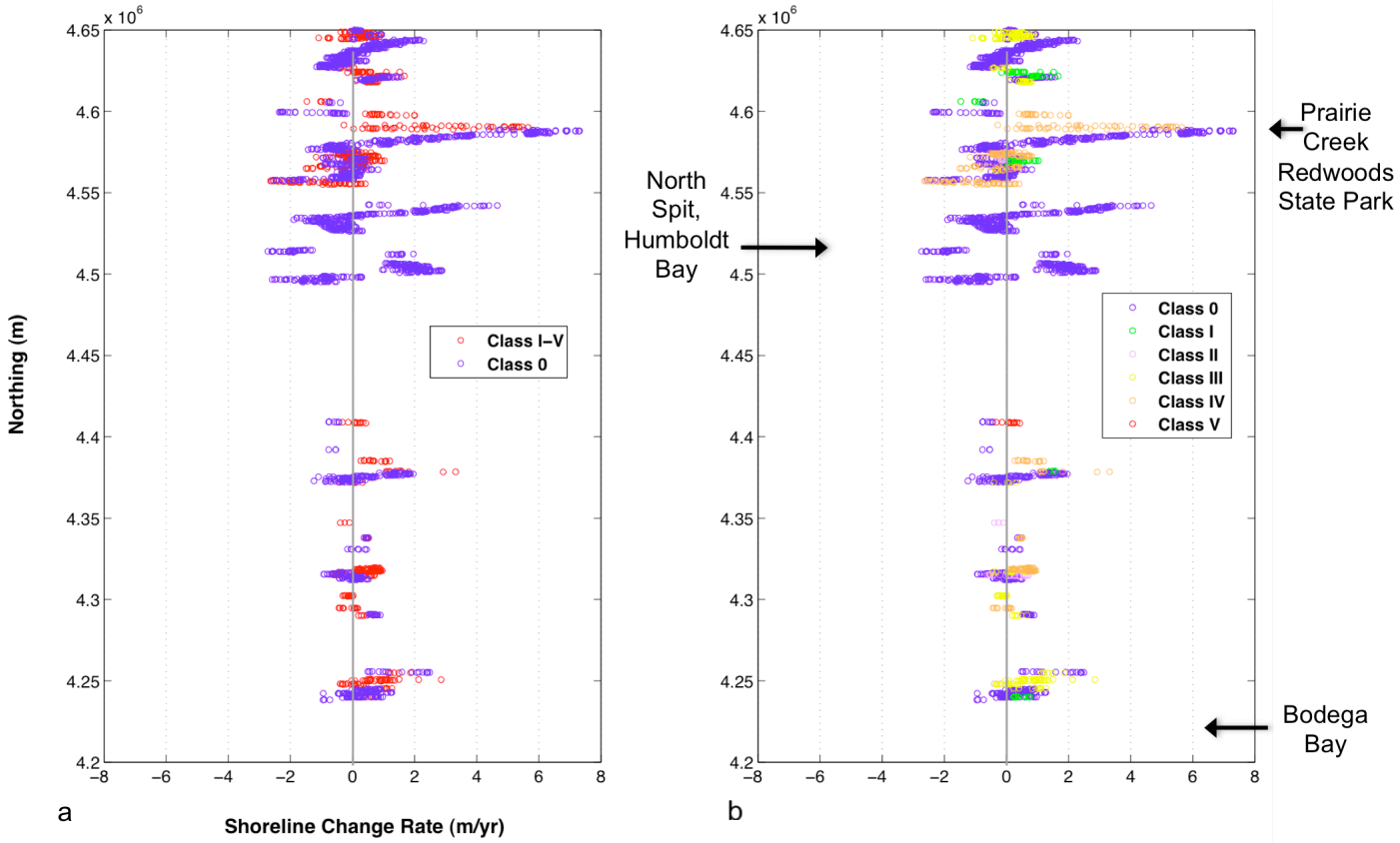

Fig. 1.21: Scatter plots of UTM Northing (m) vs. short-term historic shoreline change rates plotted by (a) the presence or absence of a back-beach barrier and (b) separated by class for Northern California

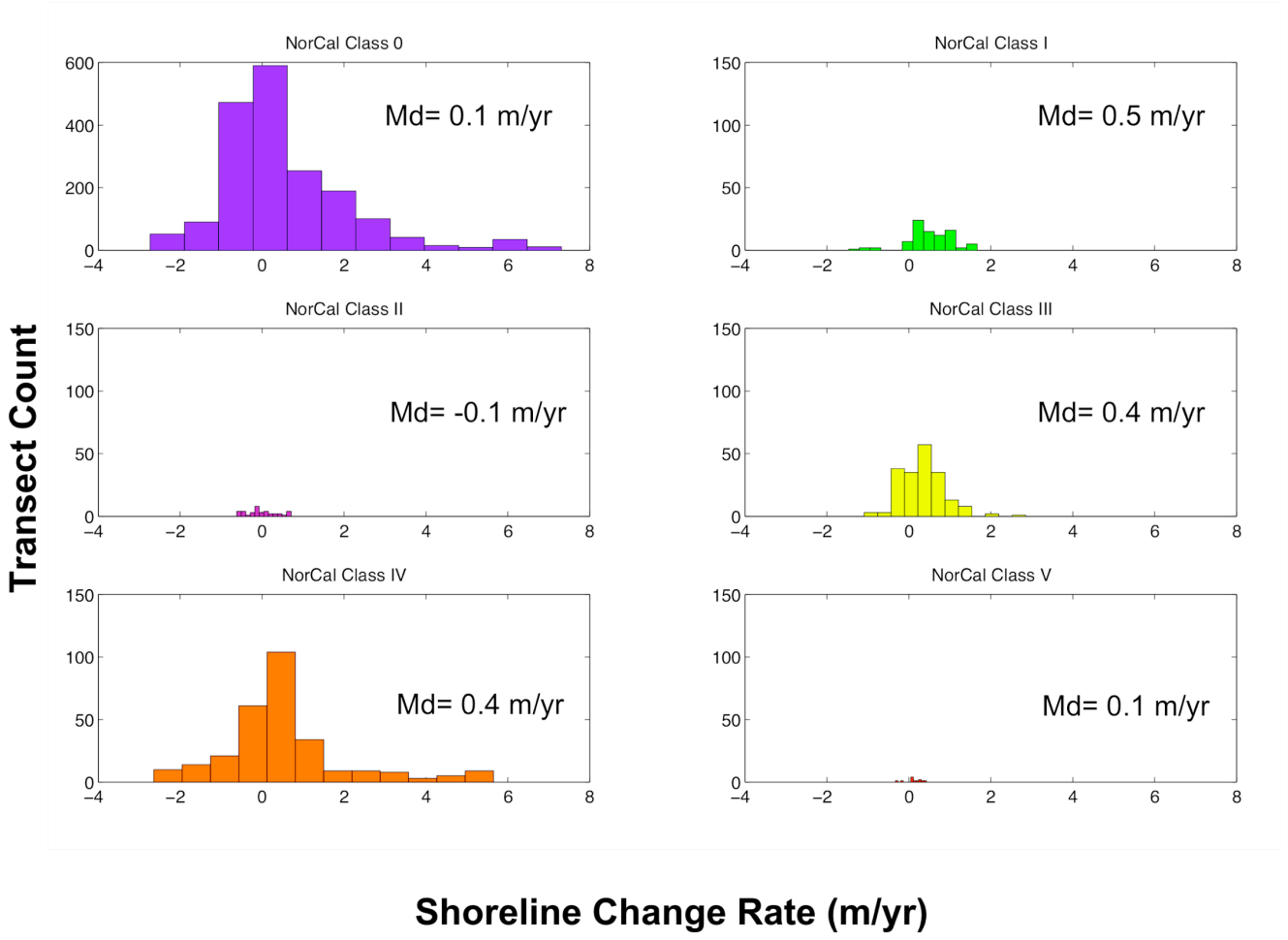

Fig. 1.22: Histograms of sandy shoreline short-term shoreline change rate distributions by class for Northern California with median shoreline change rates. The 'count' within each bin is equal to the number of transects within the specified shoreline rate of change interval.

The medians of all class shoreline change rate distributions are accretional (+0.1 m/yr to +0.5 m/yr) except for Class II, which has a median shoreline change rate of -0.1 m/yr. Mann-Whitney U-tests were conducted between Class 0 and Class I distributions, Class 0 and Class II distributions, Class 0 and Class III distributions, Class 0 and Class IV distributions, and Class 0 and Class V distributions to test for a statistically significant difference in the median shoreline change rates between beaches of varying degrees of back-beach immobility (i.e., with a back-beach barrier) and beaches without a back barrier. The null hypothesis that the samples (Northern California Class 0 and Northern California Class I shoreline change rates, Class 0 and Class II change rates, etc.) are drawn from the same distributions (have the same median) fails to be rejected at the 5% significance level for all Classes (compared with the Northern California Class 0 distribution) except for Class I (Table 1.9).

Table 1.9: Mann-Whitney U-Test results comparing Classes I-V shoreline change rate distributions with Class 0 distributions for Northern California

	Reject null hypothesis at the 5% significance level?
	Northern California
Class I	yes
Class II	no
Class III	no
Class IV	no
Class V	no

1.5.2 Central California

The Central California coast as defined by the National Assessment of Shoreline Change report extends to El Capitan State Beach north of Santa Barbara. In this report, Central California includes all of Santa Barbara County, which extends the defined Central California coastline by approximately 50 km in comparison. The average short-term shoreline change rate for the Central California region is strongly erosional, at -0.5 m/yr. The maximum rate of accretion of +4.7 m/yr occurred in northern Santa Barbara County at

Vandenberg Air Force Base (see Fig. 1.18), and corresponds to a Class 0 shoreline (Fig. 1.23 a, b). The maximum short-term erosion rate of -5.6 m/yr occurred at Guadalupe Dunes south of Pismo Beach in San Luis Obispo County and also corresponds to a Class 0 shoreline. The distributions of shoreline change rates for each sandy shoreline classification reflect the relatively high proportion of Class 0 and Class III sandy shoreline along the Central California coast (Fig. 1.24).

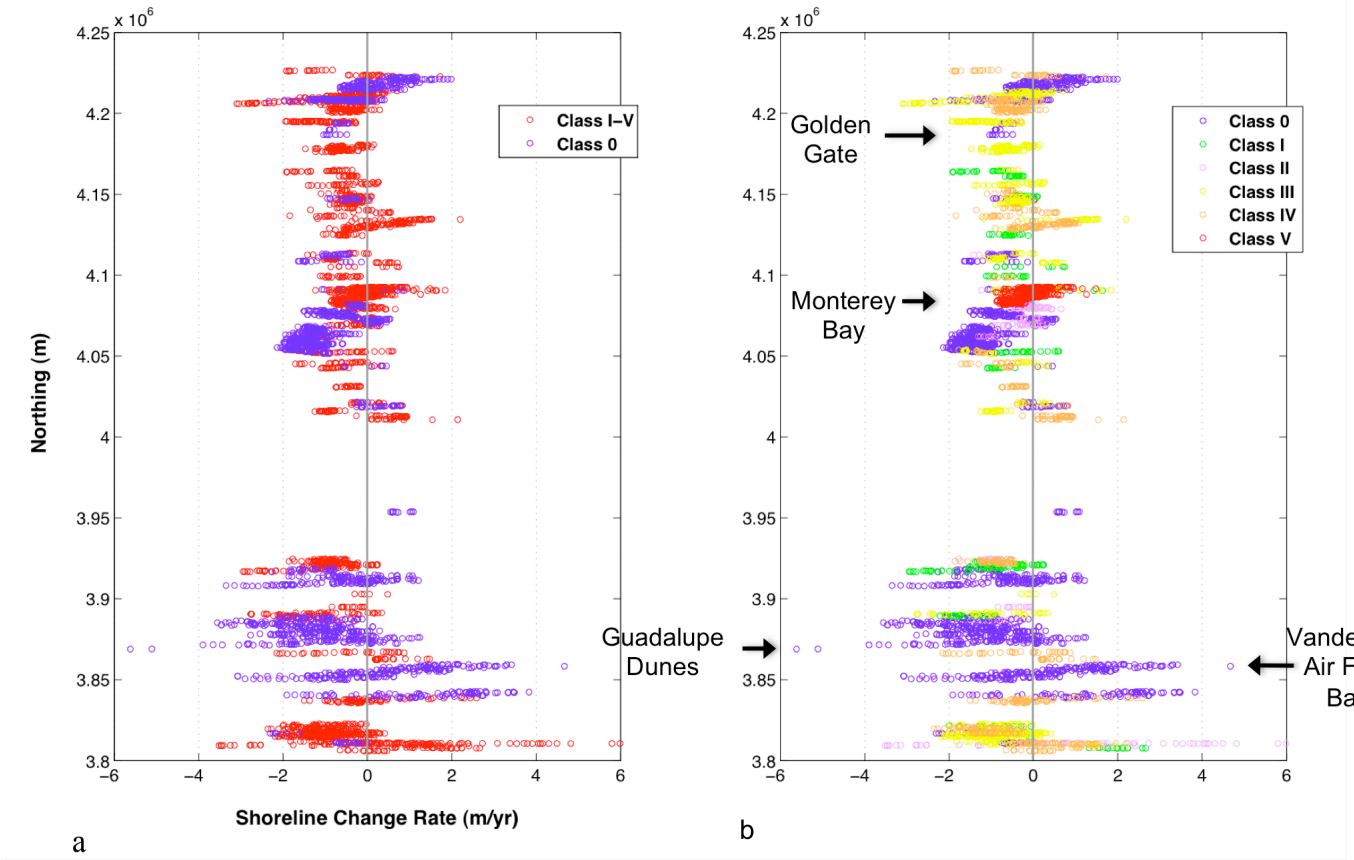

Fig. 1.23: Scatter plots of UTM Northing (m) vs. short-term historic shoreline change rates plotted by (a) the presence or absence of a back-beach barrier and (b) separated by class for Central California

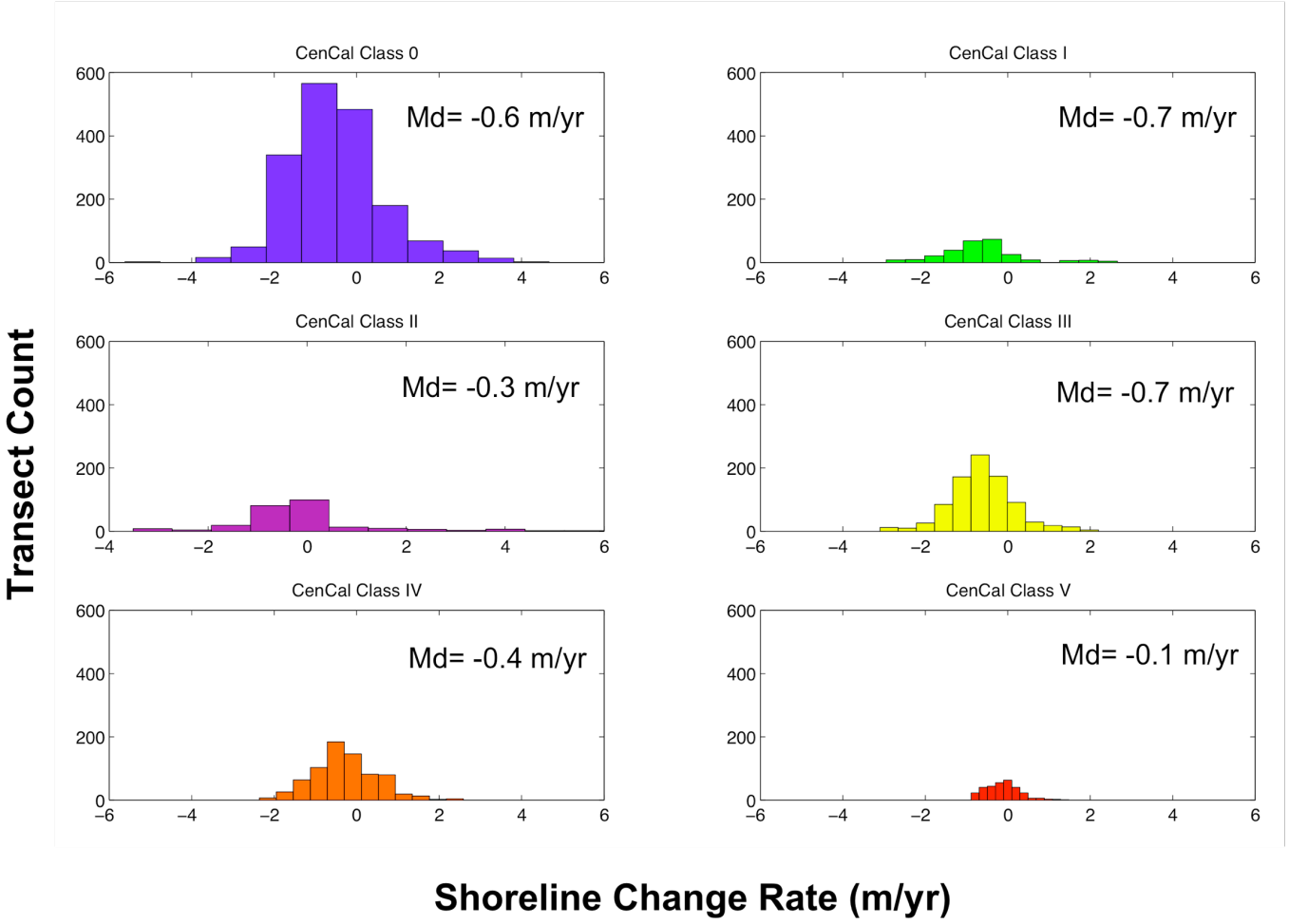

Fig. 1.24: Histograms of sandy shoreline short-term shoreline change rate distributions by class for Central California with median shoreline change rates. The 'count' within each bin is equal to the number of transects within the specified shoreline rate of change interval.

The medians of all class distributions are erosional, with the Class I and III medians corresponding to the highest erosion rate of -0.7 m/yr, and the Class V median corresponding to the lowest erosion rate of -0.1 m/yr. The null hypothesis that the samples (Central California Class 0 and Central California Class I shoreline change rates, Class 0 and Class II change rates, etc.) are drawn from the same distributions is rejected for Classes II, IV, and V, but fails to be rejected for Classes I and III (Table 1.10).

Table 1.10: Mann-Whitney U-Test results comparing Classes I-V shoreline change rate distributions with Class 0 distributions for Northern and Central California

	Reject null hypothesis at the 5% significance level?	
	Northern California	**Central California**
Class I	yes	no
Class II	no	yes
Class III	no	no
Class IV	no	yes
Class V	no	yes

1.5.3 Southern California

The average short-term shoreline change rate for the Southern California coast from Ventura County to the U.S.-Mexico border is erosional at -0.1 m/yr. The maximum short-term accretion rate of +6.8 m/yr occurred south of Dana Point Harbor at Doheny State Beach (see Fig. 1.20), and corresponds to a Class I shoreline (Fig. 1.25 a, b). The maximum short-term erosion rate of -5.5 m/yr occurred just south of Port Hueneme in Ventura County at Ormond Beach, and corresponds to a Class I shoreline. The distributions of shoreline change rates for each sandy shoreline classification show the relatively high proportion of Class II and IV sandy shoreline along the Southern California coast (Fig. 1.26).

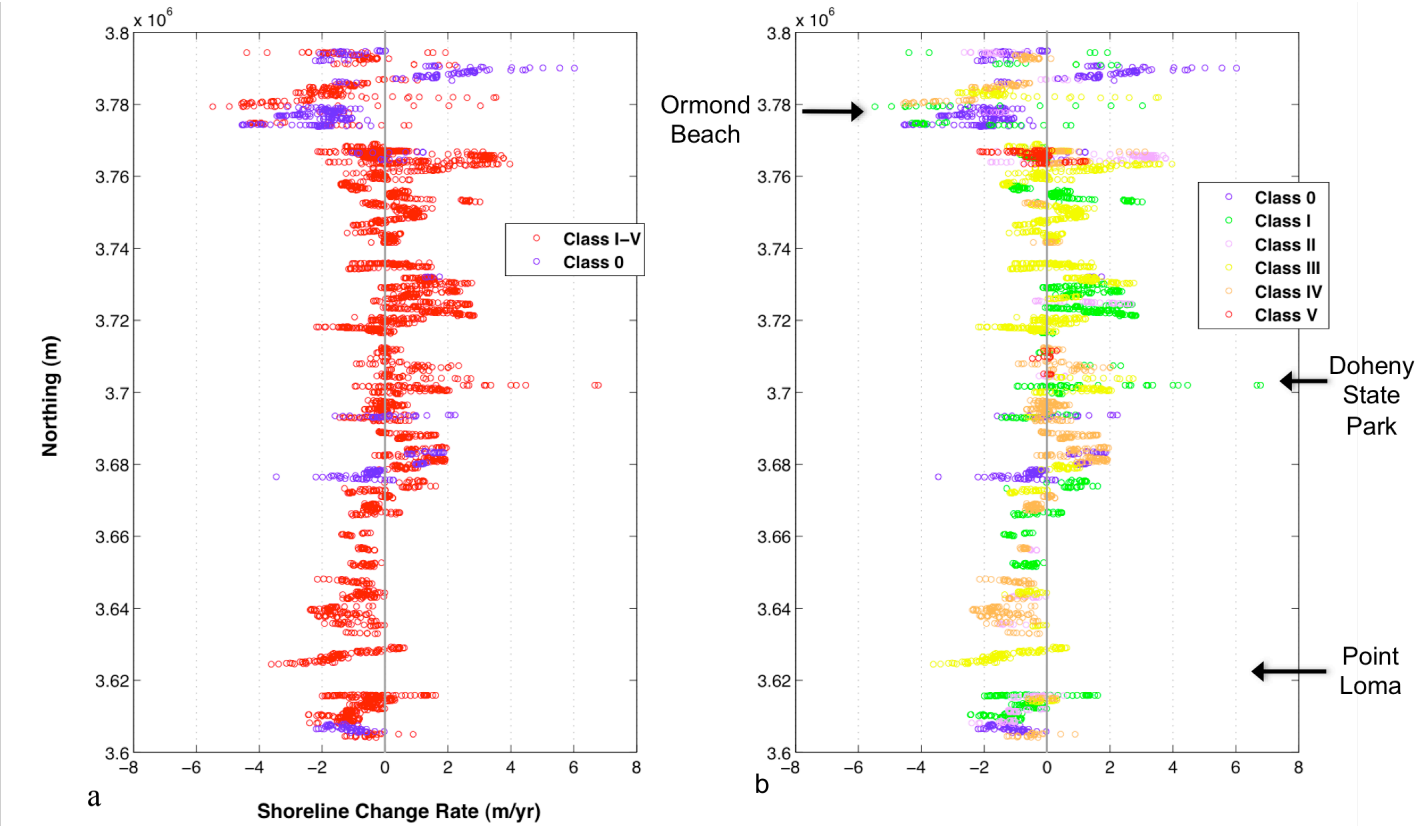

Fig. 1.25: Scatter plots of UTM Northing (m) vs. short-term historic shoreline change rates plotted by (a) the presence or absence of a back-beach barrier and (b) separated by class for Southern California

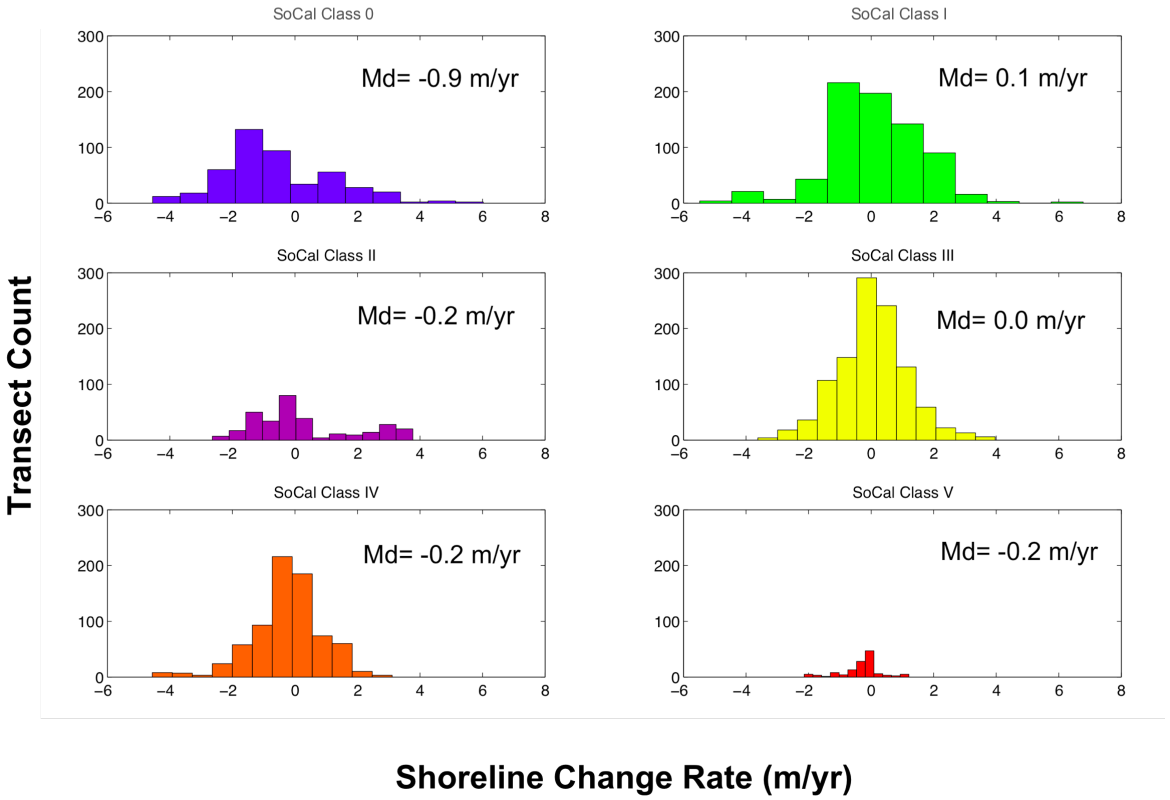

Fig. 1.26: Histograms of sandy shoreline short-term shoreline change rate distributions by class for Southern California with median shoreline change rates. The 'count' within each bin is equal to the number of transects within the specified shoreline rate of change interval.

The median shoreline change rate for Classes 0, II, IV, and V are erosional (-0.2 m/yr for Classes II,IV, and V to -0.9 m/yr for Class 0), while the Class I median is accretional (+0.1 m/yr) and the Class III median is zero. In contrast to Northern California, the null hypothesis that the samples (Southern California Class 0 and Southern California Class I shoreline change rates, Class 0 and Class II change rates, etc.) are drawn from the same distributions is rejected for all classes (Table 1.11).

Table 1.11: Mann-Whitney U-Test results comparing Classes I-V shoreline change rate distributions with Class 0 distributions for Northern, Central, and Southern California

	Reject null hypothesis at the 5% significance level?		
	Northern California	**Central California**	**Southern California**
Class I	yes	no	yes
Class II	no	yes	yes
Class III	no	no	yes
Class IV	no	yes	yes
Class V	no	yes	yes

1.6 Discussion

1.6.1 Regional Shoreline Classifications and Comparisons

The three regions of the California coastline (Northern, Central, and Southern) are distinct in terms of the sandy shoreline back beach classifications. The total sandy shoreline of the Northern California coast is 74% Class 0, which equates to 20% of the total length of open ocean sandy shoreline along the entire California coastline and 47% of the total Class 0 sandy shoreline along the entire California coast. In comparison, the Central California Class 0 sandy shoreline makes up 17% of the total length of California's sandy shoreline and 41% of the total length of statewide Class 0 shoreline, and Southern California Class 0 makes up only 5% of the total length of sandy shoreline and 12% of the total statewide Class 0 shoreline. The high proportion of unrestrained sandy shoreline in Northern California is

primarily a result of the comparatively low coastal population and thus lower proportion of back-beach development, and may also be due to the high proportion of publically owned sandy shoreline. Twenty-four percent of the total Class 0 publically owned sandy shoreline along the California coast lies within the four northern counties. However, the Northern California coastline is also rugged and characterized by rocky bluffs and cliffs, accounting for 20% of the total statewide length of Class IV sandy shoreline.

Central California as defined in this study contains 46% of the total coastline and 42% of the total sandy shoreline, accounting for the relatively high percentages of each shoreline class. Although Central California is more highly populated than Northern California, two significant stretches of publically owned sandy shoreline at Point Reyes in Marin County and Vandenberg Air Force Base in Santa Barbara County account for 42% of the sandy shoreline in Central California denoted as Class 0, which is 41% of the total statewide length of Class 0 beach. Central California also contains the highest proportion both regionally (6%) and statewide (69%) of Class V highly immobile sandy shoreline, most of which is concentrated in the northeastern Monterey Bay between New Brighton State Beach and the Santa Cruz-Monterey County Line. The sandy shoreline in this region is backed by a combination of high bluffs topped by infrastructure, as well as infrastructure directly on the beach, which has resulted in significant placement loss of the beach (Fig. 1.27). Much of this infrastructure is fronted by rip-rap or seawalls.

Fig. 1.27: Class V shoreline at New Bright State Beach in Central California. The high classification is due to the presence of infrastructure not only on the bluffs, but also on the back beach fronted by coastal armoring (rip-rap) (photo by Kenneth and Gabrielle Adelman)

The presence of rip-rap or seawalls fronting infrastructure or bluffs is an important indication of the state of mind of coastal managers or property owners as well as the present and potential future state of the beach. It demonstrates that coastal property owners and/or coastal managers as well as the local or statewide coastal regulatory agencies have indicated that protecting back beach or bluff top infrastructure has a higher priority than preserving the beach, and that coastal retreat will most likely not be considered until the beach is essentially completely inundated or eroded. There are several examples of 'drowned' sandy beaches along the Southern California coastline that have been sacrificed in favor of protecting shorefront residences (Fig. 1.28). These shorelines in Southern California would be classified as a 'V' in the sandy shoreline catalog; however, many of these beaches were excluded due to a lack of significant subaerial beach area. As a result, Southern California has a lower proportion of Class V shoreline compared with Central California.

Fig. 1.28: Solimar Beach in Ventura County, Southern California: An example of a 'drowned' beach due to coastal armoring (photo by Kenneth and Gabrielle Adelman)

The total length of Southern California sandy shoreline as defined for this study makes up almost a third of the total length of statewide sandy shoreline, whereas the total Southern California coastline (beaches + bluffs/cliffs) consists of only about 23% of the total California coastline. The Southern California sandy shoreline statistics reflect the significant anthropogenic manipulation of the Southern California coastal zone. The highest proportion (31%) of Southern California sandy shoreline is Class III, and significant portions also fall within Class I and Class IV designations. The Class III designations in part reflect the long stretches of wide beaches in places like Santa Monica that are backed by dense, but low-lying infrastructure. Such beaches have been artificially widened by intentional or opportunistic nourishment. Since the 1930s, 100 million m^3 of sand have been added to Southern California littoral cells (Flick, 1993)—a much larger volume of sand than is typically introduced by rivers and streams—which has resulted in the wide beaches today that serve as some of the most popular tourist destinations in California. Coastal engineering structures

such as jetties and groins have also contributed to artificial widening of many Southern California beaches.

The large proportion of Class I shoreline can be attributed to the Pacific Coast Highway 1, which runs close to the shoreline along most of the Southern California coast. While the highway in most cases does not serve as a physically elevated barrier to landward beach migration, it is a crucial piece of infrastructure not only for connecting coastal communities, but also for supporting California's important tourist economy, as it is a popular destination and resource for coastal sightseers and beachgoers. Therefore, the landward migration of a beach fronting the highway would either be physically restricted by coastal armoring measures as the highway becomes threatened by an encroaching shoreline, or steps would need to be taken to reroute the highway inland, a measure that would be both costly and inconvenient.

1.6.2 Publically Owned Sandy Shoreline

One of the important results of this study is the relationship between publically owned sandy shoreline and particular shoreline classifications. Thirty-seven percent of the total length of cataloged sandy shoreline is publically owned beach, either due to a state/county park or reserve designation, wildlife refuge, or the presence of a military base. Fourteen percent of the total length of California's sandy shoreline and 38% of the total length of publically owned sandy shoreline is Class 0 publically owned beach, whereas only 4% is highly immobile Class IV-V publically owned sandy shoreline. Sixty-eight percent of the total length of publically owned sandy shoreline in Northern California is Class 0. In Southern California, 45% of publically owned sandy shoreline is Class 0 or Class I. In Southern California, publically owned beaches such as state or county parks tend to have parking lots or sparse infrastructure (facilities) in the back beach compared with the more 'wild' Northern California coastline.

In general, publically owned beaches have restrictions for back beach development, and thus tend to have either no back-beach barriers, or low-to-moderate barriers depending

on the presence of roadways, parking lots, or bluffs. The effects of public ownership of beaches are apparent in places like Ventura County, where the juxtaposition of a publically owned state beach with a city beach results in a significant difference in beach characteristics—beach width and particularly the landward extent of the back beach—alongshore (Fig. 1.29).

Fig. 1.29: San Buenaventura State Beach (left of the groin) directly adjacent to Ventura public beach (right). Although the presence of the groin has widened the state beach, it is clear in comparing the back beach extents that back-beach development on the public beach side has contributed to beach narrowing and placement loss (photo by Kenneth and Gabrielle Adelman)

This finding suggests that the current designation of beaches as state parks, wildlife refuges, and military bases will most likely aid in the preservation and persistence of these particular beaches in the future as sea level rises and the beaches are able to migrate landward. Closing or eliminating state parks and state beaches would be detrimental not only to California's coastal tourism economy, but also to the fate of many of California's beaches.

Such a proposal was in fact put forth initially in 2009 by Governor Schwarzenegger, although it excluded many of the popular state beaches in Southern California.

1.6.3 Shoreline Classifications and Rates of Change

Visual inspection of the historical shoreline change rate scatter plots colored by class (Figs. 1.21, 1.23, 1.25) do not show obvious correlations between patterns in change rates and specific classifications. The most apparent pattern of color banding (continuous bands of identically-colored data points on the plots) is a result of alongshore variation (an increase or decrease) in shoreline change rates along a continuous stretch of beach that has been given a single classification, and reflects the fact that there are multiple transects reporting a range of rates intersecting that particular stretch of uniformly-classed beach. Historic shoreline change rates, particularly in Southern California, may result largely from coastal armoring and coastal engineering structures, as well as beach nourishment. The construction or existence of a groin, jetty, or breakwater over the past 40 years could have resulted in positive short-term shoreline change rates for the beach directly updrift of the structure due to the trapping of littoral drift sediments, and negative shoreline change rates downdrift of the structure for beaches that were subsequently starved of littoral sediments. This was observed for the beaches north and south of Oceanside Harbor in Southern California after the harbor jetties were constructed in 1968 and began to trap littoral drift sand (Flick, 1993). Beach nourishment would have also resulted in artificially positive shoreline change rates (or negative, if unsuccessful projects were conducted immediately prior to the earliest shoreline) depending on when the nourishment occurred relative to the date of the shoreline position data and the success of the nourishment project.

Results of the Mann-Whitney rank-sum U-tests either indicate that there is a statistically significant difference between the median shoreline change rates of beaches without back-beach barriers and beaches with varying degrees of back-beach barriers if the null hypothesis that the samples are drawn from the same distribution is rejected at the 5% significance level, or that there is no statistically significant difference between median

shoreline change rates if the null hypothesis fails to be rejected. The U-test results show an interesting pattern between the Northern, Central, and Southern coasts. For the Northern California coast, the null hypothesis failed to be rejected for almost all back barrier classes (II-V) tested against the Class 0 distribution, yet in Southern California the opposite case is true. The null hypothesis in Central California was rejected for three of the five back barrier classes (II, IV, and V).

It is important to note that rejection of the null hypothesis does not indicate a cause and effect relationship between a back-beach barrier and shoreline erosion or accretion, or that there is any direct relationship at all between the two, but it suggests the possibility of a direct or indirect relationship. It cannot be concluded that back-beach barriers necessarily contribute to erosion of the shoreline. In Southern California, the Class 0 median shoreline change rate is actually significantly more negative (erosional) compared with Classes I-V. It is hypothesized that this may result from the artificial widening and stabilization of popular and developed sandy beaches in Southern California. In Northern California, the median shoreline change rate of both the Class I distribution (for which the null hypothesis was rejected) and Class 0 distribution is accretional; however, it is significantly more accretional for the Class I distribution. It is possible that the differences between Northern and Southern California U-test results could be due to the differences in coastal development and anthropogenic influence on the regional coastal zone, and that the Central California coast represents a sort of 'transition zone.' More detailed testing of the additional questions and hypotheses that arise from these preliminary statistical results in future studies could have important implications for California coastal policy, coastal management and coastal development, and regional sea-level rise adaptation and mitigation plans.

1.7 Conclusions

Future sea-level rise and potential increases in storm event frequency and intensity could lead to a landward-moving shoreline; indeed, this is already the case in several

locations along the California coast. A sandy shoreline migrating towards a natural undeveloped bluff could potentially result in a preserved beach provided that the rate of bluff erosion can keep up with shoreline migration. Alternately, landward shoreline migration that threatens anthropogenic coastal development leaves us with four options: take no action; armor the shoreline or bluff toe and potentially lose the beach; nourish the beach, a costly and not always successful solution; or retreat. As beaches are ephemeral features and can undergo significant changes over not only seasonal time scales, but also interannual or decadal time scales that might not be captured by the existing aerial photo and satellite imagery datasets, it will be important to continue updating the sandy shoreline classification catalog with new and improved datasets in the future. Comparisons of updated catalogs to the one presented in this report could provide additional information about the longer-term variability of beach widths along the California coast and potential correlations with interannual to decadal climate variability (ENSO events, PDO cycles) as well as the impacts of future anthropogenic modifications of and influences on the California coastal zone.

CHAPTER 2

Extreme Water Levels, Sea-Level Rise, and the Future of California's Sandy Beaches

2.1 Introduction and Background

Climate change and sea-level rise are a concern for a wide variety of populations globally for reasons ranging from environmental and ecological effects, to economic impacts, to basic survival and adaptation. Although the current estimates for global eustatic sea-level rise of a few mm/year seem insignificant on short time scales, projected sea-level rise of 18 (IPCC, 2007) to 140 cm or more (Vermeer and Rahmstorf, 2009) by 2100, in conjunction with extreme storm events, could mean extensive inundation for low-lying coastal regions and erosion or retreat for coastal cliffs, bluffs, and dunes.

2.1.1 Sea Level Variability

Variations in sea level occur on several spatial and temporal scales. The semidiurnal and diurnal harmonic tidal constituents cause the most significant regular changes in sea level (anywhere from 0.1 to over 10 m), with periods of typically half a day. Daily tidal fluctuations are dominated by the longer period spring-neap cycle, which, in turn, is dominated by even longer period fluctuations related to variability in solar and lunar orientation and distance. Tides are the only accurately predictable component of sea-level fluctuations, although storm systems can elevate coastal water levels that persist over a few hours or days. Offshore low-pressure storm systems or tropical cyclones generate surge, a super-elevation of the mean water level typically up to 20-25 cm along the coast of California (Flick and Cayan, 1984). Perhaps more significantly, they induce increased surface gravity wave energy, resulting in extreme wave set-up and run-up at the shoreline, and can exceed still water levels orders of magnitude higher than storm surge. Elevated water levels and high wave energy due to storms are the most frequent sources of coastal property

destruction and rapid erosion, and are especially hazardous when they occur in conjunction with high tides (Storlazzi et al., 2000). On inter-annual and decadal time scales, there are periodic variations in climate patterns (El Niño, Pacific Decadal Oscillation) related to shifts in atmospheric circulation, surface air pressure, and ocean surface temperature that have an impact on ocean basin water distribution and thermal expansion, which further contribute to relative sea-level variations. Global warming-induced sea-level rise will undoubtedly be exacerbated by these higher frequency sea-level fluctuations.

2.1.2 Anthropogenic Global Warming and Sea-Level Rise

The concentrations of CO_2 and methane in the atmosphere today greatly exceed the natural concentration range for the last 650,000 years, and land and sea surface temperatures and increased rates of sea-level rise (SLR) have been concomitant with this (IPCC, 2007). The 2007 Intergovernmental Panel on Climate Change (IPCC) report states with 90% certainty that anthropogenic forcings are the main contributor to both the observed accelerated global temperature increases and eustatic sea-level rise since the last half of the 20^{th} century. During the 20^{th} century, global mean sea level rose at approximately 1.8 mm/yr, but has been rising an estimated 3 mm/yr since 1993 (Church et al., 2001) as documented by satellite altimetry. The IPCC projects global sea level to rise anywhere from 18-79 cm by the year 2095, depending on different future greenhouse gas emissions scenarios (Church, et al., 2008). In 2009, Vermeer and Rahmstorf published sea-level rise projections of 75 cm to 190 cm (average of 140 cm) by 2100 based on a simple but elegant relationship between global sea-level variations and global temperature. Since at least 1961, the main contributions to global sea-level rise have been from upper ocean (~700 m) thermal expansion (0.5 ± 0.2 mm/yr) and the melting of glaciers and ice caps (0.5 ± 0.1 mm/yr), with smaller—albeit important—contributions from deep ocean thermal expansion and mass loss from the Greenland and Antarctic ice sheets (Domingues et al., 2008). However, it is widely regarded that the IPCC (2007) estimates for the cryospheric contribution to sea level rise are too low

(e.g., Meier et al., 2007) and it is believed that these constituents are now and will have a much greater impact on sea level rise through the 21st century.

In California, sea-level rise from tide-gauge records over the last century has ranged from 10-20 cm (Cayan et al., 2006). Mean sea level along the California coast, although marked by inter-annual and decadal variability, has been rising continuously throughout most of the 20th century at a rate similar to global sea-level rise, although there has been no apparent rise since the early 1990s (Bromirski et al., 2011; Merrifield et al., 2011). This is hypothesized to be a result of the warm phase PDO regime, which has been the dominant regime since the late 1970s. However, a potential imminent shift in the PDO regime from a warm phase to a cold phase could bring a prolonged increased sea-level to the California coast, resuming and possibly exacerbating accelerated sea-level rise.

2.1.3 Climate Change, Sea-Level Rise, and Public Policy

In 2006, the Climate Action Team, a multi-agency committee created under the EPA and California Climate Change Center (CCCC), following an Executive Order from Governor Schwarzenegger for emissions reductions in the state of California, assembled a report of greenhouse gas emissions reduction strategies for mitigating future climate change. Although goals for reducing anthropogenic greenhouse gas emissions are important and necessary, several recent climate-modeling studies have found that in order to stabilize rising global temperatures, future global anthropogenic carbon emissions must be reduced to near zero (Matthews and Caldeira, 2008).

In response to the governor's Executive Order for emissions reductions, Susanne Moser of the Institute for the Study of Society and Environment at the National Center for Atmospheric Research conducted a survey on the awareness and preparedness of California coastal managers for climate change and sea-level rise (Moser, 2007). She found that although a large proportion of respondents were aware of and concerned about climate change and sea-level rise and their potential impacts, few of them felt they had the tools

necessary to integrate sea-level rise preparedness and adaptation strategies into future planning. While climate science and sea-level rise scenarios are important to present to the public, most coastal managers want to know more specific and applicable details including potential retreat rates, site-specific coastal vulnerability, and how to deal with sea-level rise and still meet management objectives. Between 2006 and 2010, several reports were published on potential sea-level rise impacts on the California coast by interagency groups such as the California Climate Change Center (Cayan et al., 2009), as well as coastal management guidelines for planning for these impacts by the Public Policy Institute of California (Hanak and Moreno, 2008), the California Natural Resources Agency (2009), and the California Ocean Protection Council's Coastal and Ocean Working Group of the California Climate Action Team (CO-CAT, 2010). As reports such as these base their management and policy recommendations on the best available science, it is necessary to continue to improve datasets and methods that will support and encourage informed and robust coastal policy.

2.2 Objectives

While sea-level rise is an inevitable consequence of global warming, a 3 mm/yr rate of sea-level rise alone is not going to be the primary factor controlling beach erosion and inundation in the short-term, although we can ultimately expect shorelines to gradually migrate landward if there are no changes in sediment supply or tectonic uplift rates do not exceed sea-level rise rates. Significant beach erosional events are typically episodic in nature, coinciding with super-elevated storm water levels and high wave energy. Therefore, the main objective for this study is to employ an extreme water level recurrence interval model to assess probabilistic cross-shore shoreline translation and subsequent inundation of beaches in California that would result from historic extreme water levels and sea-level rise scenarios of 18 cm, 79 cm, and 140 cm by 2100. This study focuses on beaches with high

attendance rates and the presence of a back-beach barrier, and assesses changes in both the still water level (SWL), as well as additional expected inundation due to run-up. A back-beach barrier with an elevation greater than the fronting beach sets a physical limit to the extent of landward translation of the shoreline. It is expected that the low (18 cm) sea-level rise scenario will not have a significant impact on the shoreline position for most of the study beaches; however, with increasing sea-level rise scenarios (79 cm and 140 cm), there will be a tipping point for gently-sloping beaches where once the foreshore berm elevation is exceeded, the shoreline position will migrate landward at a higher rate that is inversely proportional to the backshore slope. It is also expected that with the addition of run-up, the static still water shoreline will transform into a dynamic shoreline that oscillates about the mean predicted water level and adds a significant component to inundation predictions and erosion potential.

2.3 Methods

The following methods were applied to eight study beaches in California chosen based on high recreational use and the presence of a back-beach barrier: Mission Beach in San Diego, Huntington Beach, Santa Monica Beach, Redondo Beach, Ventura Beach, Santa Barbara East Beach, Santa Cruz Main Beach, and Ocean Beach in San Francisco (Fig. 2.1).

Fig. 2. 1: Locations of study beaches

2.3.1 Lidar and Interpolated Beach Surfaces

The main data used in this study are high-resolution lidar data collected during low tide in October of 1997 as part of the Airborne Lidar Assessment of Coastal Erosion (ALACE) project conducted by NOAA, NASA, and the U.S. Geological Survey. Airborne lidar data are collected by a low-flying aircraft equipped with a laser scanner and RTK-GPS. As the aircraft flies parallel to the shoreline, a series of mirrors reflect laser pulses over a 30-degree wide conical swath, typically at a rate of 2,000-5,000 pulses per second. A sensor records the time difference between laser emission from the aircraft and reflection back from the earth. The resulting elevation point data are simultaneously georeferenced by the GPS during data collection.

The 1997 lidar data were downloaded from the NOAA Coastal Service Center as first-return, raw X, Y, Z (longitude, latitude, elevation) points in UTM zones 10 and 11 (NAVD88 vertical datum) with a vertical RMS error of about 15 cm and a horizontal error of about 100 cm/1 m. The raw data points were interpolated by elevation into continuous gridded beach surfaces in ArcGIS using a natural neighbor interpolation algorithm (Watson, 1988). This algorithm approximates the value of a grid cell based on the nearest data point, and is appropriate for lidar datasets due to the high lidar point densities, as well as the algorithm's preservation of sudden changes in slope, which is useful for identifying manmade structures such as those that might define a back-beach barrier. A constant grid cell size of 0.5 x 0.5 m was used for all interpolations to maximize spatial resolution and minimize processing time.

Contours constraining the beach area of interest—the beach region from the Mean High Water (MHW) shoreline to the back-beach barrier—were extracted from the interpolated surfaces using a combination of contouring and slope analysis in ArcGIS as well as georeferenced aerial photo consultation. The MHW elevation is the vertical datum onto which sea-level rise scenarios are projected in this study, and were determined from local tide gauge data obtained from the NOAA National Ocean Service Center for Operational

Oceanographic Products and Services (NOAA NOS/CO-OPS; Table 2.1) and extracted from the beach raster surfaces as smoothed contours. The contoured MHW elevation was deemed for the purposes of this study a robust and acceptable approximation for the intersection of the MHW line with the beachface with uncertainty governed by the error in the raw data and in the interpolation method. For beaches with back-beach barriers of significant height (i.e., a seawall), the seaward edge of the back-beach barrier was delineated using the Slope tool in ArcGIS, which calculates the maximum rate of change of elevation between cells, in conjunction with contouring and aerial photo "ground truthing". The beach area of interest was then extracted from the original interpolated surface using a masking function within the ArcMap Spatial Analyst toolbox.

Table 2. 1: Mean high water (MHW) elevations, recorded sea-level rise rates, and tide gauge locations for study beaches.

Study Beach	Tide Gauge	MHW (m above NAVD88)	Recorded Sea-Level Rise Rate (mm/yr)
Mission Beach, San Diego	La Jolla Stn. 9410230	1.34	2.07 ± 0.29
Huntington Beach	Los Angeles Outer Harbor Stn. 9410660	1.39	0.83 ± 0.27
Redondo Beach	Santa Monica Stn. 9410840	1.37	1.46 ± 0.40
Santa Monica Beach	Santa Monica Stn. 9410840	1.37	1.46 ± 0.40
Ventura Beach	Santa Barbara Stn. 9411340	1.38	1.25 ± 1.82
Santa Barbara East Beach	Santa Barbara Stn. 9411340	1.38	1.25 ± 1.82
Santa Cruz Main Beach	Monterey Stn. 9413450	1.46	1.34 ± 1.35
Ocean Beach, San Francisco	San Francisco Stn. 9414290	1.61	2.01 ± 0.21

2.3.2 Recurrence Intervals of Extreme Water Levels

The recurrence interval, or return period, is the average time interval between occurrences of past random events. Recurrence intervals describe the frequency of events of various magnitudes, and are useful for assessing the probability of these events and magnitudes occurring in any given specified time period. In this sense, a recurrence interval distribution is not a forecasting tool, but rather can provide a range of probabilities derived for particular events from historic data. Recurrence intervals are commonly used in flood-frequency analysis and flood-zone mapping, as well as earthquake and volcanic eruption potential. A shift in the recurrence interval of events of a given magnitude can indicate larger scale changes in the system that governs these events, such as the climate system.

The probability of an event equal to or exceeding a certain magnitude each year is referred to as the annual probability of exceedance, and is the magnitude ranking (m) of each event divided by the number of events in the record (n) plus one. The event of greatest magnitude is assigned a ranking of m=1. The recurrence interval of an event is the inverse of the exceedance probability:

$$\text{Probability of Exceedance, } P = \frac{m}{n+1} \qquad (2.1)$$

$$\text{Recurrence Interval, } RI = \frac{1}{P} \qquad (2.2)$$

High probabilities of exceedance (P) indicate more frequently occurring events, and conversely low P values indicate less frequently occurring events of greater magnitude. For this study, a 1% exceedance probability is equivalent to a 100-year event.

For this study, recurrence interval and exceedance probability distributions of observed extreme high still water levels (SWL) and extreme SWL plus run-up were generated for each study beach from historic tide gauge records of maximum water levels. Data were derived from the same NOAA NOS/CO-OPS tide gauge records used to determine MHW elevations for each beach. The NOAA extreme high water level records are the water levels recorded by the tide gauges during storms, and include the astronomical tide, storm surge, and set-up, but do not incorporate run-up, and thus are considered measurements of the still water level elevation during an extreme water level event. In terms of a dynamic shoreline, this is the elevation about which swash oscillates. The data were filtered to include only the highest recorded water level for each year on record, sorted in decreasing order of maximum SWL, and assigned a rank, m, with m=1 corresponding to the first data point. Exceedance probability and recurrence interval distributions were constructed using Equations 2.1 and 2.2, and represent a range of extreme still water levels referenced to modern MHW elevations. In other words, these distributions are applicable for current mean sea level.

The effects of an 18 cm, 79 cm, and 140 cm sea-level rise on the extreme still water level distributions were determined by assuming a static beach state and projecting the three sea-level rise scenarios onto modern extreme SWL elevations at every 10% exceedance probability within the distributions. For example, a modern extreme SWL of 1.00 m above MHW with a 50% probability of exceedance would increase to a SWL of 1.18 m, 1.79 m, and 2.40 m above MHW with an 18 cm, 79 cm, and 140 cm rise in sea level, respectively. To quantify the impacts of increasing extreme still water levels associated with each sea-level rise scenario on a particular beach, the fractional area of the beach within the elevation values defined by the extreme SWL exceedance probabilities were calculated by appropriately binning the interpolated lidar beach surface grid cell elevations, summing the number of grid cells within each bin, multiplying the result by the grid cell dimensions (0.5 m^2), and finally dividing by the total beach area. For each study site, the cumulative fractional area of the beach that would be inundated with each 10% decrease in exceedance

probability (lower P corresponds with higher extreme water levels) was calculated. These values thus represent the percent of the total beach area that would be inundated under increasing still high water levels.

2.3.3 Recurrence Intervals And Exceedance Probabilities Of Extreme Still Water Levels Plus Run-Up

The still high water level represents the elevation about which the mean high water shoreline oscillates during a storm event of a certain magnitude. The total area of the beach impacted by the storm event is greater when wave run-up is also added into the equation. Run-up is a combination of the shoreward transfer of momentum due to wave breaking (set-up) and swash oscillations on the foreshore. Run-up, in conjunction with parameters such as the beach slope, maximum beach elevation, and sediment characteristics, governs the time-varying position of the shoreline about the still-water level and the maximum landward extent of swash motions, and is of significant concern with regards to erosion potential. Run-up is a function of the beach slope, ß (tangent of the slope angle), the deep-water significant wave height, H_o, and the deep-water wavelength, L_o, which scales as the square of the peak wave period, T:

$$L_o = \frac{gT^2}{2\pi} \qquad (2.3)$$

There are several empirically derived formulas for determining run-up on a beachface, most of which are either a function of the Iribarren number (ξ_o)—a ratio between the beach steepness and deep-water wave steepness (Equation 2.4)—for intermediate or reflective (ξ_o>0.3) beaches (Hunt, 1959; Holman, 1986), or are derived from 'Iribarren-like'

relationships of beach slope (β), deep-water wave height (H_o), and deep-water wavelength (L_o) for more dissipative (ξ_o<0.3) beaches (Ruggiero et al., 2001; Stockdon et al., 2006).

$$\xi_o = \frac{\beta}{\sqrt{\frac{H_o}{L_o}}} \tag{2.4}$$

Swash oscillations are a combination of low-frequency incident (0.05 Hz <f <0.2 Hz) and infragravity (f <0.05 Hz) motions. Gently sloping dissipative beaches are typically dominated by infragravity motion, while reflective beaches are dominated by incident wave motions. Including both of these frequencies in empirical run-up formulas has been shown to improve run-up parameterizations for intermediate and reflective beaches (Stockdon et al., 2006).

For this study, an empirical formula for 2% exceedance run-up height (R_2) derived by Stockdon et al. (2006) that incorporates both the incident and infragravity swash components was used to determine the highest 2% of predicted run-up heights associated with extreme SWL exceedance probabilities for modern still high water levels, SWL plus 18 cm, SWL plus 79 cm, and SWL plus 140 cm for each study beach:

$$R_2 = 1.1\left((0.35\beta\sqrt{H_o L_o}) + \frac{\sqrt{H_o L_o (0.563\beta^2 + 0.004)}}{2}\right) \tag{2.5}$$

For beaches with ξ_o<0.3, the infragravity component was removed and Equation 2.5 simplified to:

$$R_2 = 0.043\sqrt{H_o L_o} \tag{2.6}$$

This simplification has been shown to improve predictive capabilities of run-up on highly dissipative beaches (Ruggiero et al., 2001; Stockdon et al., 2006).

Site-specific deep-water significant wave heights and peak wave periods used to calculate wavelengths were determined from the NOAA National Buoy Data Center (NBDC) buoy data archives. H_o is the average deep-water significant wave height and T_p is the period is the average peak period calculated from five years (2006-2010) of hourly wave data from each buoy. Table 2.2 lists the study beaches, their respective buoy data sources, and significant wave height, wave period, and wavelength statistical parameters.

Table 2. 2: Study beach mean deep-water significant wave heights, mean wave periods, and mean wavelengths used in run-up calculations and the associated buoy sources

Study Beach	Buoy Source	Mean H_o (m)	Mean T_o (s)	Mean L_o (m)
Mission Beach San Diego	Mission Bay Stn. 46231	1.18	7.7	92.3
Huntington Beach	San Pedro Stn. 46222	1.00	6.7	70.7
Redondo Beach	Santa Monica Bay Stn. 46221	1.04	7.1	73.9
Santa Monica Beach	Santa Monica Bay Stn. 46221	1.04	7.1	73.9
Ventura Beach	East Santa Barbara Stn. 46053	1.26	6.1	57.9
Santa Barbara East Beach	East Santa Barbara Stn. 46053	1.26	6.1	57.9
Santa Cruz Main Beach	Monterey Stn. 46042	2.24	7.4	85.0
Ocean Beach San Francisco	Pt. Reyes Stn. 46214	2.55	7.8	96.0

For intermediate to reflective beaches, (ξ_o>0.3), ß is the average foreshore slope of the alongshore length of beach analyzed. To calculate this parameter, a series of equally spaced shore-normal transects were projected from a reference offshore baseline to the backshore perpendicular to the MHW shoreline using the Digital Shoreline Analysis System extension for ArcGIS (Thieler et al., 2009). Topographic beach profiles were extracted from each transect, and the average foreshore slope—the slope between the MHW shoreline and the berm crest—was calculated from the range of profiles.

2.4 Study Site Specifics and Results

2.4.1 Mission Beach, San Diego

Location, Oceanography, and Beach Morphology

Mission Beach is located on a 3-km long, north-south trending sand spit bounded to the north by Pacific Beach and to the south by a jetty at the entrance to Mission Bay. It is located in the Mission Beach subcell of the Mission Bay littoral cell, which extends from Scripps Canyon in the north to Point Loma in the south. The beach width relative to the 1997 lidar data of the 2.3-km stretch of Mission Beach analyzed in this study varies between about 60-75 m in the northern end to 45-50 m in the south, with an average foreshore slope of about 5 degrees.

Although early beach profile studies conducted by Bruun (1954) suggest that Mission Beach was a stable system with little natural sediment loss, the shoreline has been significantly impacted by episodic storm activity. During the 1982-83 El Niño, the Mission Beach MHW line retreated 30 m (100 ft) over a period of about seven months (Thompson, 1987). The dramatic beach changes that transpired over a period of months took several years to recover.

La Jolla tide gauge records from 1924-2006 indicate that the mean sea-level rise trend for the San Diego region has been 2.07 ± 0.29 mm/yr, which is equivalent to 0.21 m

(0.68 ft) of rise over a 100-year period. The highest observed still water level at Mission Beach occurred in November, 1997, and reached almost 1 m above MHW.

Back-Beach Development, Coastal Engineering Structures, and Nourishment History

Development on Mission Beach began in the early 1900s, and in the 1940s and 1950s, the Mission Bay area was one of the fastest growing regions in California. Today, Mission Beach is backed by a low concrete seawall with an average height of 4 m above mean sea level, which separates the back-beach from dense development, including an esplanade, hotels, houses and condominiums, an amusement park, and harbor facilities (Fig. 2.2). The seawall was overtopped by waves during the 1982-83 El Niño, as well as during a large storm in January, 1988 (Flick, 2005). The three rubble-mound jetties at the entrance to Mission Bay Harbor were constructed between 1950 and 1970. Beach nourishment of the region has occurred periodically since the 1940s due to Mission Bay harbor dredging and channel maintenance, resulting in a total of over 1.2 million m^3 of sand added to Mission Beach between 1948 and 2001 (CSMW Task 3**)**. The 2006 National Assessment of Shoreline Change study conducted by the U.S. Geological Survey (Hapke et al., 2006) found that Mission Beach just north of the Mission Bay jetty had the highest short-term (1970s-1998) erosion rate in the Mission Bay littoral cell at -3.6 m/yr.

Between 2000-2004, an average of 5.2 million beachgoers visited Mission Beach annually (Dwight et al., 2007). This attendance rate is nearly twice as high as any other beach in San Diego County. Beachgoers also spent over $133 million annually at Mission Beach, which is about 2% of the total annual spending at all California beaches combined (King and Symes, 2003).

Fig. 2.2: San Diego Mission Beach back-beach barrier (photo by E.L. Harden)

Water-level data and datum information for the Mission Beach study were obtained from the La Jolla tide gauge station (Station ID 9410230). This station was established in 1924, with the present installation existing since 1988. The mean and diurnal tidal ranges at the station are 1.12 m and 1.62 m, respectively.

Extreme Still High Water Levels

Currently, an extreme still high water level of approximately 58 cm above MHW (192 cm above NAVD88) occurs annually on Mission Beach, while the 100-year water level reaches a height of about 98 cm above MHW (Fig. 2.3). The average extreme still high water level over the 42-year station record is 78 cm above MHW. With an 18 cm rise in sea level, an extreme still high water level of 77 cm above MHW is expected to occur annually, with the 100-year event reaching a height of 1.18 m above MHW. For a 79 cm sea-level rise, the

predicted annual and 100-year recurrence interval extreme still high water levels increase to 138 cm above MHW and 178 cm above MHW, respectively. Finally, with a 140 cm rise in sea level, annual and 100-year recurrence interval still high water levels jump to 199 cm above MHW and 238 cm above MHW, respectively. The beach area that would be inundated annually with a 140 cm sea-level rise is 83%, which is 57% more than the area that would be inundated today from a 100-year extreme high water event (26%; Fig. 2.4). Figures 2.5, 2.6, 2.7, and 2.8 show annual probability of inundation maps for Mission Beach extreme still water levels under current, 18 cm, 79 cm, and 140 cm sea-level rise scenarios.

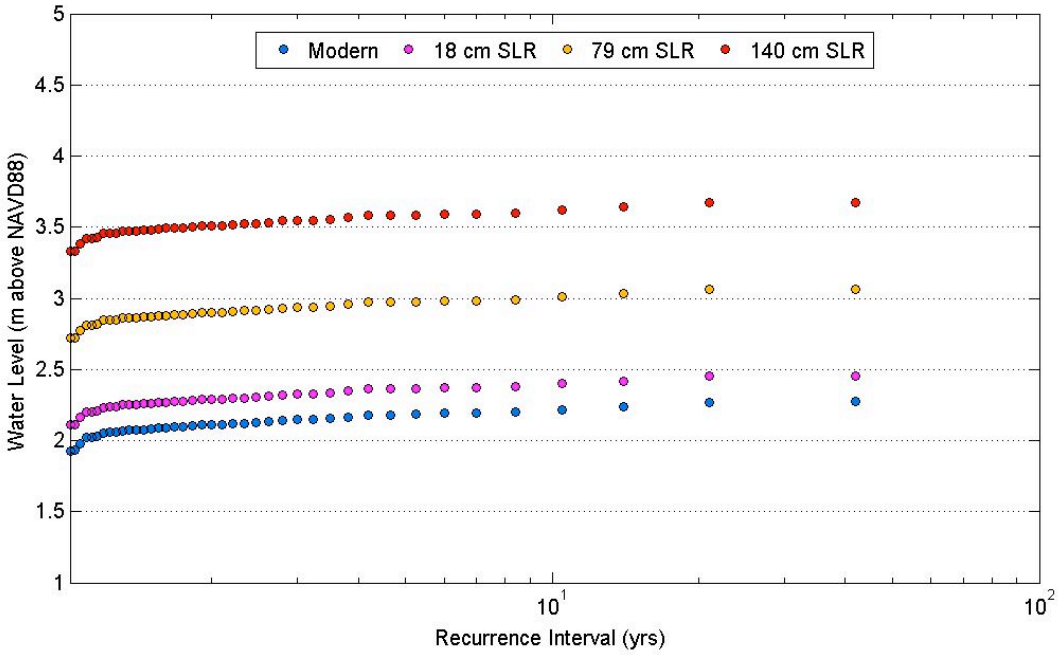

Fig. 2.3: Extreme still high water level vs. recurrence interval for San Diego Mission Beach for current, +18 cm, +79 cm, and + 140 cm sea level scenarios

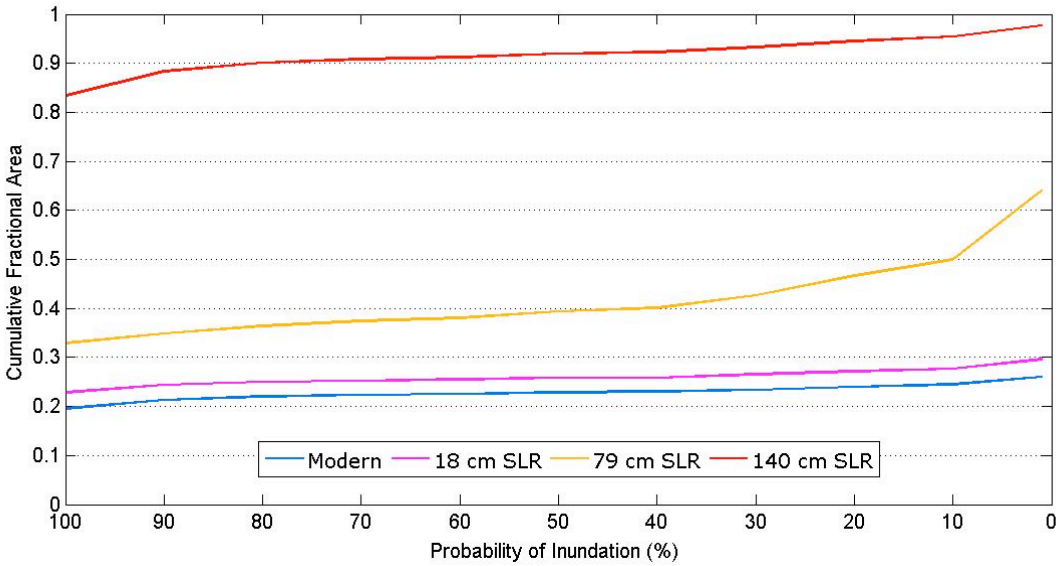

Fig. 2.4: Cumulative fractional beach area vs. probability of inundation for extreme still high water levels under current, +18 cm, + 79 cm, and + 140 cm sea level scenarios for San Diego Mission Beach

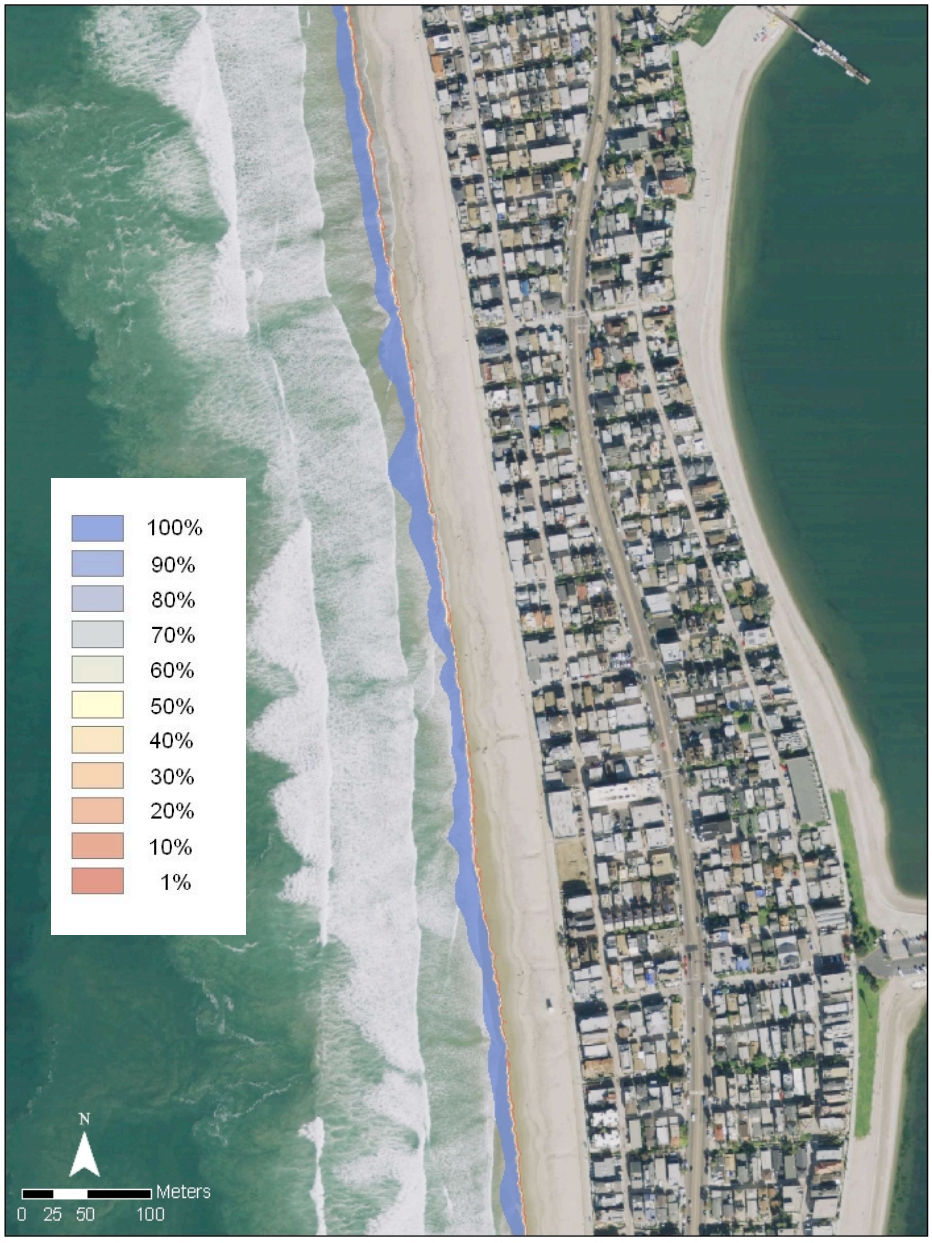

Fig. 2.5: Annual probability of inundation map for Mission Beach extreme still high water levels at current sea level

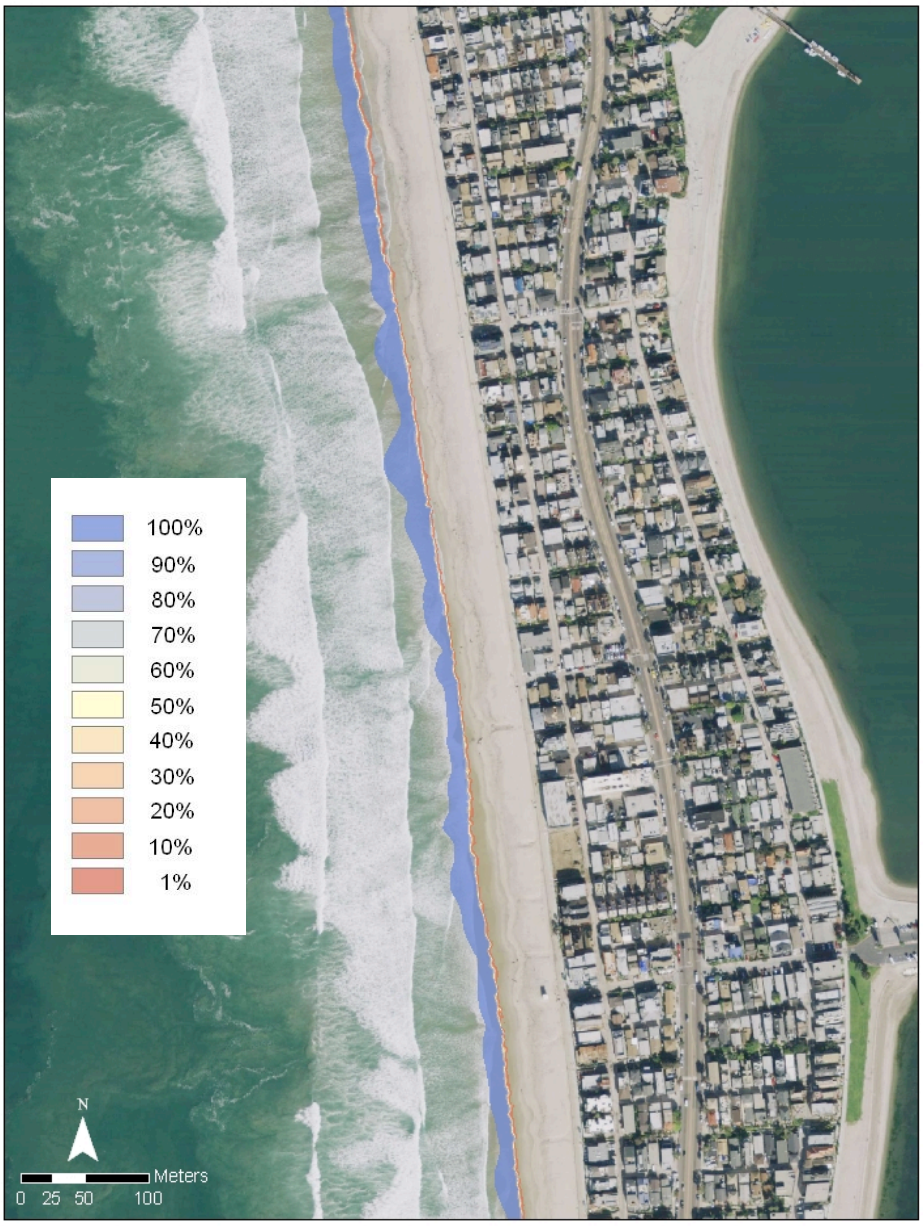

Fig. 2.6: Annual probability of inundation map for Mission Beach extreme still high water levels with 18 cm of sea-level rise

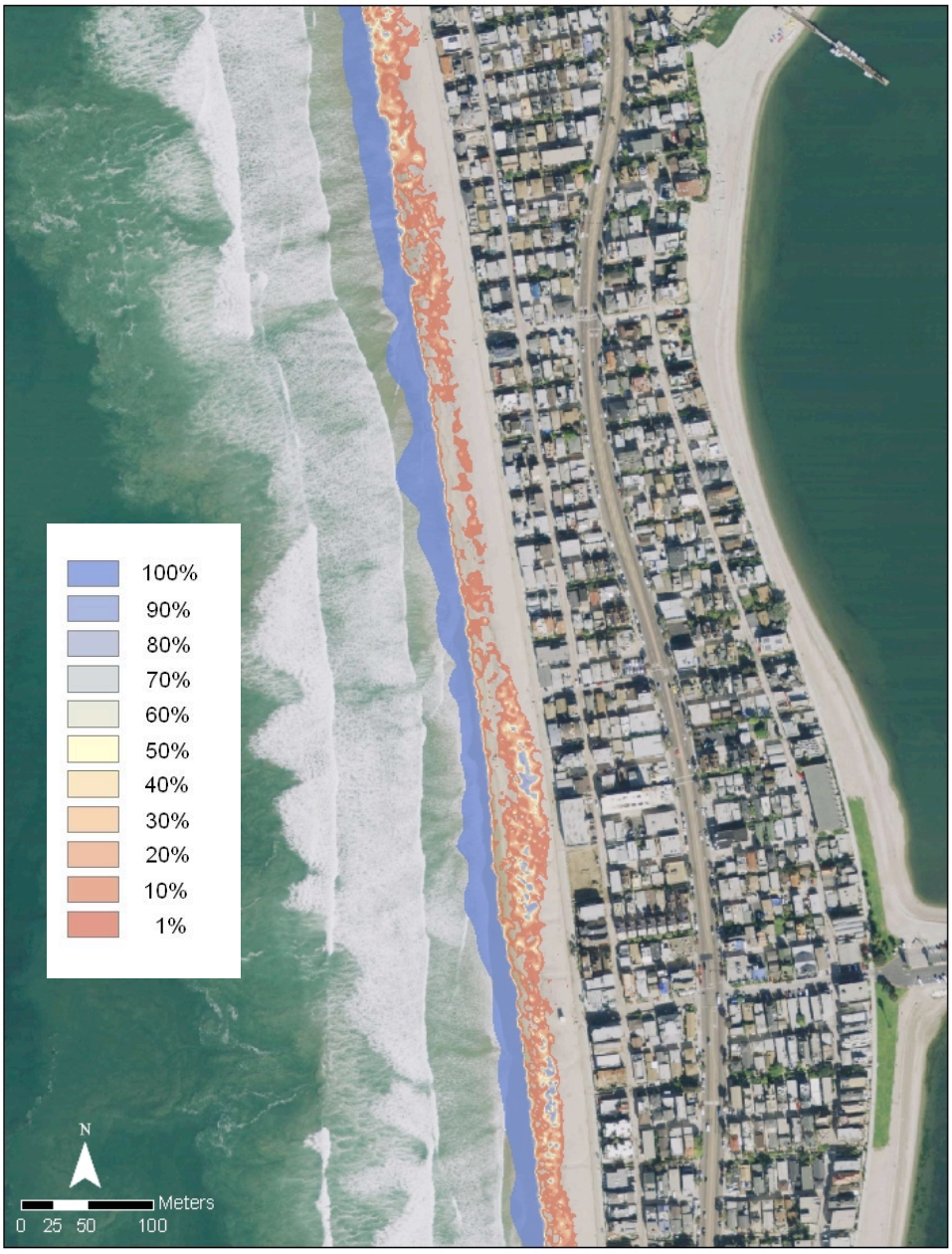

Fig. 2.7: Annual probability of inundation map for Mission Beach extreme still high water levels with 79 cm of sea-level rise

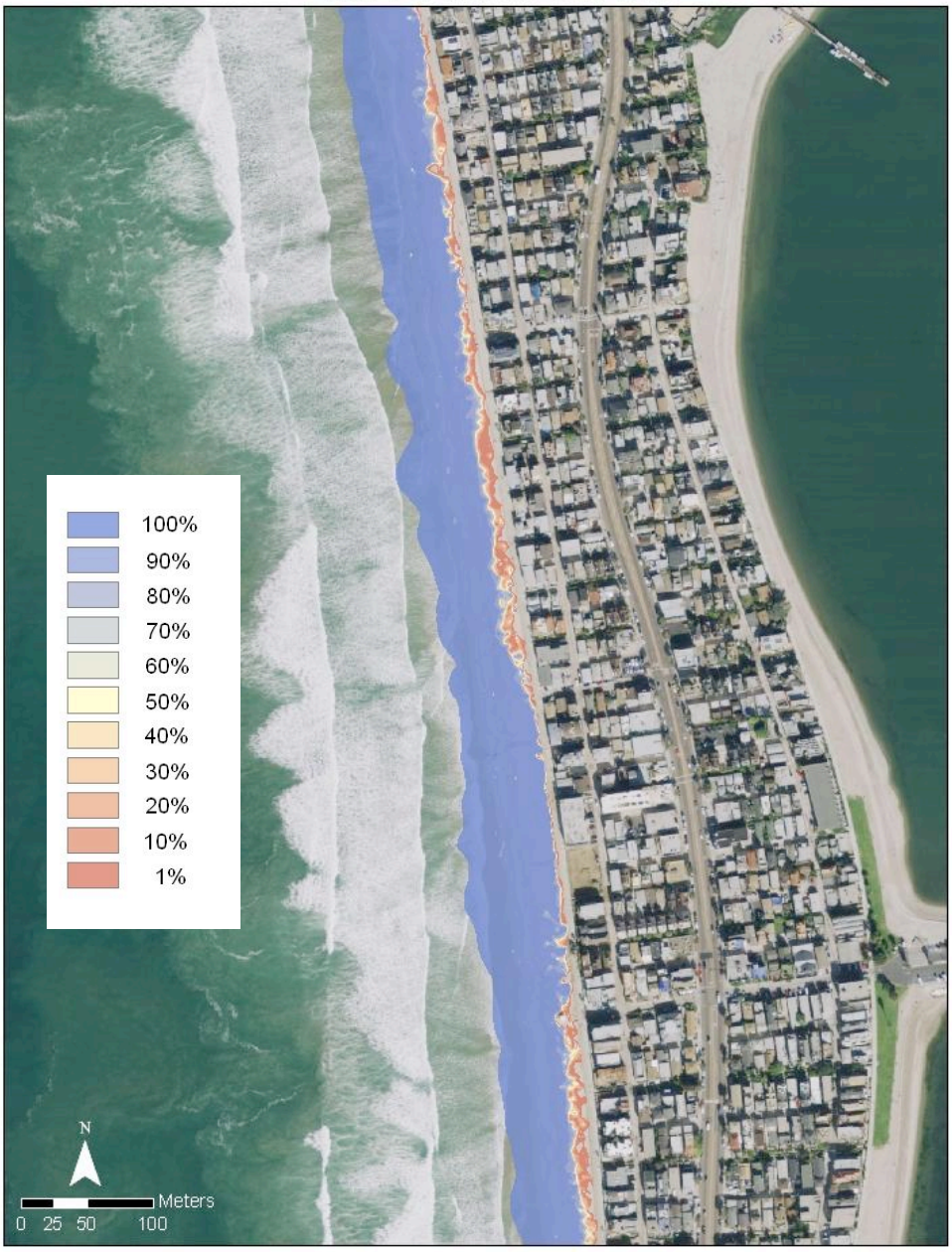

Fig. 2.8: Annual probability of inundation map for Mission Beach extreme still high water levels with 140 cm of sea-level rise

Extreme Still High Water Levels Plus Run-up

Average L_o and H_o from the Mission Bay deep-water buoy records were 92.3 m and 1.18 m, respectively, for Mission Beach, with an average foreshore beach slope (ß) of 0.05 and an Iribarren number of 0.44. The resulting value for the average 2% exceedance run-up on Mission Beach is 62 cm. This doubles the annual extreme high water event at current sea level, and with an 18 cm sea-level rise, the 100% exceedance level with run-up is equivalent to the 1% exceedance level at current sea level with no run-up, plus nearly half a meter. In the case of a 140 cm sea-level rise, the 2% exceedance run-up above the still water level would result in periodic inundation of 100% of the beach area occurring at least once annually, compared to inundation of 27% of the beach area that currently occurs annually (Fig. 2.9).

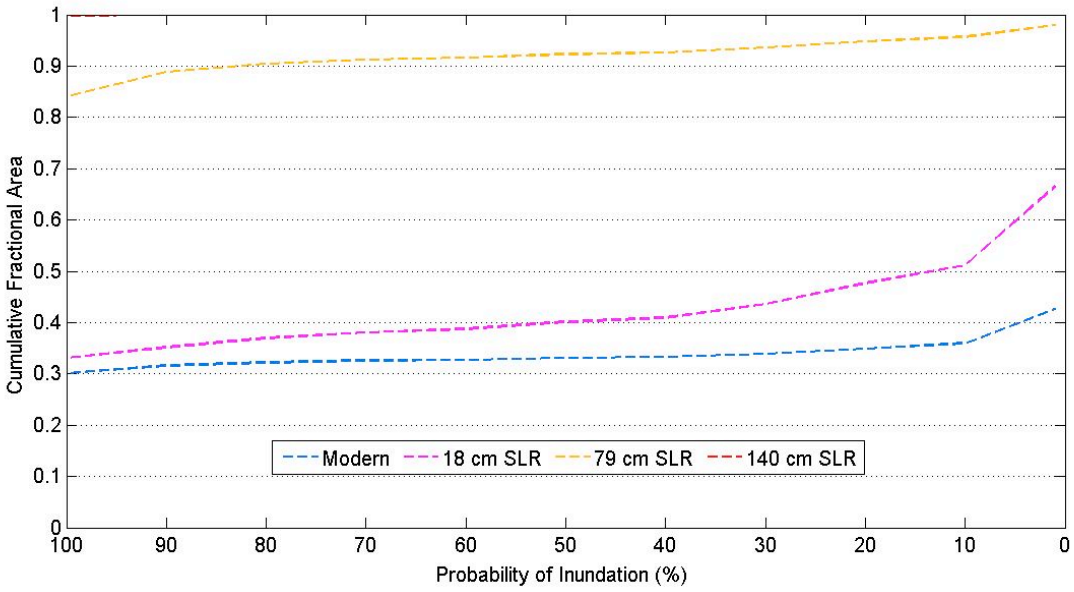

Fig. 2.9: Cumulative fractional beach area vs. annual probability of inundation for extreme high water levels plus run-up at current, + 18 cm, + 79 cm, and + 140 cm sea level scenarios for Mission Beach

2.4.2 Huntington Beach

Location, Oceanography, and Beach Morphology

The section of Huntington Beach analyzed in this study is a part of Huntington City Beach, an area maintained by the city as opposed to the conjoining beaches to the north and south (Bolsa Chica State Beach and Huntington State Beach), which are state parks. Together these beaches extend for more than 14 km along the San Pedro littoral cell coast, which extends south from Point Fermin to the Newport Submarine Canyon. Sand is supplied to Huntington Beach by the Santa Ana River, as well as from longshore transport of beach sediment from nourishment to the north.

The Huntington Beach shoreline is oriented northwest-southeast within the Southern California Bight. During the summer, Huntington Beach receives waves from the south-southwest, and because of its orientation, can experience large waves from tropical storms off the coast of Central America. Although swell from the northwest is most common, swells directly from the west or south can result in increased erosion and rip currents along the shoreline (Griggs et al., 2005).

Back-beach Development, Coastal Engineering Structures, and History

Huntington Beach beaches are generally wide due to the down coast transport of nourishment sediment; however, where the beach is narrow, bluff retreat threatens infrastructure and could potentially encroach on the Pacific Coast Highway, which runs along the bluff edge.

Dynamics of the San Pedro littoral cell have been influenced by river damming, which has resulted in a 66% annual reduction in natural sediment supply to the cell. Despite extensive nourishment to beaches within this cell, there has still been a significant net reduction in sediment supply of about 100,000 m^3/year (Slagel and Griggs, 2008). Another factor that has been connected to beach retreat from anthropogenic activity is ground

subsidence due to the withdrawal of oil from local fields between 1933 and 1964 (Flick, 1993), which was equated to over 5 million m^3 of sand lost from the beach.

Huntington Beach has also been the focus of various water quality and beach health studies (Grant et al., 2001; Boehm et al., 2002), as the Orange County Sanitation District wastewater outfall is located just seaward of the Huntington Beach surf zone. In 1998, Huntington Beach was the subject of an environmental damages lawsuit that resulted from a 1990 crude oil spill 1.5 miles off the coast by the steam tanker, the American Trader (Chapman and Hanemann, 2001). The American Trader oil spill highlighted the importance of beach and coastal recreation for Huntington Beach and the other Orange County beaches affected by the spill, as well as the difficulty in assigning a quantitative 'value' to beach recreational use. The lawsuit that followed several years after the incident included an economic analysis of the lost recreational use based on beach attendance rates and modeled rates for the period of beach closure (Chapman and Hanemann, 2001). The study conducted by Chapman and Hanemann was one of the first quantitative economic analyses of beach recreational 'value' done for the US West Coast. Despite the environmental concerns and challenges, Huntington Beach still rates highly among value assessments and attracts over 6.5 million beach visitors annually (Dwight et al, 2007).

Today, the Huntington City Beach back beach is developed with residential and commercial developments, as well as long parking lots and the Pacific Coast Highway (Fig 2.10). A low seawall protects much of this development from extreme wave events. Extensive wetlands exist behind much of Huntington State Beach. The Huntington Beach Pier, originally constructed in 1912 and rebuilt several times over the years due to repeated storm damage, is one of the longest piers on the west coast.

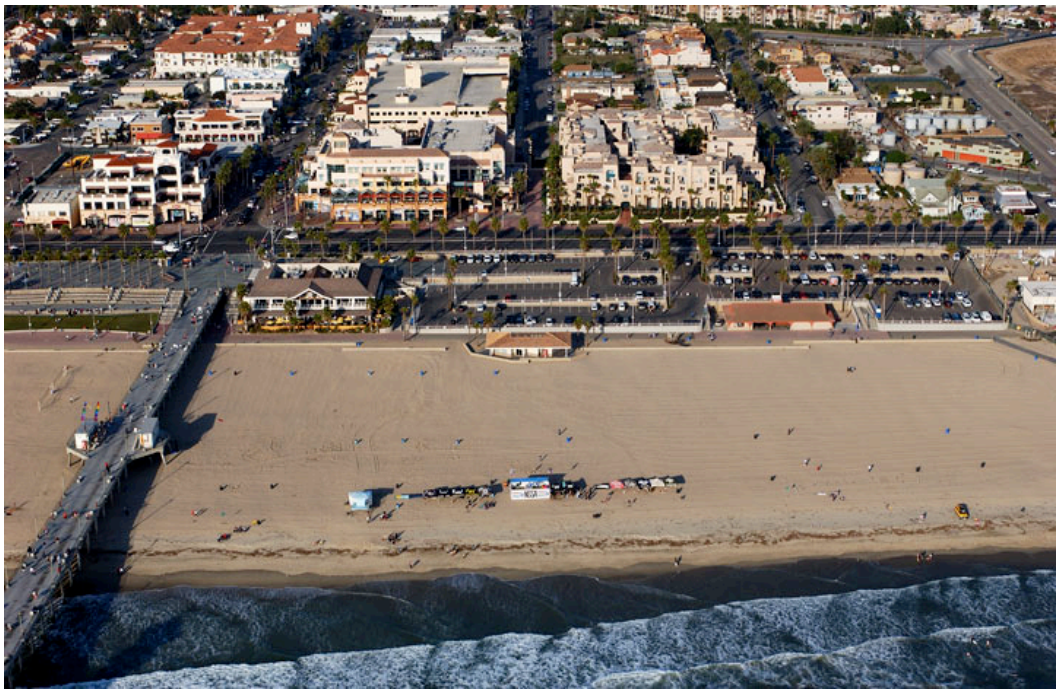

Fig. 2.10: Oblique aerial photograph of Huntington City Beach and the Huntington Beach Pier. Extensive parking lots flank the back beach, and the Pacific Coast Highway runs between the parking lots and landward dense development (photo by Kenneth and Gabrielle Adelman)

Water-level data and datum information for the Huntington Beach study were obtained from the Los Angeles Outer Harbor tide gauge station (Station ID 9410660). This station was established in 1923, with the present installation existing since 1990. The mean and diurnal tidal ranges at the station are 1.16 m and 1.67 m, respectively.

Extreme Still High Water Levels

Based on historic records, extreme still water levels at Huntington Beach currently annually reach or exceed 0.65 m above MHW and have a 1% chance annually of exceeding 1 m above MHW (Fig. 2.11). The average extreme still high water level from the period between 1970 and 2011 is 0.79 m above MHW. With an 18 cm sea-level rise, the 100% exceedance extreme still high water level increases 0.83 m above MHW, equivalent to a 28%

exceedance extreme still high water level today. A 100% exceedance extreme still water level with a 79 cm sea-level rise would be equivalent to a <1% exceedance level today, and with a 140 cm sea-level rise, the 100% exceedance value jumps to almost 170% of the current 100% exceedance level. This would mean that an extreme high water event that occurs once every 100 years at current sea level would not only occur annually with a 140 cm sea-level rise, but would annually exceed this level by at least 44%. A 1% exceedance level with a 140 cm sea-level rise would only inundate about 31% of the total beach area analyzed, while currently the 100% exceedance level inundates only about 7% of the total area (Fig. 2.12). With an 18 cm, 79 cm, and 140 cm sea-level rise, inundation due to the annual extreme still water event is only about 9%, 15%, and 22% of the total beach area, respectively (Figs. 2.13, 2.14, and 2.15).

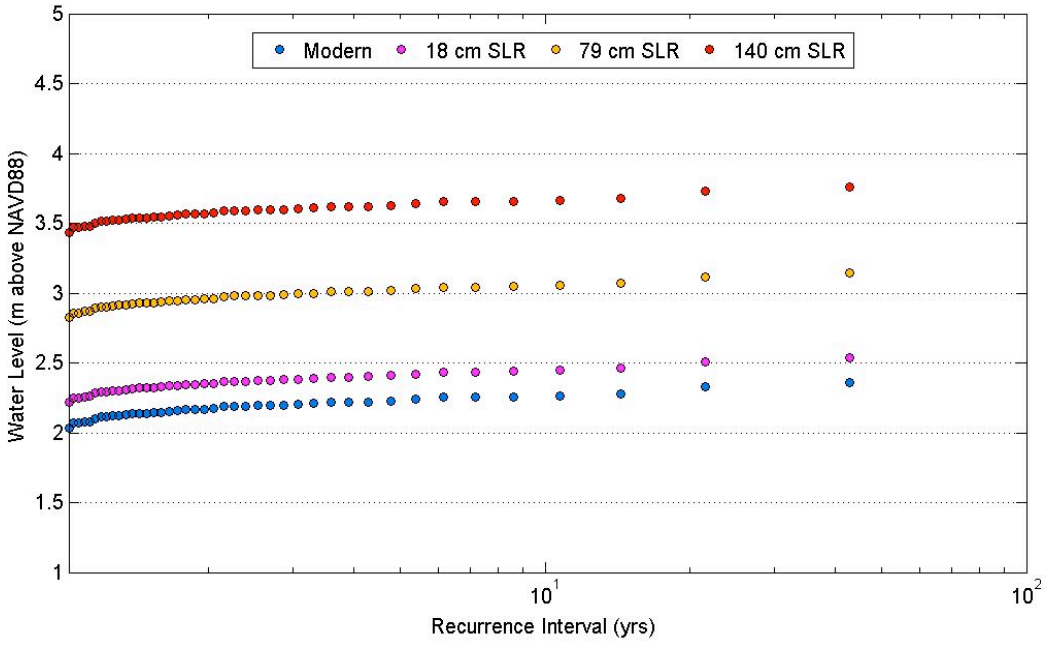

Fig. 2.11: Extreme still high water level vs. recurrence interval for Huntington Beach for current, + 18 cm, + 79 cm, and + 140 cm sea level scenarios

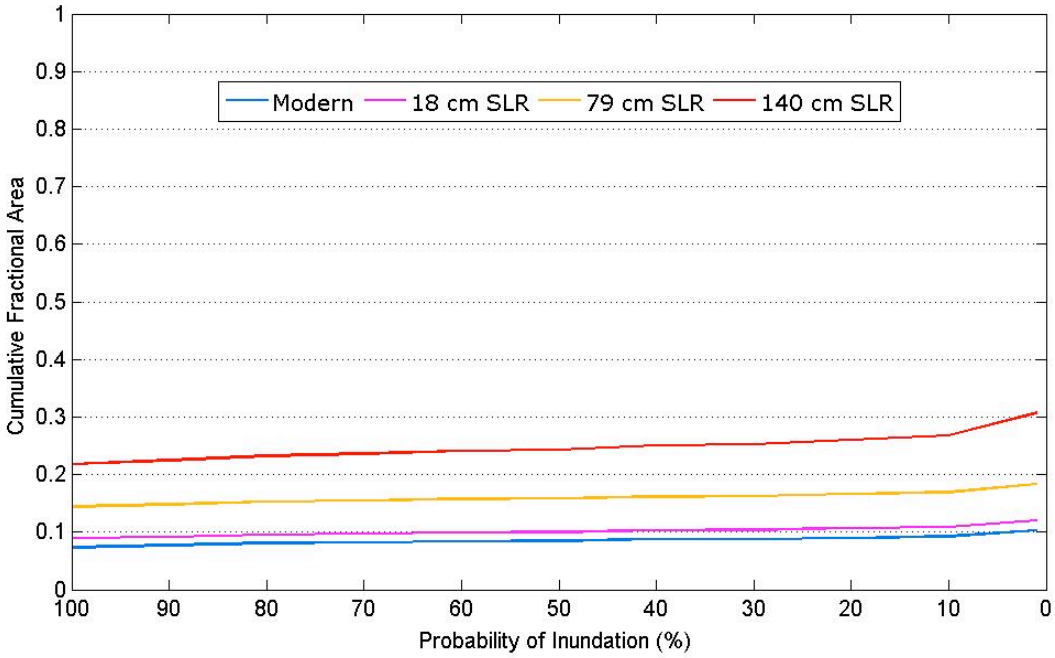

Fig. 2.12: Cumulative fractional beach area vs. probability of inundation for extreme still high water levels under current, +18 cm, + 79 cm, and + 140 cm sea level scenarios for Huntington Beach

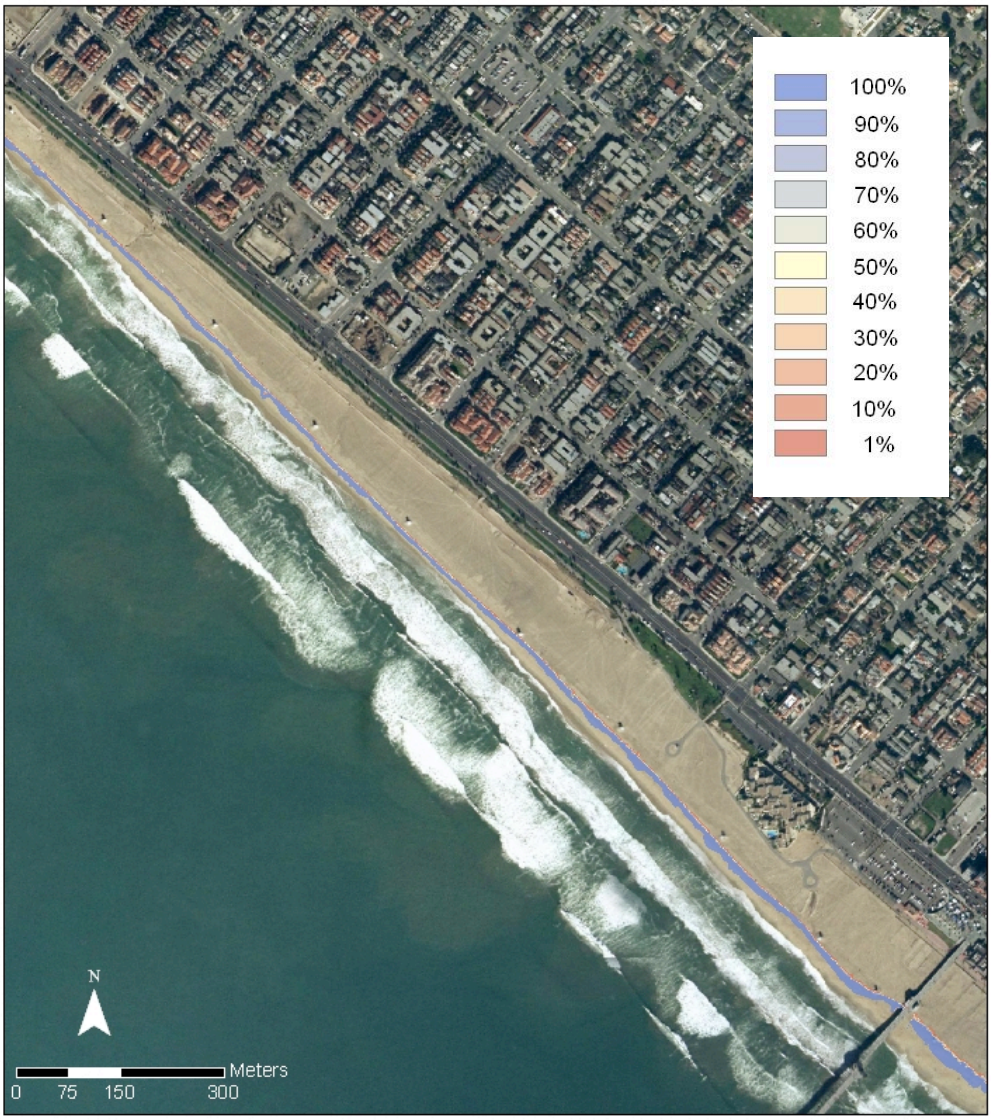

Fig. 2.13: Annual probability of inundation map for Huntington Beach extreme still high water levels with an 18 cm sea-level rise

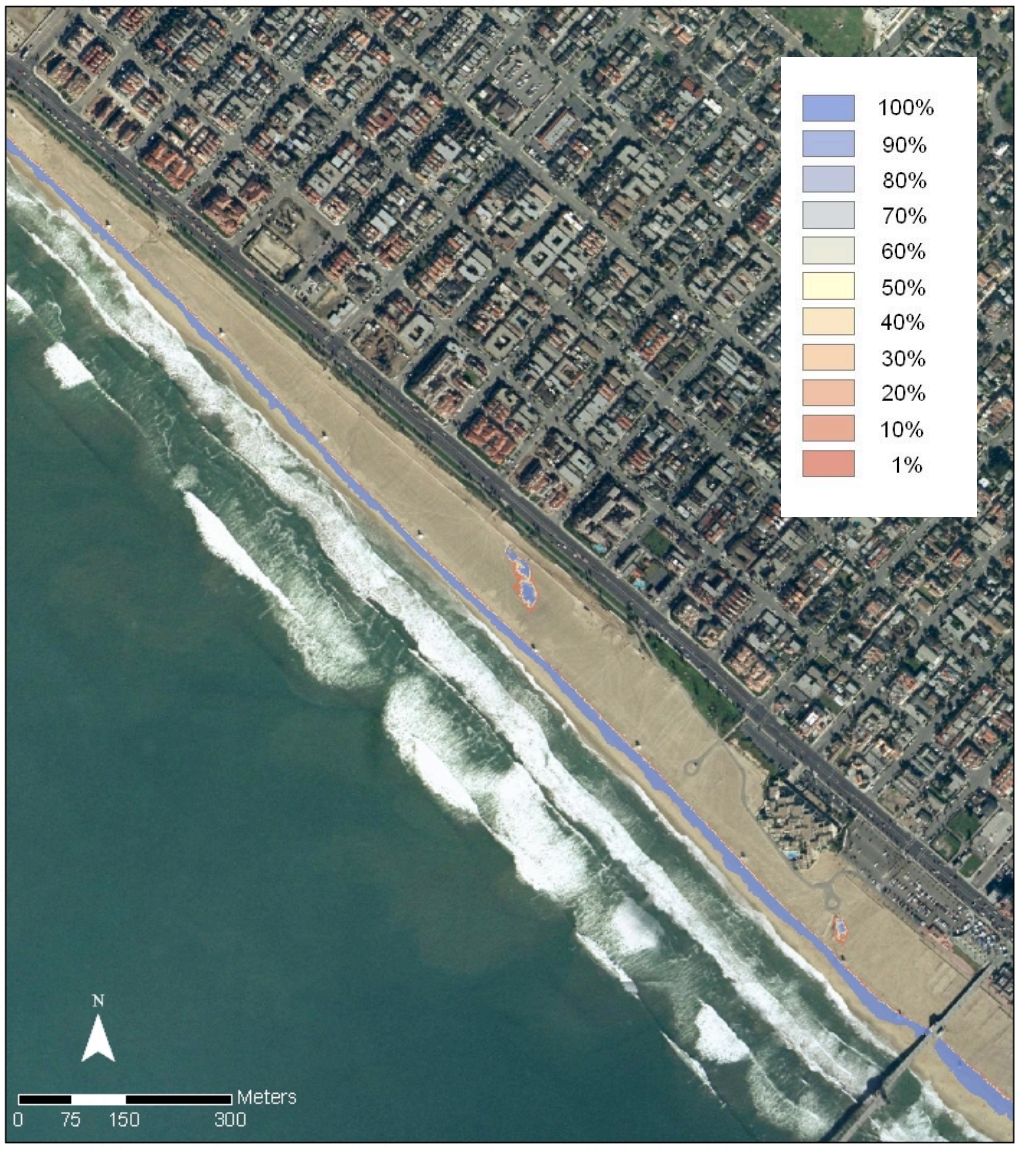

Fig. 2.14: Annual probability of inundation map for Huntington Beach extreme still high water levels with a 79 cm sea-level rise

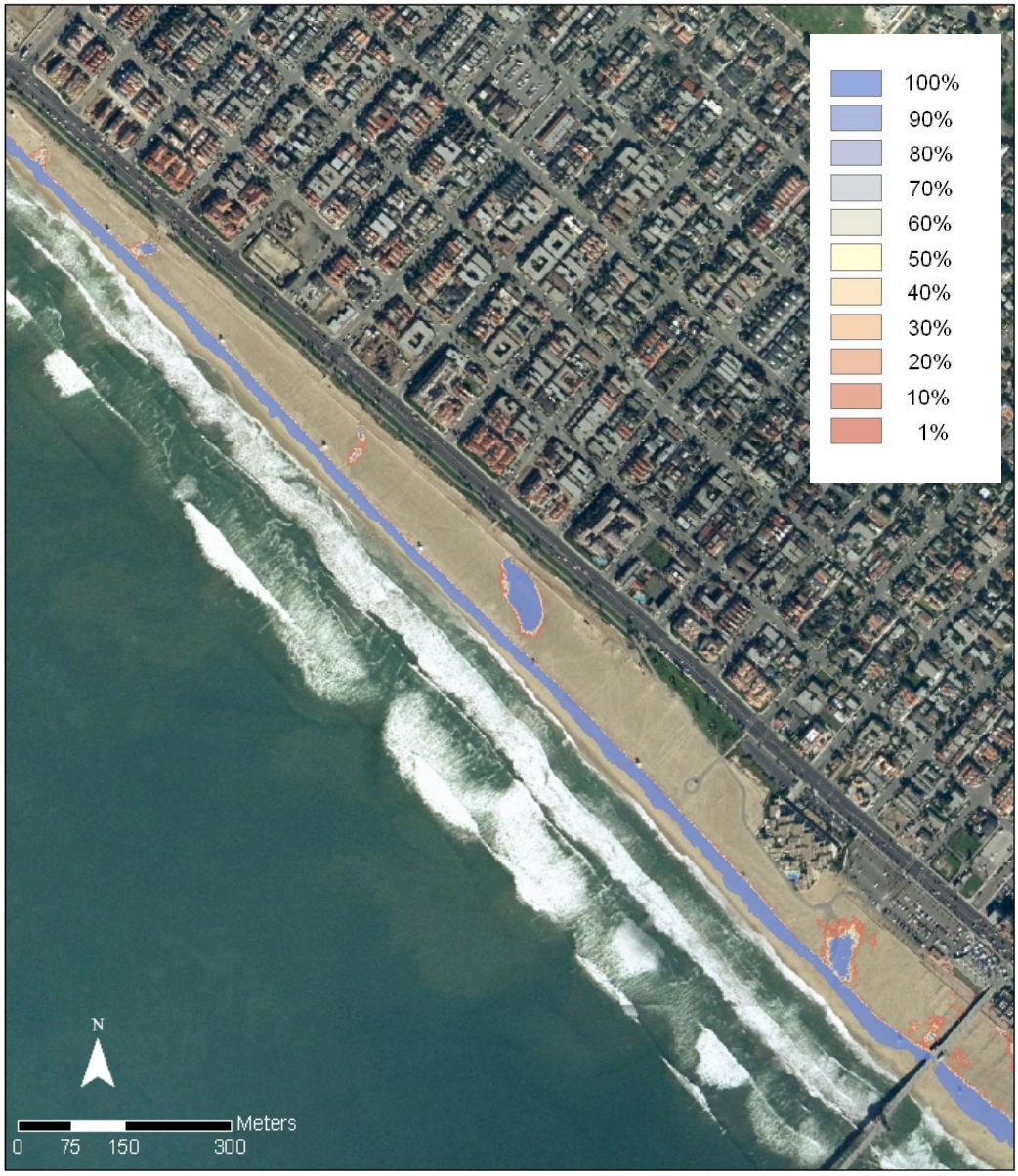

Fig. 2.15: Annual probability of inundation map for Huntington Beach extreme still high water levels with a 140 cm sea-level rise

Extreme Still High Water Levels Plus Run-up

Average L_o and H_o from the San Pedro deep-water wave buoy records 70.7 m and 1.00 m, respectively, with an average foreshore beach slope (ß) of 0.1 and an Iribarren number of 0.83. The resulting 2% exceedance run-up height is 0.77 m. This translates into a 1.60 m above MHW 100% exceedance extreme high water level with run-up at current sea level, and a 2.81 m above MHW 100% exceedance level with run-up with a 140 cm sea-level rise. At the 1% exceedance level, the current extreme still high water elevation jumps to 1.77 m above MHW and the extreme still water level with run-up and a 140 cm sea-level rise jumps to 3.17 m above MHW. This results in a doubling of the cumulative beach area that would be inundated by a 100% exceedance extreme high water level by an extreme high water level + run-up compared to the still water level results alone for both the current sea level (7% to 14% inundation) and with a 140 cm sea-level rise (22% to 48% inundation; Fig. 2.16). At the 1% exceedance level with run-up, 63% of the beach would be inundated.

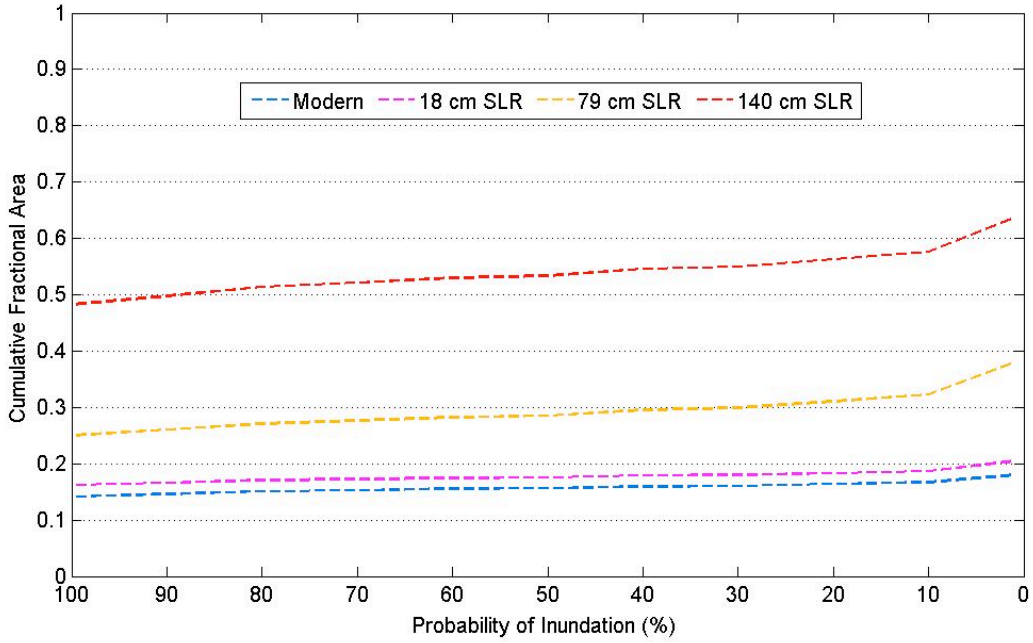

Fig. 2.16: Cumulative fractional beach area vs. annual probability of inundation for extreme high water levels plus run-up at current, + 18 cm, + 79 cm, and + 140 cm sea level scenarios for Huntington Beach

2.4.3 Redondo Beach

Location, Oceanography, and Beach Morphology

Redondo Beach in Los Angeles County is located at the southeastern end of Santa Monica Bay between Torrance Beach and the Palos Verdes Peninsula in the south and the Redondo Submarine Canyon to the north. Average littoral drift rates are about 23,000 m^3 per year (Griggs et al., 2005), with transport predominantly to the southeast. Offshore of Redondo Beach, the continental shelf is quite narrow. Before the late 1800s, low sand hills, which were part of a larger 13-km long dune field extending north along the Santa Monica Bay, characterized the backshore region of Redondo Beach. The once extensive sand hills have been heavily urbanized in the last century, anchoring sand that probably once supplied the beaches or was swept offshore during storm or high wave events.

Back-beach Development, Coastal Engineering Structures, and Nourishment History

Redondo Beach was subject to widespread unchecked urban development from the late 1800s until the California Coastal Act was passed in 1976. As a result, the modern back beach north of King Harbor is highly developed with commercial and residential infrastructure, low seawalls, a bike path, harbor facilities, and roadways. Where the beach is not directly backed by man-made infrastructure, mainly south of the harbor, it is bounded by medium-to-high sloping bluffs armored in areas by low and mid-bluff walls.

King Harbor is a man-made harbor that was built in 1956 and is protected by a rubble-mound breakwater. The breakwater had significant impacts on Redondo Beach State Park to the south, including sediment starvation and ultimately beach narrowing. Nourishment activity began for beach restoration and erosion control purposes in the early 1940s, and in the late 1960s and early 1970s, a 2-km long stretch of Redondo Beach was widened to an average width of 68 m (Fischer and Arredondo, 1999). The nearly 5-km long stretch of beach south of the harbor is divided by the Topaz Street groin, which has contributed significantly to the retention of sand on the beach to the south (Fig. 2.17; Wiegel, 2002).

Redondo Beach has one of the highest coastal population densities in Southern California, at almost 3,400 people per coastal km, and hosts an average of 2.4 million beachgoers annually (Fischer and Arredondo, 1999; Dwight et al., 2007).

Fig. 2.17: Aerial photo of the Redondo Beach Topaz Street groin and back-beach development (photo by Kenneth and Gabrielle Adelman)

Water-level data and datum information for the Redondo Beach study were obtained from the Santa Monica tide gauge station (Station ID 9410840). This station was established in 1932 with the present installation existing since 1992. The mean and diurnal tidal ranges at the station are 1.15 m and 1.66 m, respectively. A 2.3 km long stretch of Redondo Beach was analyzed in this study, with an average width of about 61 m and a range of about 25-90 m.

Extreme Still High Water Levels

At current sea level, the annual extreme still high water level at Redondo Beach is equal to or greater than 2.02 m above NAVD88 (0.65 m above MHW). With an 18 cm, 79 cm, and 140 cm sea-level rise, this number increases to 2.20 m above NAVD88 (0.83 m above MHW), 2.81 m above NAVD88 (1.44 m above MHW), respectively, which equate to an

average cross-shore MHW shoreline migration during these extreme events of 10 m, 13 m, and 18 m, respectively (Fig. 2.18). With a 1% exceedance extreme still high water level, these numbers increase to 12 m, 17 m, and 23 m of shoreline migration. However, an extreme still high water level at the 1% exceedance level and with a 140 cm sea-level rise is only projected to inundate about 36% of the beach, with the current annual extreme still high water level inundating only about 12% of the beach (Fig. 2.19, 2.20). With an 18 cm, 79 cm, and 140 cm sea-level rise, inundation due to the annual extreme still water event affects about 15%, 23%, and 30% of the total beach area, respectively (Figures 2.21, 2.22, 2.23).

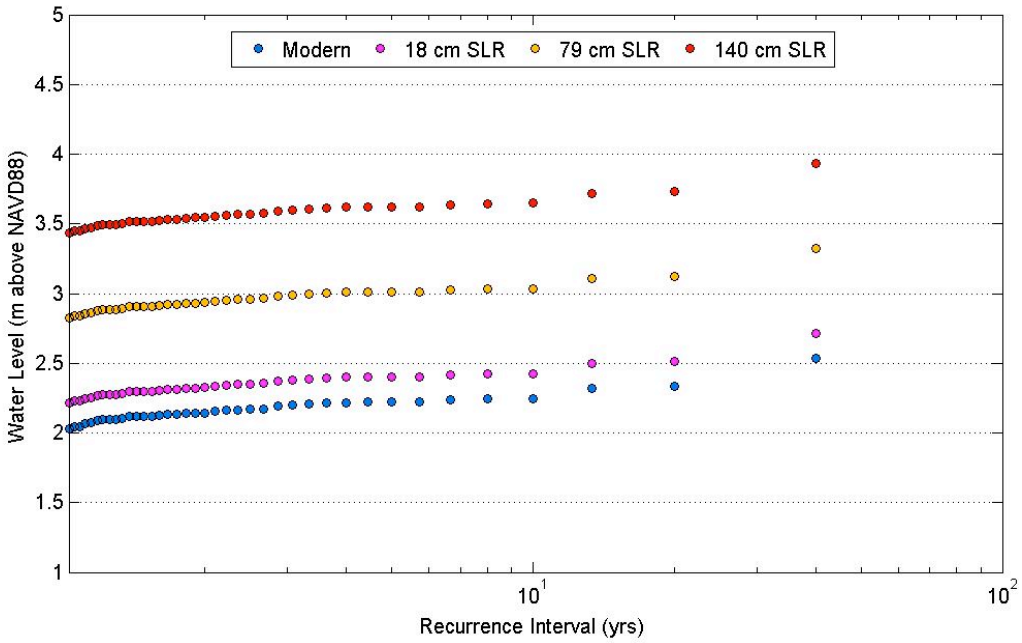

Fig. 2.18: Extreme still high water level vs. recurrence interval for Redondo Beach for current, + 18 cm, + 79 cm, and + 140 cm sea level scenarios

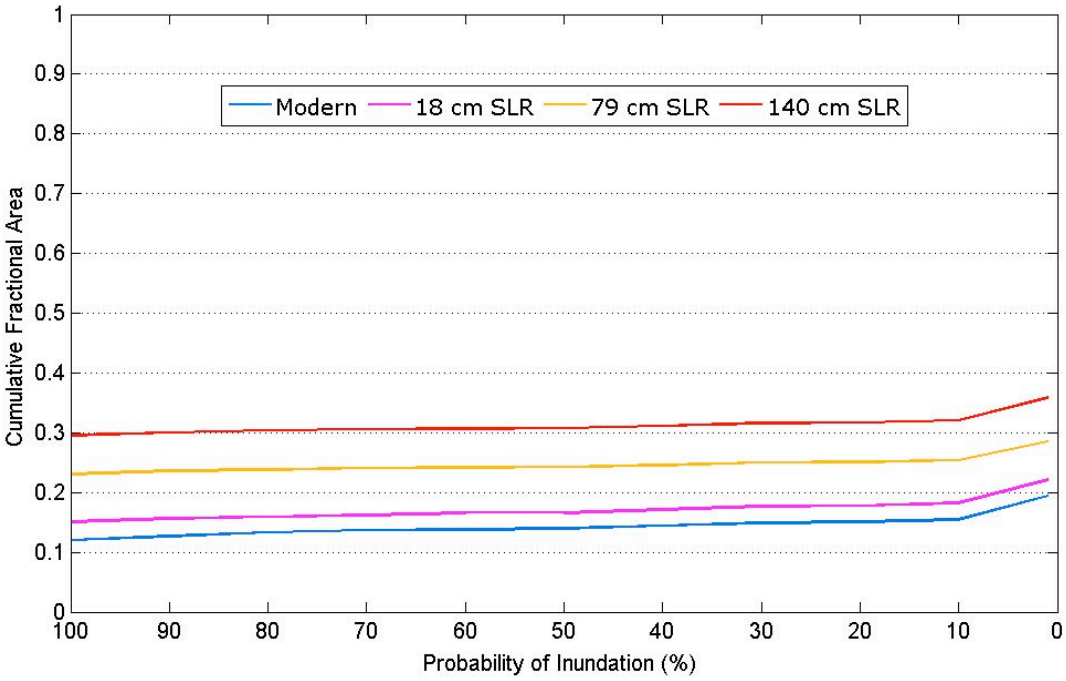

Fig. 2.19: Cumulative fractional beach area vs. probability of inundation for extreme still high water levels under current, +18 cm, + 79 cm, and + 140 cm sea level scenarios for Redondo Beach

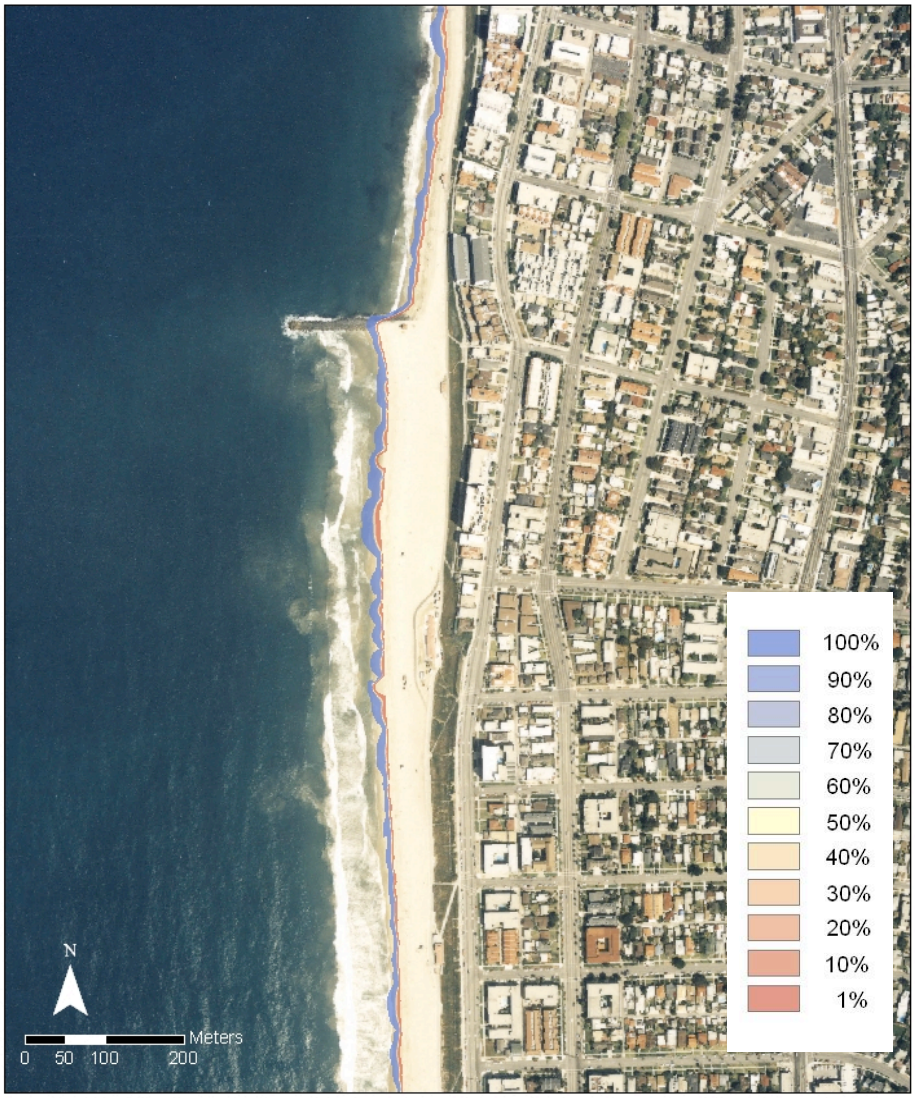

Fig. 2.20: Annual probability of inundation map for Redondo Beach extreme still high water levels for current sea level

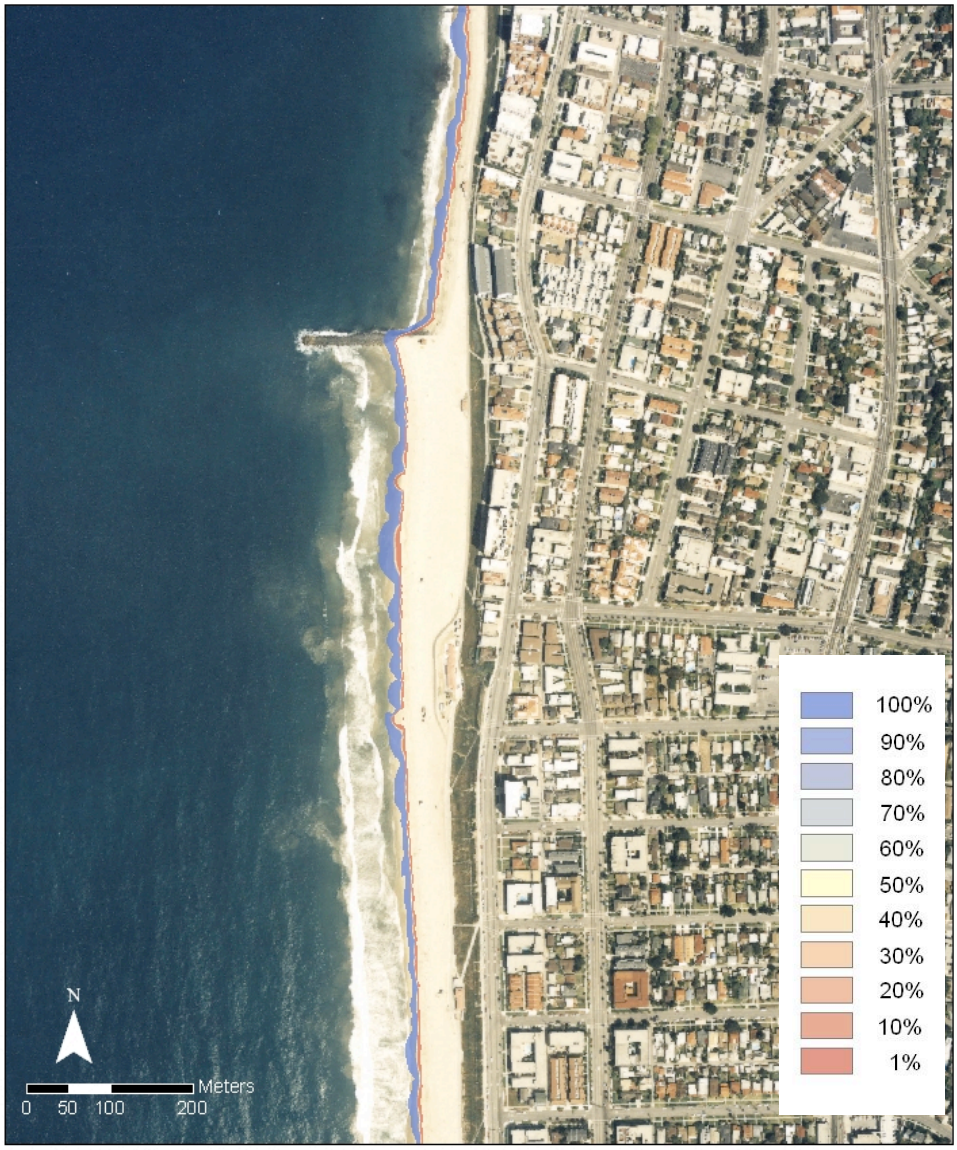

Fig. 2.21: Annual probability of inundation map for Redondo Beach extreme still high water levels with an 18 cm sea-level rise

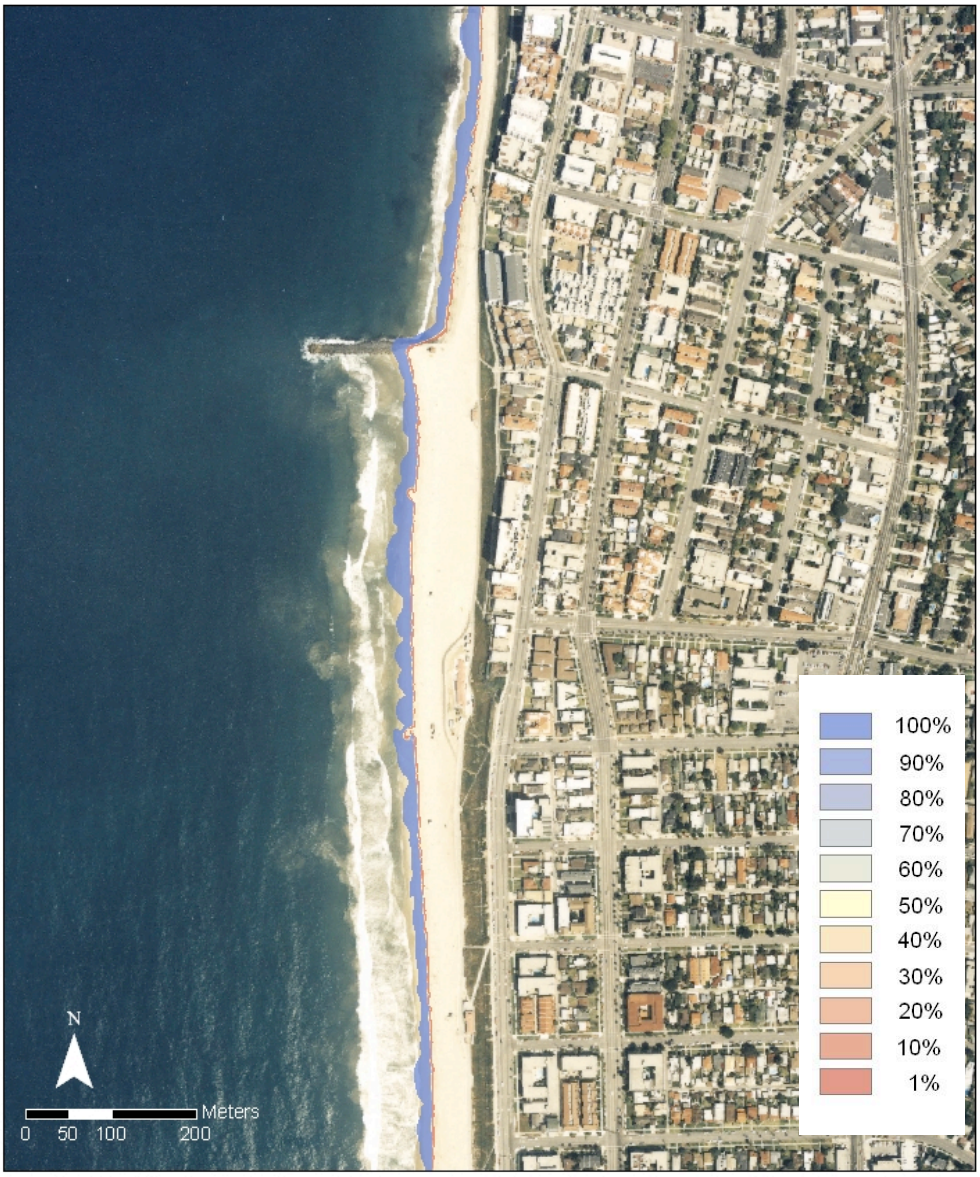

Fig. 2.22: Annual probability of inundation map for Redondo Beach extreme still high water levels with a 79 cm sea-level rise

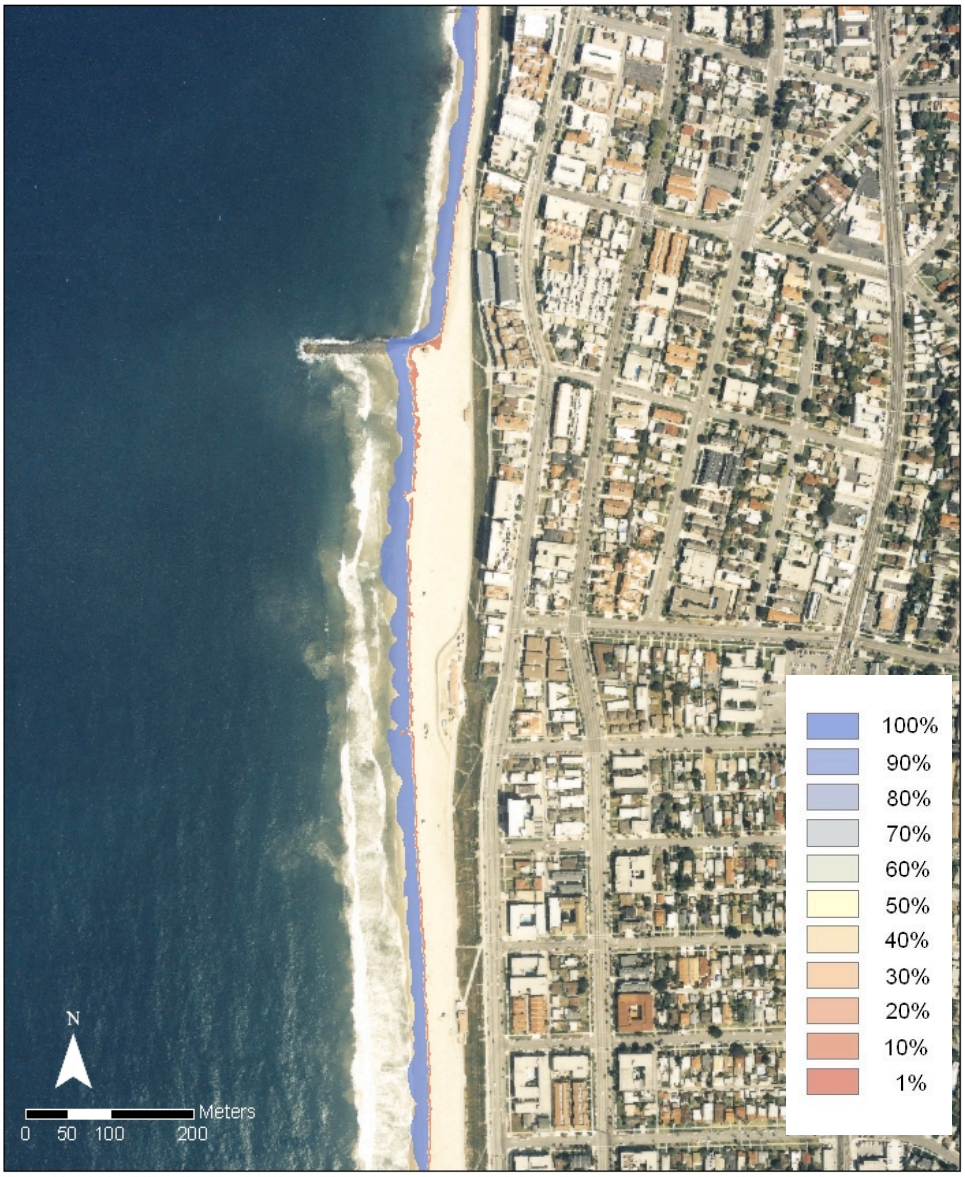

Fig. 2.23: Annual probability of inundation map for Redondo Beach extreme still high water levels with a 140 cm sea-level rise

Extreme Still High Water Levels Plus Run-up

Average L_o and H_o from the Santa Monica Bay deep-water wave buoy records are 73.9 m and 1.04 m, respectively, with an average foreshore beach slope (ß) of 0.09 and an Iribarren number of 0.75. This results in a 2% exceedance run-up elevation of 0.74 m. This addition of run-up increases the extent of the beach area periodically inundated during annually occurring extreme high water events by ~10% for all sea level scenarios. The 1% exceedance inundation extents also increase by about 10% for current, +18 cm, and + 79 cm sea levels with the inclusion of run-up, but for a 140 cm sea-level rise the 1% exceedance extent increases from 36% to 72% of the total beach area analyzed (Fig. 2.24).

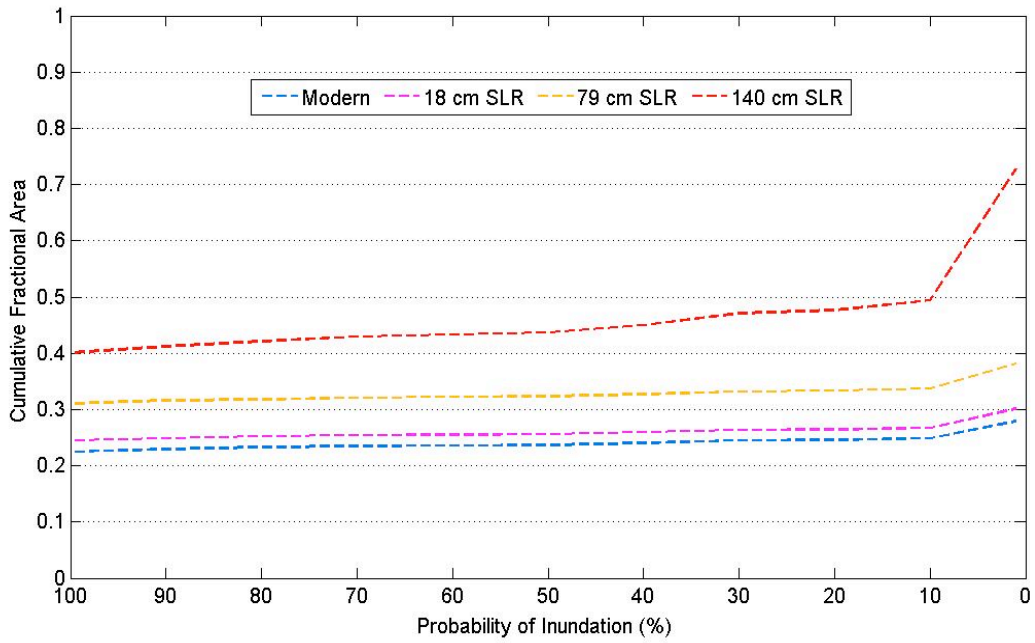

Fig. 2.24: Cumulative fractional beach area vs. annual probability of inundation for extreme high water levels plus run-up at current, + 18 cm, + 79 cm, and + 140 cm sea level scenarios for Redondo Beach

2.4.4 Santa Monica

Back-beach Development, Coastal Engineering Structures, and Nourishment History

Santa Monica is located in the Santa Monica Bay north of Venice Beach and Marina Del Rey. The beaches are generally wide and flat due to extensive nourishment and sand retention efforts. In their natural state, the beaches of Santa Monica were much narrower (Flick, 1993; Clayton, 1991). River damming in the Santa Monica littoral cell has resulted in a 30% decrease in the natural sediment normally supplied by these rivers (Patsch and Griggs, 2006).

The Los Angeles County coastline is extensively developed and engineered. The narrow Santa Monica beaches of the early 1900s have been significantly widened by beach nourishment activities that began in the 1930s (Clayton, 1991; Hapke et al., 2006). In 1947-1948, 11 km of Santa Monica Bay beaches were nourished with 10 million m^3 of sediment, which widened the beaches to an average width of 180-250 m. Over twice this amount of sand total has been added to beaches in the Santa Monica littoral cell since 1938. In general, Santa Monica natural beach widths increased by 45-150 m due to nourishment that occurred mainly before the 1970s (Patsch and Griggs, 2006). Although nourishment activities have decreased since then, the wide, stable Santa Monica beaches observed today are maintained by sand retention structures and are primarily artificial.

Dense development, including hotels, condos, and other infrastructure, parking lots, pedestrian and bike paths, and coastal armoring structures such as a low seawall and revetment forms the majority of the back beach in Santa Monica. Where artificial nourishment hasn't modified the back beach morphology, construction and development have leveled it. It is not uncommon to see large parking lots, hotels, and even recreational facilities such as skate parks, basketball courts, and open-air gyms built out onto the beach (Fig. 2.25), resulting in extreme placement loss of the beach in several areas.

Fig. 2.25: Aerial photo of the Santa Monica parking lot directly adjacent to the Santa Monica pier (photo by Kenneth and Gabrielle Adelman)

Water-level data and datum information for the Santa Monica Beach study were obtained from the Santa Monica tide gauge station (Station ID 9410840). This station was established in 1932 with the present installation existing since 1992. The mean and diurnal tidal ranges at the station are 1.15 m and 1.66 m, respectively.

Extreme Still High Water Levels

Since the same tide gauge data was used for the Santa Monica analysis as for Redondo Beach, the Santa Monica extreme still water level recurrence interval results are identical to the Redondo Beach results; however, what these results mean for shoreline migration and beach inundation are site-specific. At Santa Monica Beach, current 100% exceedance extreme still high water levels result in an average of only about 6 m of landward shoreline migration, while with a 140 cm sea-level rise, the 100% exceedance level results in about 30 m of landward shoreline migration, equivalent to inundation of about 7% and 23% of

the total analyzed beach area, respectively (Figs. 2.26, 2.27). At the 1% exceedance level for a 140 cm sea-level rise, approximately 51% of the total beach area analyzed would be inundated.

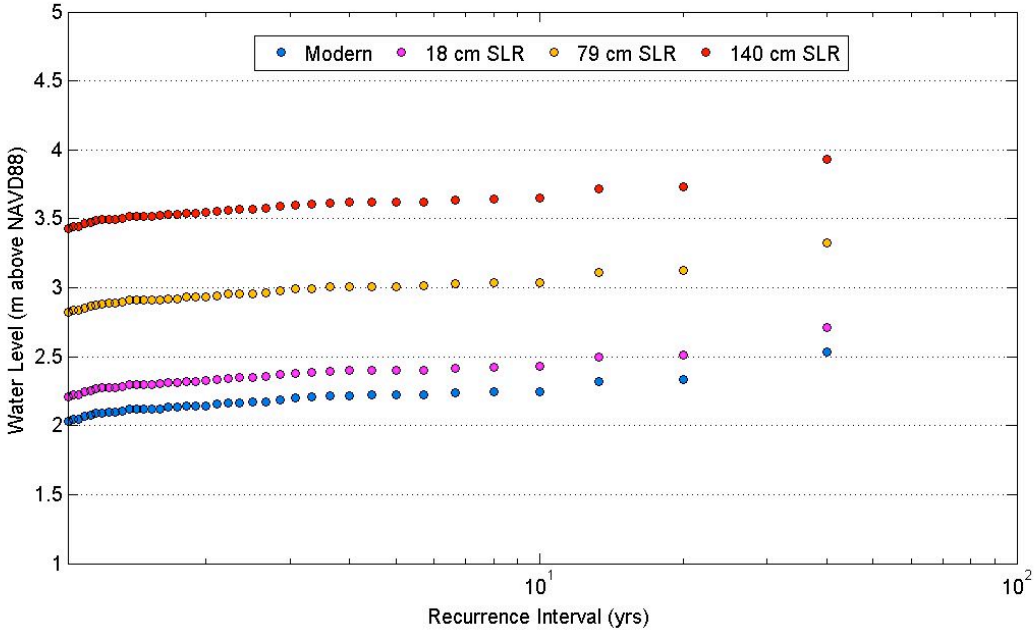

Fig. 2.26: Extreme still high water level vs. recurrence interval for Santa Monica Beach for current, + 18 cm, + 79 cm, and + 140 cm sea level scenarios

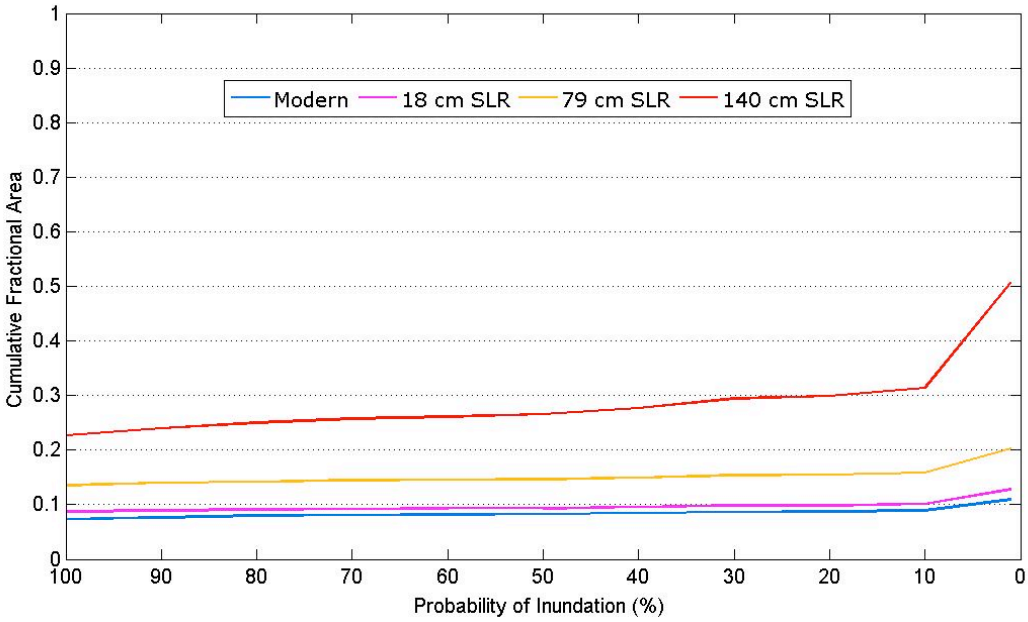

Fig. 2.27: Cumulative fractional beach area vs. probability of inundation for extreme still high water levels under current, +18 cm, + 79 cm, and + 140 cm sea level scenarios for Santa Monica Beach

Extreme Still High Water Levels Plus Run-up

Average L_o and H_o from the Santa Monica Bay deep-water wave buoy records are 73.9 m and 1.04 m, respectively, with an average foreshore beach slope (ß) of 0.06 and an Iribarren number of 0.48. This results in a 2% exceedance run-up elevation of 0.56 m, and thus increases the current 100% exceedance extreme high water level from a still water level of 0.66 m above MHW to 1.22 m above MHW with run-up, and the 100% exceedance with a 140 cm sea-level rise from 2.06 m above MHW to 2.62 m above MHW. When run-up is included, the 100% exceedance beach inundation increases from 23% of the total beach area analyzed to 53% with a 140 cm sea-level rise, and for a 1% exceedance, these numbers rise from 51% to 76% of the total beach area analyzed (Fig. 2.28).

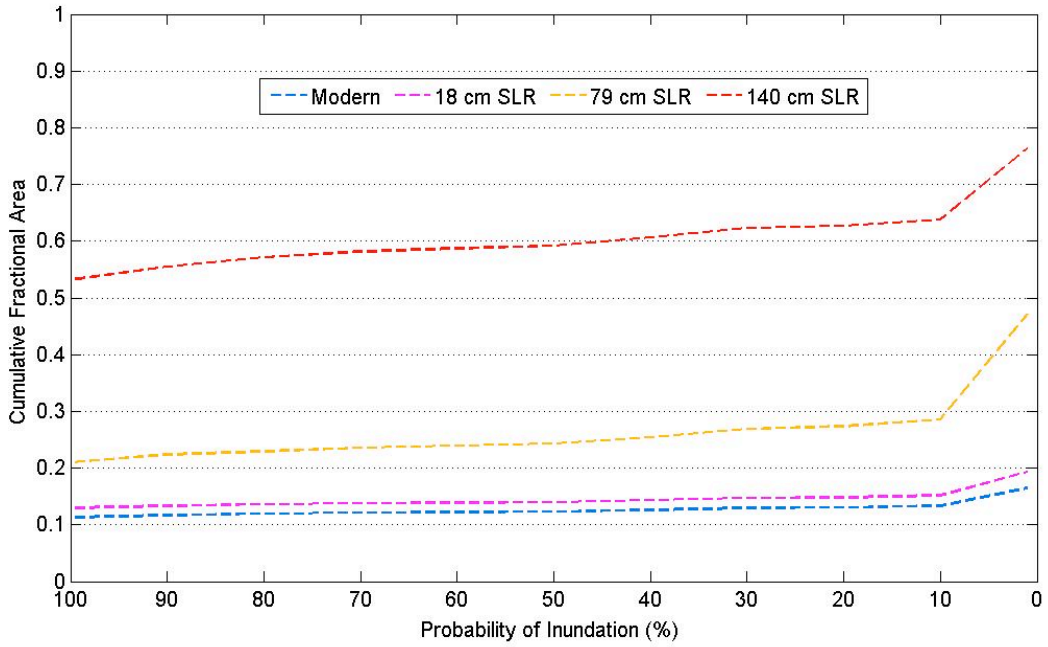

Fig. 2.28: Cumulative fractional beach area vs. annual probability of inundation for extreme high water levels plus run-up at current, + 18 cm, + 79 cm, and + 140 cm sea level scenarios for Santa Monica Beach

2.4.5 Ventura Beach

Location, Oceanography, and Beach Morphology

Ventura Beach is located south of Point Conception in Pierpoint Bay. It is also part of the Santa Barbara littoral cell, and littoral drift is predominantly to the southeast. The average annual littoral drift rate at Ventura based on harbor dredging records is between 450,000-750,000 m^3/year, which is over twice as high as littoral drift rates at Santa Cruz or Santa Barbara, and more than 20 times as high as the rate at Redondo Beach (Griggs et al., 2005). The groin field at San Buenaventura State Beach gives the shoreline a characteristic notched plan-form profile (Fig 2.29), where sand has accumulated into fillet beaches on the northwest sides of the groins. As at Santa Barbara East Beach, most of the waves approaching the Ventura coast come from due west through the Santa Barbara Channel.

Back-beach Development, Coastal Engineering Structures, and Nourishment History

Lower-than-average precipitation between 1948 and 1959 caused a reduction in sediment yield from the Ventura River, which outlets just north of the bay. The Matilija Dam was completed in 1948 on Matilija Creek, trapping sediment from flowing downstream. The reduction in sediment supply from the combination of these two events resulted in about 90 m of beach erosion between the Ventura and Santa Clara Rivers (Griggs et al., 2005). Seven groins were subsequently built just south of San Buenaventura State Beach between 1962 and 1967, and 670,000 m^3 were placed on the shoreface to mediate the erosion problem. The beach was nourished almost annually during the 1980s using Ventura Marina dredge disposal. In 1998, Ventura County resolved to remove the dam; however, questions surrounding the impacts of releasing the accumulated sediment have delayed any action.

The Ventura Marina, protected by two rock rubble jetties and a down coast groin, was built in 1963 and immediately affected by rapid shoaling of sand at the entrance. On average, 150,000 m^3 of sediment are dredged from the entrance annually in order to keep the channel open. Since the marina's construction in the 1960s, a detached breakwater, an offshore breakwater, extensions to the north jetty, and another groin have all been constructed in attempts to mediate the shoaling of the harbor's entrance, although the harbor continues to be subject to annual maintenance dredging (Patsch and Griggs, 2007). The section of Ventura Beach analyzed in this study is backed mainly by dense residential and commercial development.

Fig. 2.29: Aerial photo of the characteristic notched planform profile of Ventura Beach due to an extensive alongshore groin field (photo by Kenneth and Gabrielle Adelman)

Water-level data and datum information for the Ventura Beach study were obtained from the Santa Barbara tide gauge station (Station ID 9411340). This station was established in 1974 with the present installation existing since 1990. The mean and diurnal tidal ranges at the station are 1.12 m and 1.65 m, respectively.

Extreme Still High Water Levels

At current sea level, extreme still high water levels range from 0.58 m above MHW at the 100% exceedance level to 0.84 m above MHW at the 1% exceedance level (Fig. 2.30). These still water levels would result in approximately 11% to 14% inundation of the total beach area analyzed, respectively (Fig. 2.31). For each sea-level rise scenario, the range of percent area of inundation is no more than 6% between the 100% exceedance levels and 1% exceedance levels. With a 140 cm sea-level rise, the extreme still high water level is

projected to inundate no more than 40% of the total beach area analyzed at the lowest exceedance probability.

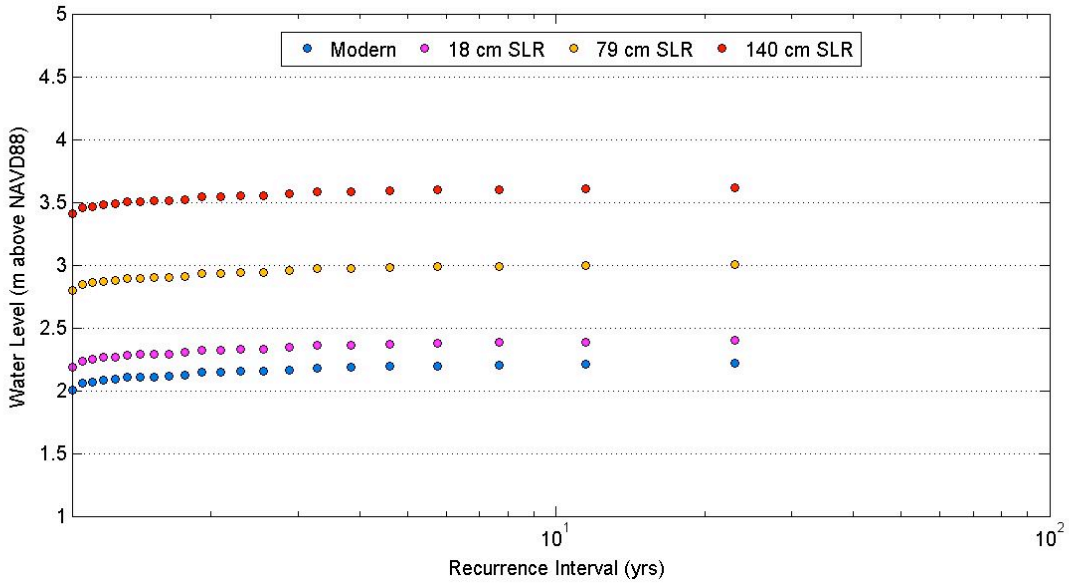

Fig. 2.30: Extreme still high water level vs. recurrence interval for Ventura Beach for current, + 18 cm, + 79 cm, and + 140 cm sea level scenarios

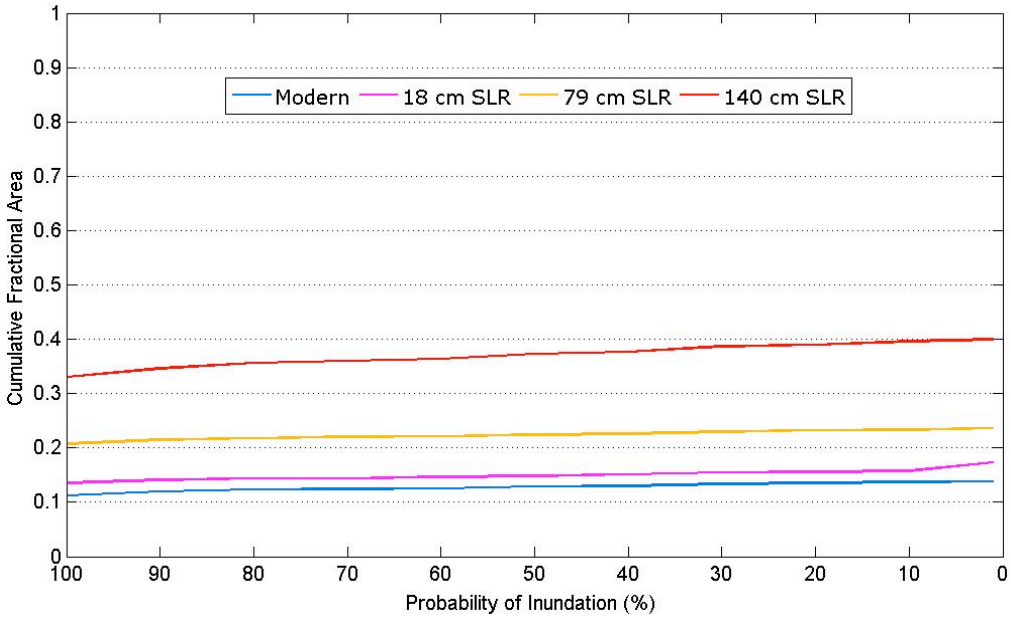

Fig. 2.31: Cumulative fractional beach area vs. probability of inundation for extreme still high water levels under current, +18 cm, + 79 cm, and + 140 cm sea level scenarios for Ventura Beach

Extreme Still High Water Levels Plus Run-up

Average L_o and H_o from the East Santa Barbara deep-water wave buoy records are 57.9 m and 1.26 m, respectively, with an average foreshore beach slope (ß) of 0.082 and an Iribarren number of 0.57. When the resulting 0.69 m 2% exceedance run-up is included in water level calculations, the current 1% exceedance extreme water level almost doubles from 0.83 m above MHW to 1.53 m above MHW. With an 18 cm and 79 cm sea-level rise, the 100% exceedance extreme water levels increase to 1.50 and 2.11 m above MHW, respectively. These water levels correspond to 22% and 35% beach inundation, while at the 100% exceedance level with a 140 cm sea-level rise, 73% of the total beach area analyzed is projected to be inundated (Fig. 2.32).

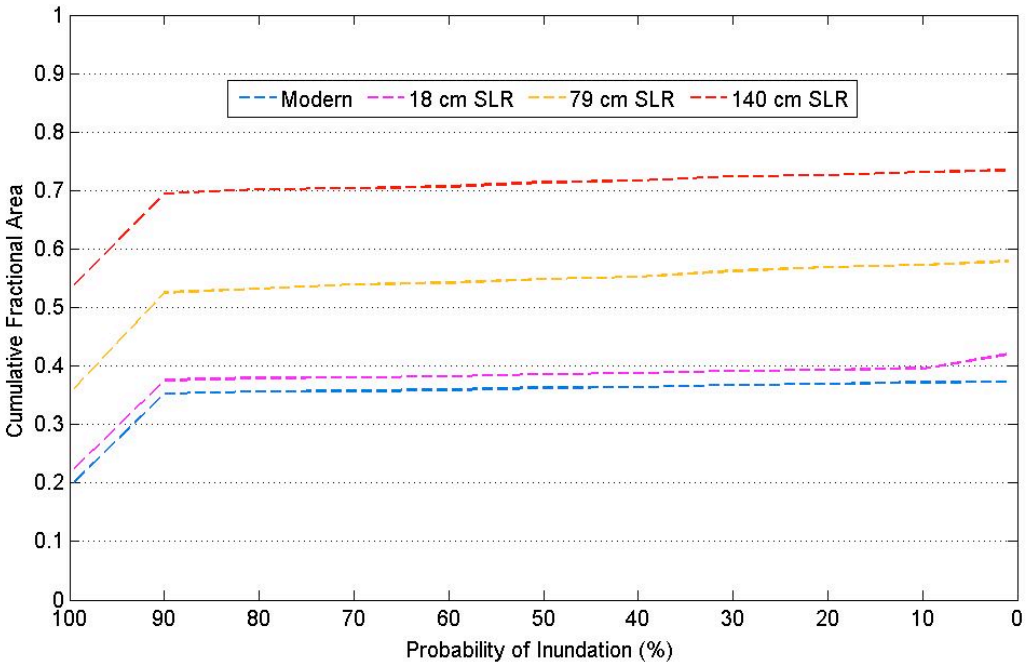

Fig. 2.32: Cumulative fractional beach area vs. annual probability of inundation for extreme high water levels plus run-up at current, + 18 cm, + 79 cm, and + 140 cm sea level scenarios for Ventura Beach

2.4.6 Santa Barbara East Beach

Location, Oceanography, and Beach Morphology

Santa Barbara East Beach is located in the Santa Barbara littoral cell, which extends from the Santa Maria River to the Mugu Submarine Canyon at Point Mugu. Approximately 230,000 m^3 of sediment move eastward through the cell annually (Griggs et al., 2005). The west-to-east littoral drift direction is a direct result of the dominant swell approach from the west, focused through the Santa Barbara Channel. The south-facing orientation of the coastline at Santa Barbara in the Southern California Bight shelters it from large wave events from the northwest. The average significant wave height at Santa Barbara East Beach is less than 0.5 m. Storm waves from the south, most common during El Niño events, however, can have significant effects on dynamics within the Santa Barbara cell. High-energy waves

approaching from the south can temporarily reverse the direction of littoral drift, moving it westward.

The area analyzed in this study is a 1.6 km-long stretch of East Beach located 0.8 km east of Stearn's Wharf. Just eastward of this study region, steep bluffs and narrow beaches dominant the coastline.

Back-beach Development, Coastal Engineering Structures, and Nourishment History

The L-shaped breakwater of the Santa Barbara harbor was constructed in 1928. The initial design was for a detached breakwater, intended to direct longshore transport of sand through the harbor to beaches to the east; however, due to a reduction in the lee of the detached breakwater, the harbor began to fill with sediment (Griggs et al., 2005). The breakwater was then extended to Point Castillo soon after it was built. The breakwater became a significant barrier to littoral drift down coast, and as a result, beaches east of the harbor were starved of their normal sediment supply, leading to significant beach erosion in the 1930s. Today, erosion down coast has been alleviated due to the dredging and down coast disposal of sand from harbor dredging. Annually an average of 220,000 m^3 of sand is dredged from the harbor and disposed of on East Beach.

The section of East Beach analyzed in this study is backed by a pedestrian/bike path, parking lots, flat grassy expanses, parking lots, some vegetated dunes, and sparse infrastructure (Fig. 2.33). Cabrillo Boulevard runs parallel to the shoreline just beyond the back beach. During the 1982-83 El Niño, a combination of large waves and that struck at high tide inundated East Beach all the way back to Cabrillo Boulevard.

Fig. 2.33: Aerial photo of a portion of East Beach, Santa Barbara. The back beach is characterized by occasional infrastructure as well as parking lots and Cabrillo Blvd. (photo by Kenneth and Gabrielle Adelman)

Water-level data and datum information for the Santa Barbara East Beach study were obtained from the Santa Barbara tide gauge station (Station ID 9411340). This station was established in 1974 with the present installation existing since 1990. The mean and diurnal tidal ranges at the station are 1.12 m and 1.65 m, respectively.

Extreme Still High Water Levels

At current sea level, extreme still high water levels range from 0.58 m above MHW at the 100% exceedance level to 0.84 m above MHW at the 1% exceedance level (Fig. 2.34). This corresponds to between 10% and 13% inundation of the total beach area analyzed (Fig. 2.35). At the lowest sea-level rise projection of 18 cm, the current 20% exceedance extreme still high water level becomes the 100% exceedance, or annual extreme still high water level. With a 79 cm sea-level rise, the extreme still high water levels at the 100% and 1%

exceedance levels become 1.42 and 1.64 m above MHW, respectively, corresponding to between 24% and 41% inundation of the total beach area analyzed. When total sea-level rise is increased to 140 cm, 88% of the beach area is inundated at the 100% exceedance level, and 95% at the 1% exceedance level. With an 18 cm, 79 cm, and 140 cm sea-level rise, inundation due to the annual extreme still water event affects at least 12%, 25%, and 88% of the total beach area, respectively (Figures 2.36, 2.37, 2.38).

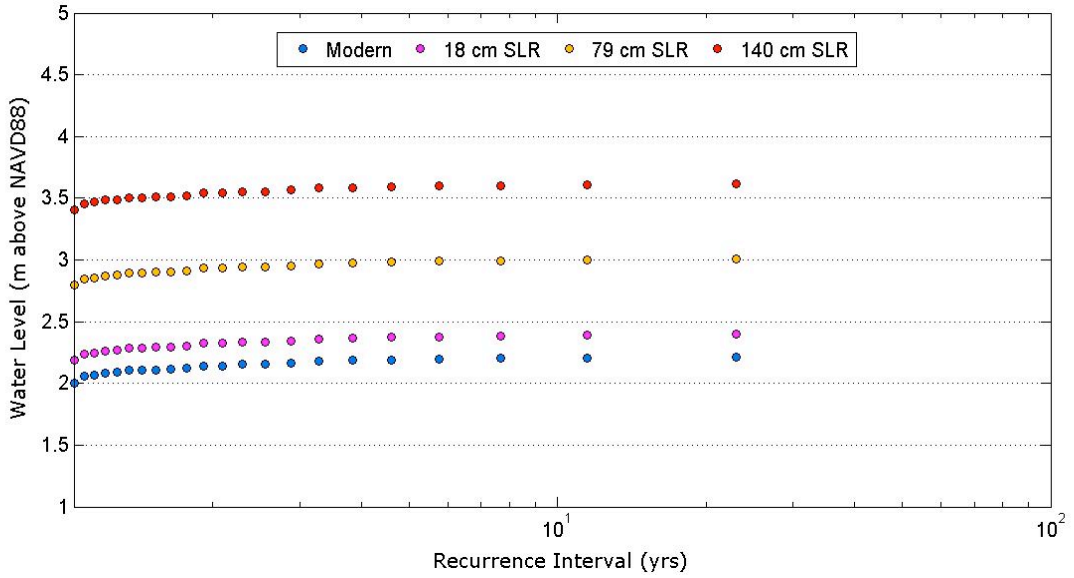

Fig. 2.34: Extreme still high water level vs. recurrence interval for Santa Barbara East Beach for current, + 18 cm, + 79 cm, and + 140 cm sea level scenarios

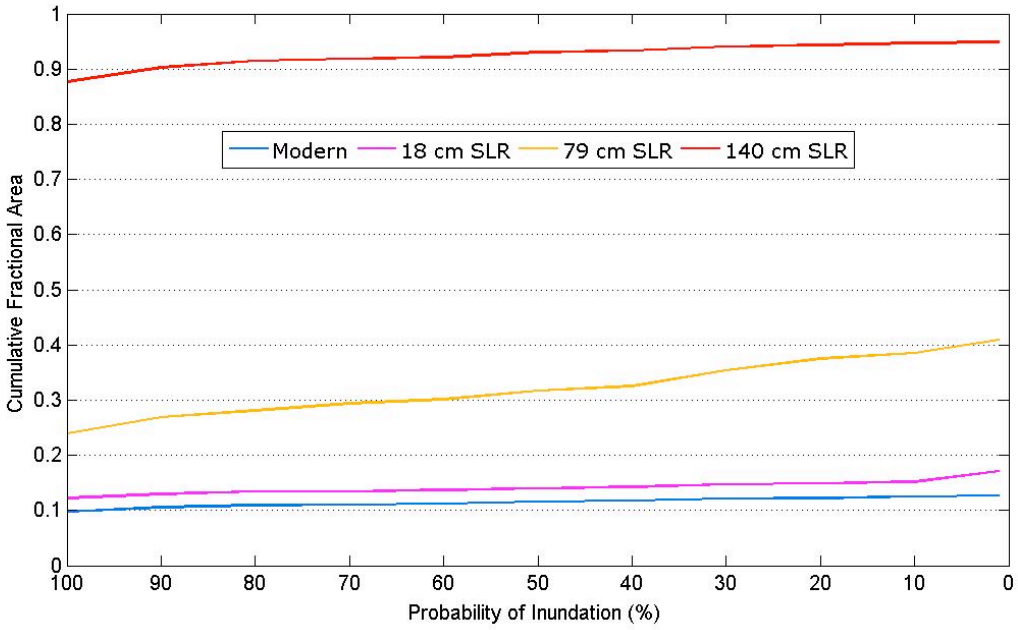

Fig. 2.35: Cumulative fractional beach area vs. probability of inundation for extreme still high water levels under current, +18 cm, + 79 cm, and + 140 cm sea level scenarios for Santa Barbara East Beach

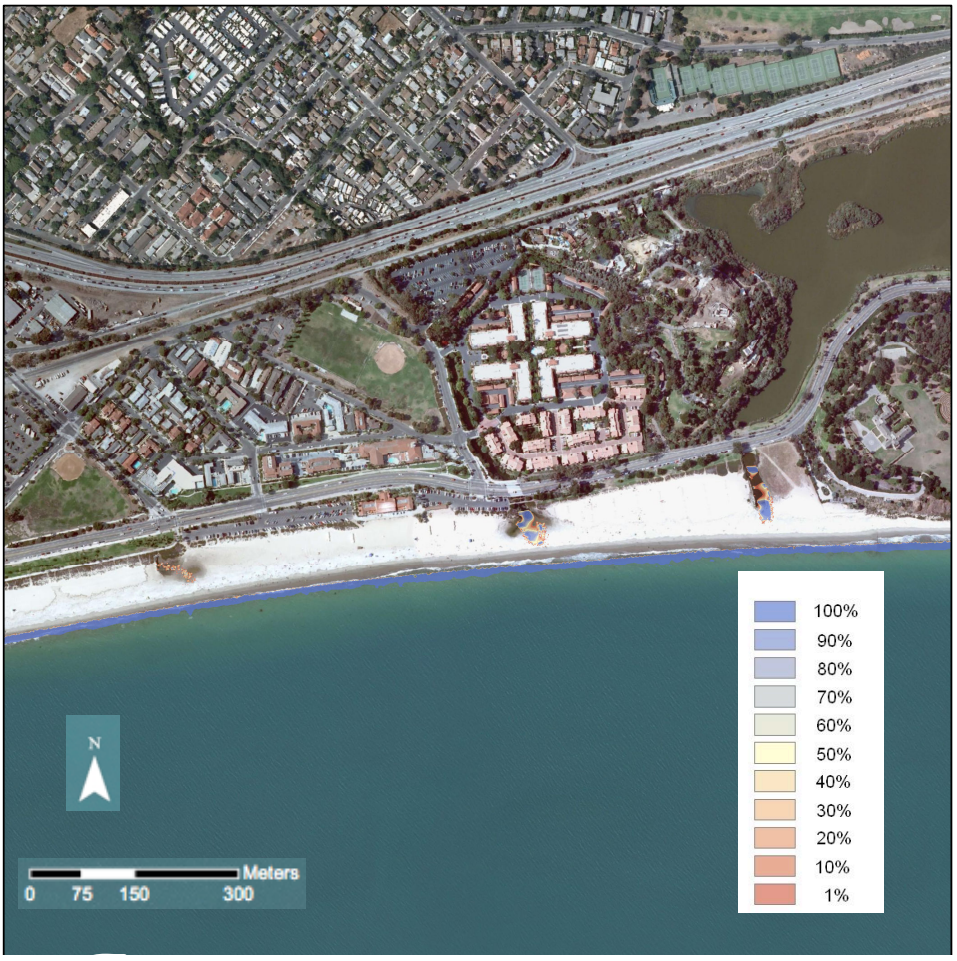

Fig. 2.36: Annual probability of inundation map for Santa Barbara East Beach extreme still high water levels with an 18 cm sea-level rise

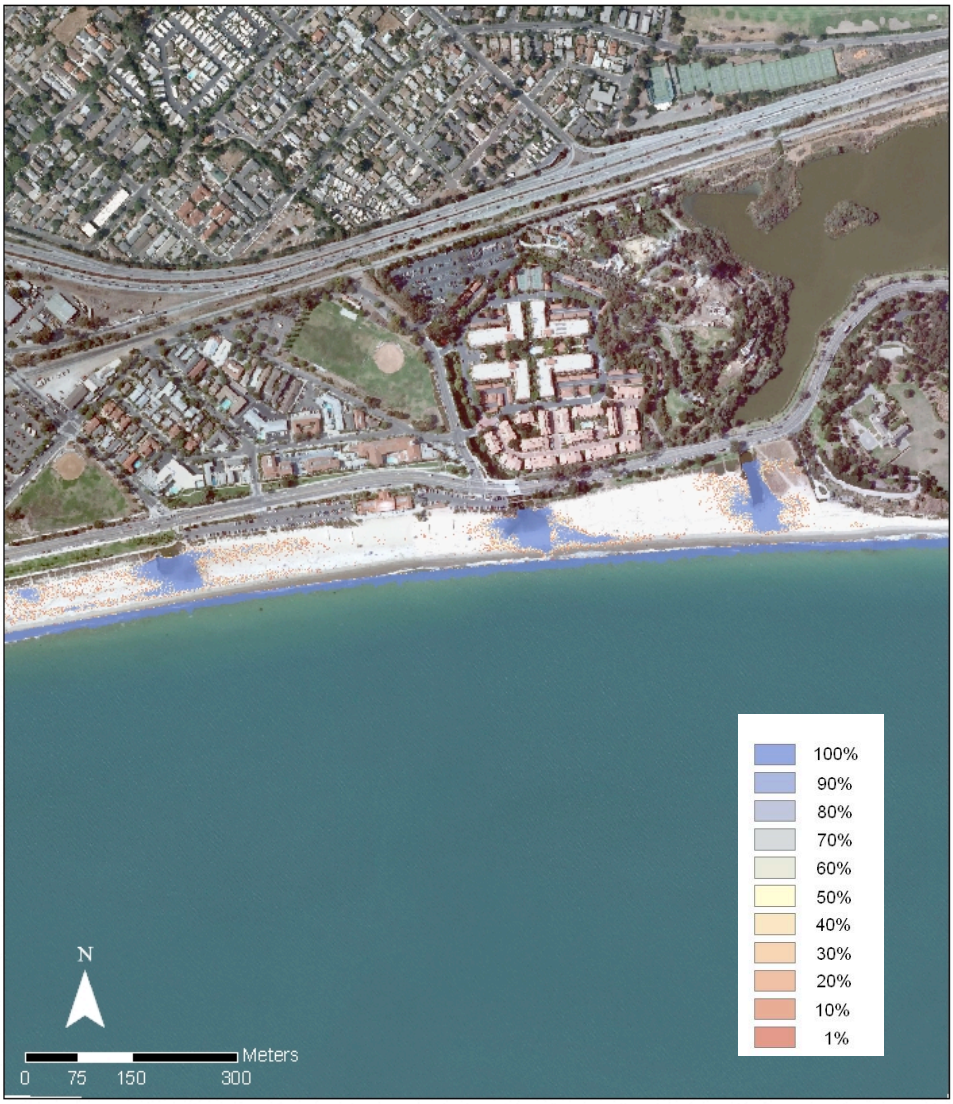

Fig. 2.37: Annual probability of inundation map for Santa Barbara East Beach extreme still high water levels with a 79 cm sea-level rise

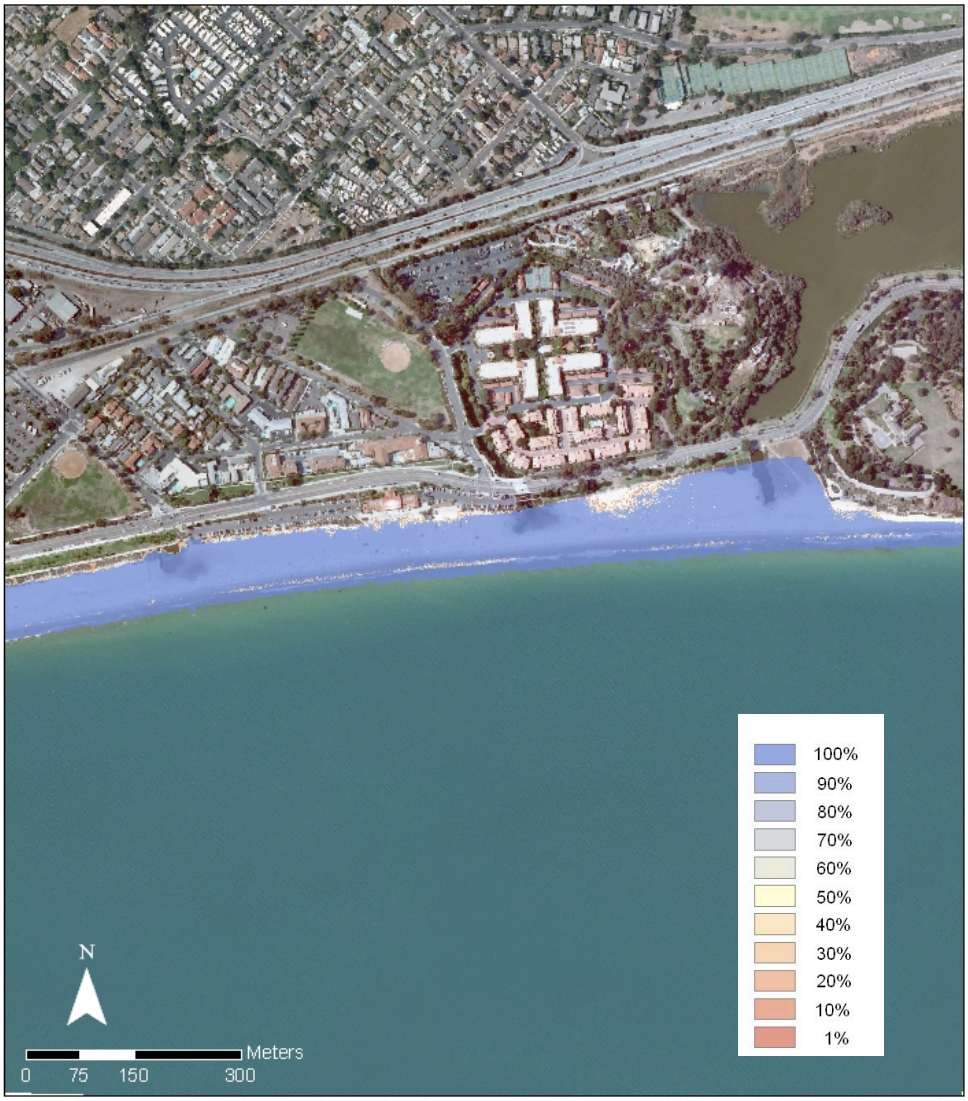

Fig. 2.38: Annual probability of inundation map for Santa Barbara East Beach extreme still high water levels with a 140 cm sea-level rise

Extreme Still High Water Levels Plus Run-up

Average L_o and H_o from the East Santa Barbara deep-water wave buoy records are 57.9 m and 1.26 m, respectively, with an average foreshore beach slope (ß) of 0.084 and an Iribarren number of 0.57. Including the resulting 2% exceedance run-up height of 0.70 m in water level calculations more than doubles the current extreme high water level elevation at the 100% exceedance level and increases the current extreme water level elevation at the 1% exceedance level from 0.84 m above MHW without run-up to 1.54 m above MHW with run-up (Fig. 2.39). The percent of total beach area inundated with a 79 cm sea-level rise increases from 24% without run-up to 92% with run-up at the 100% exceedance level, and at the 90% exceedance level the extreme water level with run-up is projected to inundate 100% of the beach area. With a 140 cm sea-level rise, it is almost 100% probable that the region of Santa Barbara East Beach analyzed will be completely inundated annually.

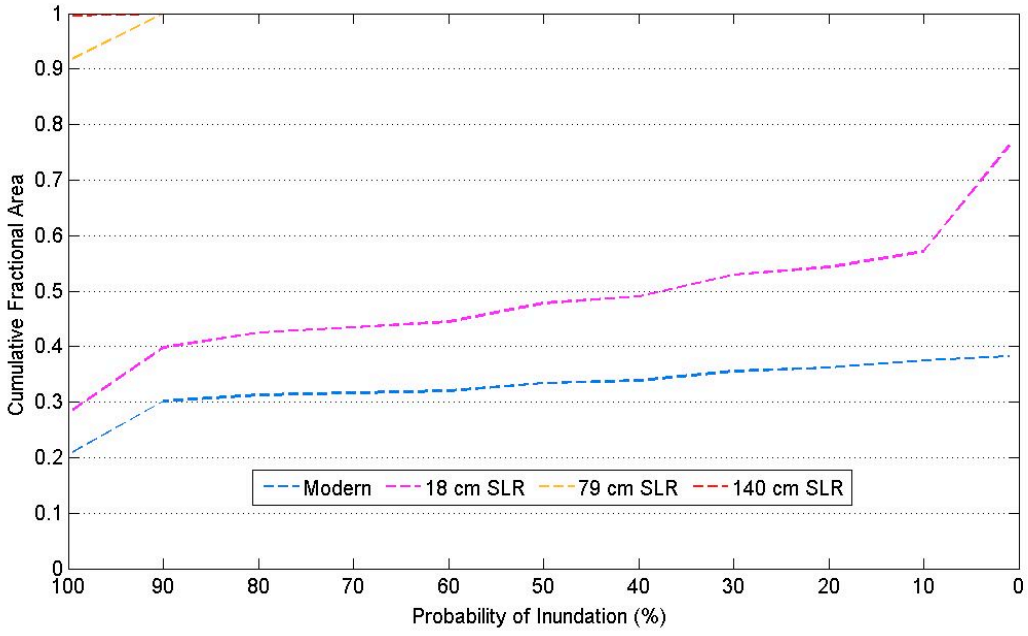

Fig. 2.39: Cumulative fractional beach area vs. annual probability of inundation for extreme high water levels plus run-up at current, + 18 cm, + 79 cm, and + 140 cm sea level scenarios for Santa Barbara East Beach

2.4.7 Santa Cruz Main Beach

Location, Oceanography, and Beach Morphology

The Santa Cruz beaches analyzed include both Main Beach (east of the Santa Cruz wharf) and Cowells Beach (west of the Santa Cruz wharf), but will be collectively referred to as Main Beach. Main Beach in Santa Cruz is an east-west trending sandy beach located on the northern end of the Monterey Bay in the Santa Cruz littoral cell. It is bounded on the east by the San Lorenzo River mouth and on the west by a rocky headland known as Point Santa Cruz (Fig. 2.40). Because of its east-west trend in the northern end of the bay and a dominant wave approach from the northwest, Santa Cruz Main Beach is a wide, well-developed stable beach. Longshore drift is to the southeast along the Santa Cruz coast, and the sand of Main Beach is supplied by up coast sources as well as by the San Lorenzo River. Although the dominant wave approach is generally from the northwest, storm waves during the fall and winter months can approach from a more southwesterly direction. Shoaling waves that approach Main Beach are refracted around Point Santa Cruz, and the wave energy is then dissipated along the approximately 1.3 km long Main Beach shoreline. The width of Santa Cruz Main Beach from the 1997 lidar data used in this study ranges between 70-140 m with an average foreshore slope of 0.08.

Fig. 2.40: Satellite image of Santa Cruz Main Beach and Point Santa Cruz (Google Earth)

Back-beach Development, Coastal Engineering Structures, and Nourishment History

Landward migration of Santa Cruz Main Beach is restricted by extensive coastal development (Fig. 2.41). The back beach is bounded mainly by the Santa Cruz Beach Boardwalk, an amusement park founded in 1907, as well as by parking lots, hotel infrastructure, a low seawall with a height of just over 4 m above sea level—the elevation above sea level of the Boardwalk and Beach Street that provides access to the boardwalk—and low bluffs that were subject to local stabilization when a cave was filled and armored with a gunite wall in 2004.

Fig. 2.41: Aerial photo of Santa Cruz Main Beach and the Santa Cruz Beach Boardwalk (photo by Kenneth and Gabrielle Adelman)

During the 1997-1998 El Niño, nearly half of the volume of sand on Cowells Beach was eroded away due to intense storm conditions (Fig. 2.42 a, b; Hapke and Richmond, 2000). The Santa Cruz Municipal Wharf, constructed in 1914, was also heavily damaged during this time, as were public roads, for a total of $3.8 million in damage during the 1997-1998 winter (Storlazzi et al., 2000).

a

b

Fig. 2.42: (a) Santa Cruz Cowells Beach after intense El Niño storms, 02/1998 (b) Santa Cruz Cowells Beach 10/1998 (U.S. Geological Survey)

Between the 1960s and 1980s, Santa Cruz County was subject to intensive coastal development. Jetties at the Santa Cruz Small Craft Harbor located west of Main Beach in the Seabright neighborhood were constructed between 1963 and 1965 and resulted in significant changes to beaches up and down coast of the harbor. Seabright Beach, immediately up coast widened significantly from 1963 until about 1980 when it seemed to reach an equilibrium width, 100 to nearly 200 meters wider than its original conditions. Beaches down coast, up to and including Capitola, were narrowed due to the trapping of littoral drift by the jetties.

Water-level data and datum information for the Santa Cruz Main Beach study were obtained from the Monterey tide gauge station (Station ID 9411340). This station was established in 1974 with the present installation existing since 1990. The mean and diurnal tidal ranges at the station are 1.12 m and 1.65 m, respectively.

Extreme Still High Water Levels

At current sea level, the annual extreme still water level that occurs at Santa Cruz Main Beach is 0.58 m above MHW, with a 1% probability each year of an extreme water level almost twice the annual level (Fig. 2.43). The 40% exceedance level at current sea level increases in frequency to the 100% exceedance level with an 18 cm sea-level rise. With a 79 cm sea-level rise, the annual extreme high water level is projected as 0.29 m higher than the 1% exceedance extreme still water level at current sea level, and with a 140 cm sea-level rise, the 100% exceedance level (1.98 m above MHW) is almost 3.5 times the current 100% exceedance level.

At current sea level, a 100% exceedance still high water level would result in inundation over 9% of the total beach area, while at the current 1% level, this increases to 21% of the beach (Figs. 2.44, 2.45). With an 18 cm sea-level rise, the annual event results in inundation of at least 12% of the beach (Fig. 2.46). The greatest range between 100% and 1% exceedance values occurs with a 79 cm sea-level rise, where the 100% exceedance level results in about 37% inundation, while the 1% exceedance level results in nearly 88% inundation (Fig. 2.47). With a 140 cm sea-level rise, between 90-100% of the beach is projected to be inundation at any exceedance level (Fig. 2.48).

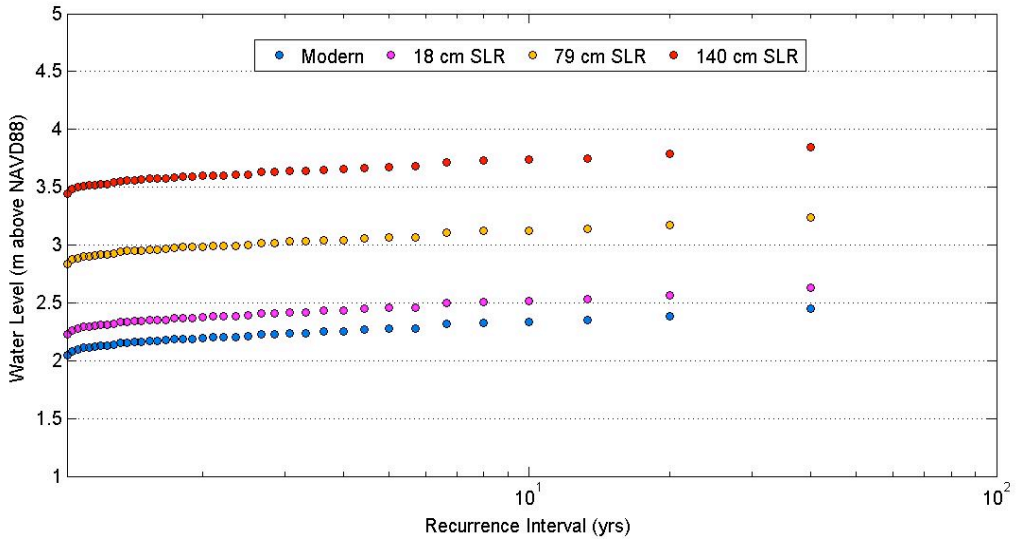

Fig. 2.43: Extreme still high water level vs. recurrence interval for Santa Cruz Main Beach for current, + 18 cm, + 79 cm, and + 140 cm sea level scenarios

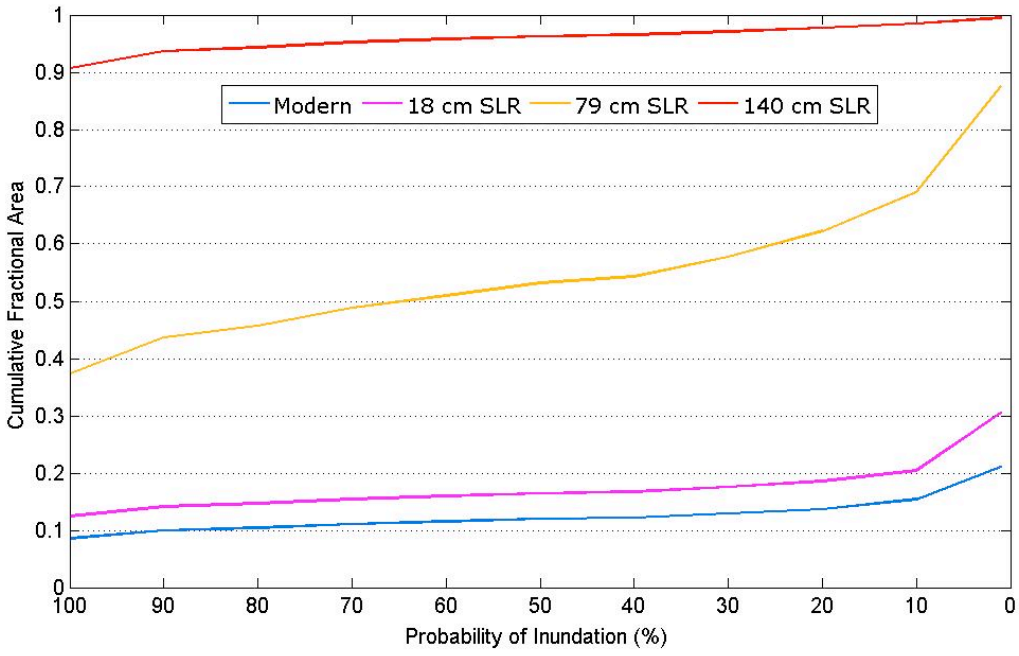

Fig. 2.44: Cumulative fractional beach area vs. probability of inundation for extreme still high water levels under current, +18 cm, + 79 cm, and + 140 cm sea level scenarios for Santa Cruz Main Beach

Fig. 2.45: Annual probability of inundation map for Santa Cruz Main Beach extreme still high water levels at current sea-level

Fig. 2.46: Annual probability of inundation map for Santa Cruz Main Beach extreme still high water levels with an 18 cm sea-level rise

Fig. 2.47: Annual probability of inundation map for Santa Cruz Main Beach extreme still high water levels with a 79 cm sea-level rise

Fig. 2.48: Annual probability of inundation map for Santa Cruz Main Beach extreme still high water levels with a 140 cm sea-level rise

Extreme Still High Water Levels Plus Run-up

Average L_o and H from the Monterey deep-water wave buoy records are 85.04 m and 2.24 m, respectively, with an average foreshore beach slope (ß) of 0.08 and an Iribarren number of 0.48. When 2% exceedance run-up levels are included in total extreme water level height, the annual extreme water height more than doubles to 1.65 m above MHW at current sea level compared to extreme still water levels. This corresponds to a 21% total beach inundation. With an 18 m sea-level rise, 28% of the total beach area is projected to be inundated at the 100% exceedance level, while at the 1% exceedance level, this number increases significantly to 76%. With a 79 cm sea-level rise, 100% of the beach is projected to be inundated as high as the 90% exceedance level, and with a 140 cm sea-level rise, it is predicted that the extreme high water level with 2% exceedance run-up will annually completely inundate Main Beach (Fig. 2.49).

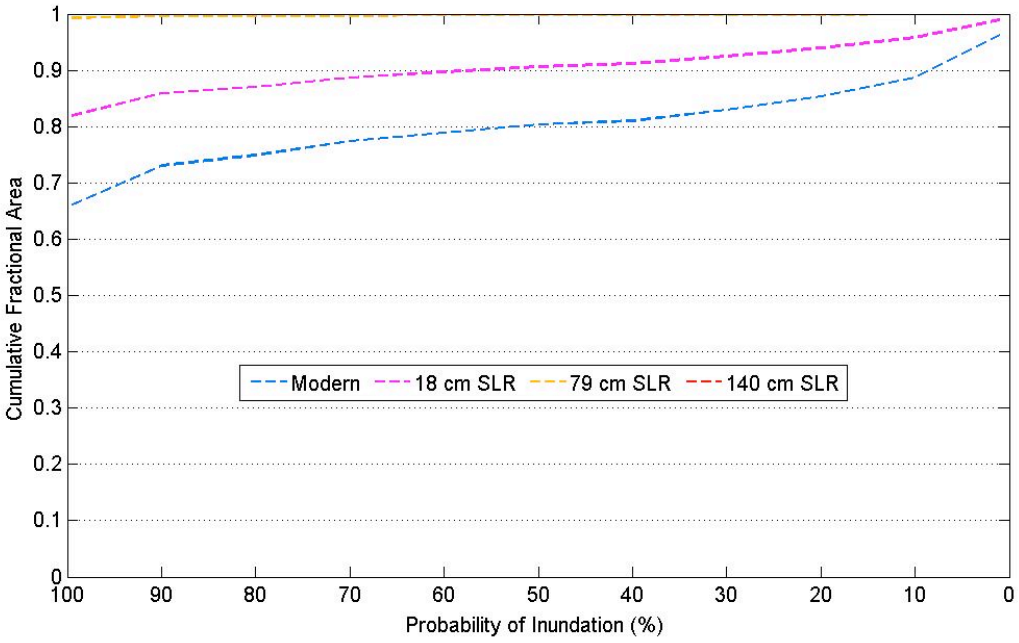

Fig. 2.49: Cumulative fractional beach area vs. annual probability of inundation for extreme high water levels plus run-up at current, + 18 cm, + 79 cm, and + 140 cm sea level scenarios for Santa Cruz Main Beach

2.4.8 Ocean Beach, San Francisco

Location, Oceanography, and Beach Morphology

Ocean Beach in San Francisco stretches 7 km from Point Lobos in the north to Fort Funston in the south. Ocean Beach is a high-energy, seasonally-wide sandy beach in the north and narrows to the south. One of the largest and oldest seawalls, the O'Shaughnessy seawall, backs the northern 1.5 km of the beach (Fig. 2.50 a). Narrow back beach dunes 7-10 m above mean lower low water in the central stretch of Ocean Beach become high sand bluffs in the southern end. Ocean Beach morphology is a product of tidal currents through the Golden Gate and wave refraction caused by the ebb tide delta (Barnard and Hanes, 2005). Fair-weather offshore wave heights average about 2.5 m, with storm waves reaching upwards of 6 m. While waves typically approaches from the northwest, westerly and southwesterly waves during storm episodes and El Niño events can alter the longshore transport direction of sand, leading to sediment starvation in the south as sediment is moved to the north. During the 1997-1998 El Nino winter, shoreline retreat at Ocean Beach was more than double the retreat during the winter of 2004-2005, a 'normal' year (Barnard et al., 2007). The southern region of Ocean Beach has been identified as an erosional hotspot attributed to changes in the Golden Gate ebb tidal delta, as well as the location of San Francisco ship channel dredge disposal site, which has increased wave energy to this portion of the beach (Barnard and Hanes, 2005); The sandy bluffs in the south are also highly unstable and have been subject to large slumps and landslides.

Back-beach Development, Coastal Engineering Structures, and Nourishment History

A massive concrete seawall 6 m above and below sea level was built along the back beach of northern Ocean Beach in 1929 and extended southward in 2005 (Griggs et al., 2005). As mentioned previously, to the south where the back beach is not backed by the seawall, it is backed by narrow sand dunes or high, unstable sandy bluffs (Fig. 2.50 b). Riprap lines a portion of these narrow sand dunes to protect the Great Highway, which runs

along the dunes, from waves, erosion, and burial due to the migration of the dunes. Erosion has become a problem at the south end of Ocean Beach and is now threatening the highway.

a

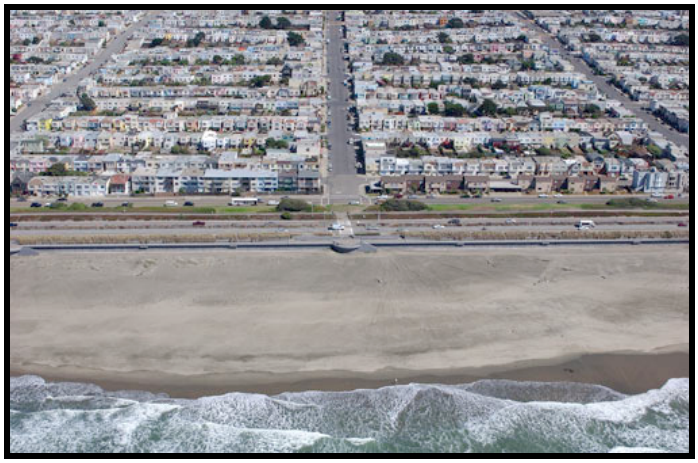

b

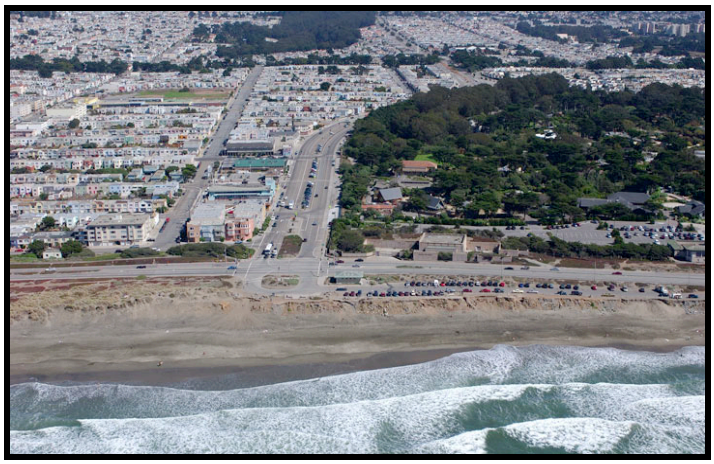

Fig. 2.50: (a) Aerial photo of Ocean Beach bounded in the backshore by the Ocean beach seawall and the Great Highway (b) Ocean Beach at Sloat Blvd, characterized by high rates of erosion (photos by Kenneth and Gabrielle Adelman)

Water-level data and datum information for the San Francisco Ocean Beach study were obtained from the San Francisco tide gauge station (Station ID 9414290). This station was established in 1854 with the present installation existing since 1988. The mean and diurnal tidal ranges at the station are 1.25 m and 1.78 m, respectively.

Extreme Still High Water Levels

The current annual extreme still high water level at Ocean Beach is 0.30 m above MHW, while there is a 50% chance annually of reaching an extreme still water height twice this value (0.61 m above MHW), and a 1% chance annually of an extreme height more than three times the annual level (1.05 m above MHW; Fig. 2.51). With an 18 cm sea-level rise, the 20% exceedance extreme still high water level at current sea level increases in frequency to the 70% exceedance level, and with a 79 cm sea-level rise, the 1% exceedance level at current sea level becomes the annual (100%) extreme still high water level. With a 140 cm sea-level rise, the 1% exceedance still high water level more than doubles the 1% level at current sea level. At the current annual exceedance level, only about 12% of the total beach area analyzed in this study is inundated (Figs. 2.52, 2.53), whereas with a 140 cm sea-level rise, this number increases to 56%. At the 1% exceedance level with a 140 cm sea-level rise, at least three quarters of the total beach area is projected to be inundated. Figs. 2.53, 2.54, 2.55, and 2.56 show annual probability of inundation maps for Ocean Beach extreme still water levels under current, 18 cm, 79 cm, and 140 cm sea-level rise scenarios, respectively.

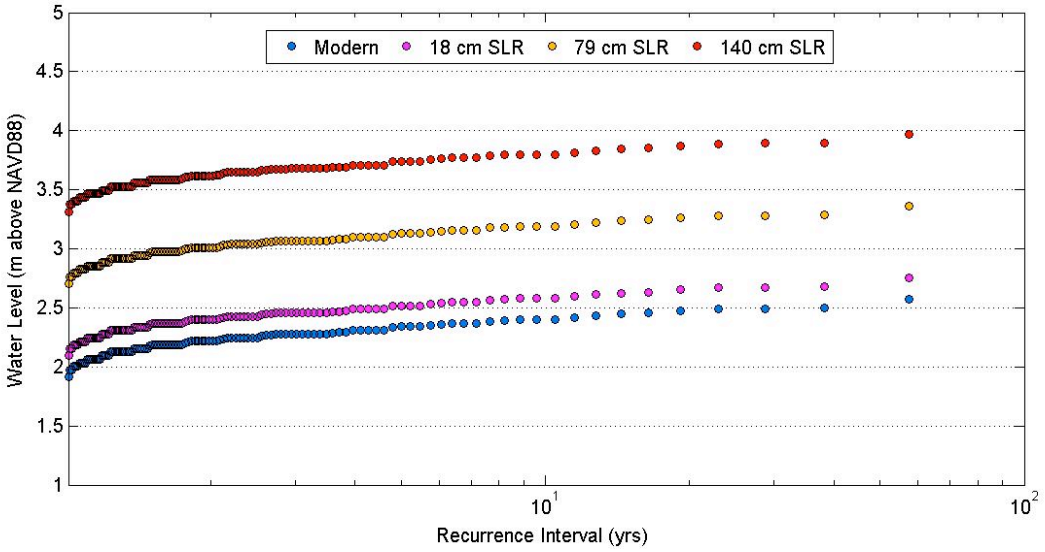

Fig. 2.51: Extreme still high water level vs. recurrence interval for Ocean Beach for current, + 18 cm, + 79 cm, and + 140 cm sea level scenarios

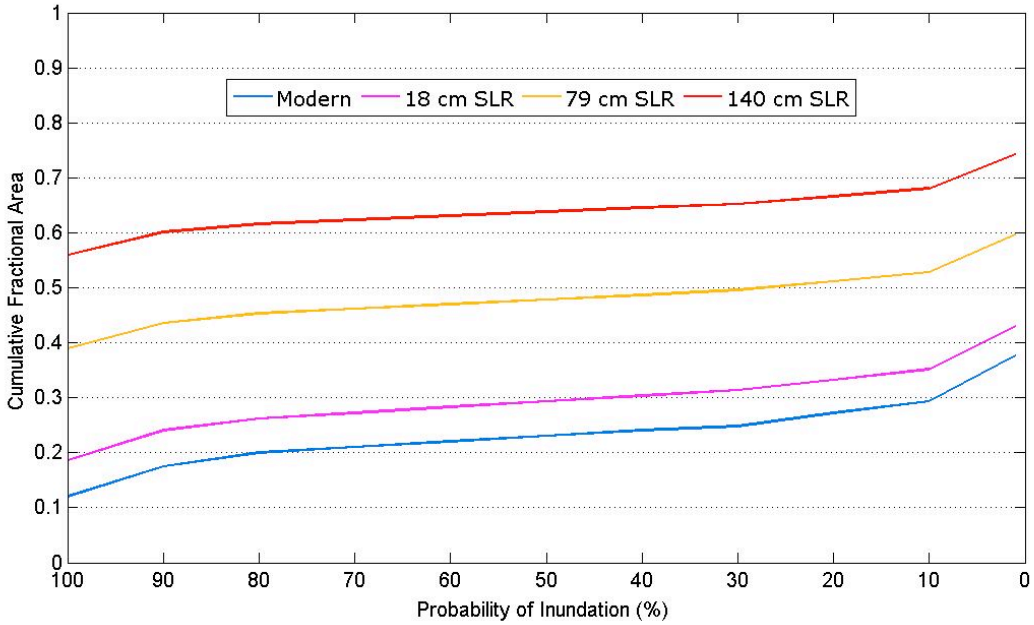

Fig. 2.52: Cumulative fractional beach area vs. probability of inundation for extreme still high water levels under current, +18 cm, + 79 cm, and + 140 cm sea level scenarios for Ocean Beach

Fig. 2.53: Annual probability of inundation map for Ocean Beach extreme still high water levels at current sea level

Fig. 2.54: Annual probability of inundation map for Ocean Beach extreme still high water levels with an 18 cm sea-level rise

Fig. 2.55: Annual probability of inundation map for Ocean Beach extreme still high water levels with a 79 cm sea-level rise

Fig. 2.56: Annual probability of inundation map for Ocean Beach extreme still high water levels with a 140 cm sea-level rise

Extreme Still High Water Levels Plus Run-up

Average L_o and H_o from the Pt. Reyes deep-water wave buoy records are 95.97 m and 2.55 m, respectively, with an average foreshore beach slope (ß) of 0.047 and an Iribarren number of 0.29. Because the Iribarren number is less than 0.3, Equation 2.6 for dissipative beaches was used to calculate a 2% exceedance run-up of 0.67 m. When run-up is included, the current extreme high water levels for Ocean Beach range from 0.97 m above MHW at the 100% exceedance level to 1.72 m above MHW at the 1% exceedance level. With a 140 cm sea-level rise, these numbers increase significantly to 2.60 m above MHW at the 100% exceedance level to 3.00 m above MHW at the 1% exceedance level. These ranges equate to approximately 35-56% beach inundation for current 100% and 1% exceedance levels, respectively, and 73-89% for 140 cm sea-level rise 100% and 1% exceedance levels (Fig. 2.57).

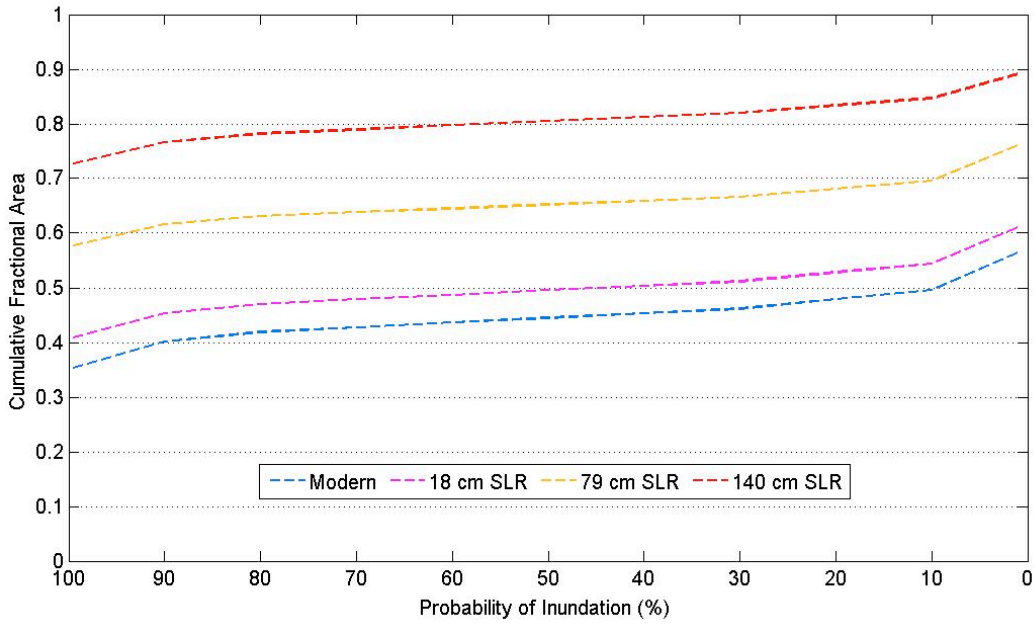

Fig. 2.57: Cumulative fractional beach area vs. annual probability of inundation for extreme high water levels plus run-up at current, + 18 cm, + 79 cm, and + 140 cm sea level scenarios for Ocean Beach

2.5 Discussion

The methods employed in this study focused on extreme water levels under various sea-level rise scenarios for the year 2100, and not projections for shorter time intervals (i.e., 2025, 2050, 2075) because coastal managers and policy makers should be planning now for conditions that could prevail in a century. Currently, sea-level rise rates and increases in temperatures are already following the most extreme IPCC projections, and there is high probability that the sea-level rise projections assessed in this study could be reached well before 2100. Also, it is important for policymakers and managers to remember that climate change related impacts will not stop in 2100, but will continue well beyond.

2.5.1 Method Caveats and Uncertainties

The methods employed in this study do not account for landward translation of the beach profile and assume maintenance of the beach foreshore slope. Potential changes in sediment supply related to climate change impacts (e.g., changes in precipitation and fluvial transport) are also not considered. The uncertainty inherent in recurrence interval projections is dependent on the length of the tide gauge record, which ranges from over one-hundred years for San Francisco to only about 20 (discontinuous) years for Santa Barbara.

The high accuracy of lidar data has been invaluable for past and present comparative studies of topographic changes and related topics; however, the high resolution of the datasets does not reduce the uncertainty inherent in sea-level rise predictions. Lidar datasets are instantaneous snapshots of topography. This is especially important to consider with regards to studies like this where probability of inundation projections are a direct function of the beach morphology. A lidar dataset for a beach is just one representation of a highly dynamic environment that changes on daily, monthly, yearly, and longer-term time scales. The lidar data used in this study represent pre-winter beach conditions when the beach is presumably widest and with a developed berm. That being said, the methods

employed in this study do have advantages over other sea-level rise and shoreline change models.

2.5.2 Advantages in Methodology

The probabilistic extreme high water level approach employed in this study has several advantages over traditional sea-level rise equilibrium profile and shoreline translation models, such as the Bruun Rule (Bruun, 1962), a popular simple mathematic model for shoreline translation with sea-level rise that has been widely used and applied, and also widely criticized for its inaccurate assumptions and oversimplifications (Thieler et al., 2000; Cooper and Pilkey, 2004). The Bruun Rule essentially predicts that an equilibrium beach profile will be maintained with increased sea level, and the profile will simply migrate upward and landward. The following are the general advantages of the methods employed in this study, as well as advantages that this study has over said simplistic equilibrium shoreline 'prediction' models:

1. This method does not aim to predict the position of the shoreline with future sea-level rise, but rather give a range of possibilities and probabilities of extreme high water levels that could occur on an annual basis under various sea-level rise scenarios. Sea-level rise alone will not be the only or main concern for coastal managers over the next 40-50 years (and beyond), but rather the extreme events that will inevitably be exacerbated by increased sea level. These extreme events are what ultimately control long-term beach stability and hold the greatest potential for beach erosion and inundation. Sea level rise will, however, be an increasingly important issue and concern for low-lying areas (San Francisco Bay and the other estuaries and bayshores) that have been developed, particularly in southern California.

2. Following on (1), this method addresses what should be the main concerns of coastal managers and policymakers—changes in extreme events that are responsible for

significant beach erosion and the destruction of coastal infrastructure—and presents results in a more effective context. Coastal managers and policymakers are much more likely to understand and be willing to work with probabilities of events of various magnitudes, rather than predictions of shoreline position or beach erosion that often entail errors and uncertainties greater than the predictions themselves.

3. The primary parameters that define a beach profile—the berm height and cross-shore position and foreshore slope—are not a function of the still water level so much as they are a function of the wave energy (which is a function of wave height and period) and swash oscillations or swash asymmetry. Therefore, it would seem reasonable that a berm would maintain its height relative to the MHW level with increasing sea level (assuming that the wave conditions do not change significantly), which is predicted by models such as the Bruun Rule. Thus, the assumption of the probabilistic extreme water method of a static beach morphology relative to the date of lidar data collection would appear to be a disadvantageous assumption. On the contrary, however, by approaching the issue of the potential impacts of sea-level rise on beaches in the context of the extreme high water levels, the probabilistic method is essentially more applicable to a winter beach state in California when berms have been temporarily eroded and moved offshore, as storm events that induce extreme high water levels occur during the high-energy winter months. Therefore the treatment of the berm with this method as a static feature relative to the October 1997 pre-winter profile lidar data would in fact provide conservative predictions of probabilities of inundation during winter beach conditions in California (when the coast is most vulnerable to wave attack) as the berm will most likely not be present as a buffer against run-up and elevated water levels.

4. The methods used in this study explore not only changes in extreme still high water levels, but also additional potential inundation due to run-up, specifically the 2% exceedance run-up, which simple mathematical models like the Bruun Rule do not account

for. As alluded to in (3), it is swash oscillations and run-up that primarily control net erosion or accretion of the beach, and thus these factors are important to consider when assessing impacts due to extreme events, which can produce destructive run-up and inundation.

2.5.3 Site-Specific Interpretations

The 8 study beaches analyzed have widely varying results. Santa Cruz Main Beach, Santa Barbara East Beach, and Mission Beach are all projected to be 90-100% inundated by 1% exceedance extreme still high water levels with a 140 cm sea-level rise, while Ocean Beach, Santa Monica, Ventura, Redondo, and Huntington Beaches are not. Redondo and Huntington Beaches appear to be the least affected by extreme still high water levels at any sea-level rise scenario, with just over 30% inundation projected for both beaches at 1% extreme still high water levels and a 140 cm sea-level rise. These results are not due to geographic variation in extreme water levels, but appear to be primarily the result of variations in beach morphology. Foreshore slope plays a significant role in moderating the cross-shore position of the elevated MHW shoreline until the water level exceeds the berm height. Huntington Beach, Redondo Beach, and Ventura Beach all have comparatively steep foreshore slopes (ß >0.08), but Santa Barbara also has a foreshore slope greater than 0.08, and is greatly affected by extreme still high water levels with a 140 cm rise in sea level. The berm height is a primary control on inundation extent, and once the berm is overtopped, there is potential for much more extensive inundation of a gently sloping or flat back beach. This can be identified in the cumulative fractionally area vs. probability of inundation graphs as a more steeply sloping curve, such as the 79 cm sea-level rise still extreme water level curve for Santa Cruz. Once the berm is overtopped, the backshore slope becomes the main variable controlling landward extent of inundation. Huntington Beach morphology based on the 1997 lidar data has a steep foreshore slope, comparatively high berm, and slightly seaward-sloping backshore (Fig. 2.58a). In contrast, Santa Cruz Main Beach generally has a more gently sloping foreshore, lower berm, and flatter backshore (Fig. 2.58b).

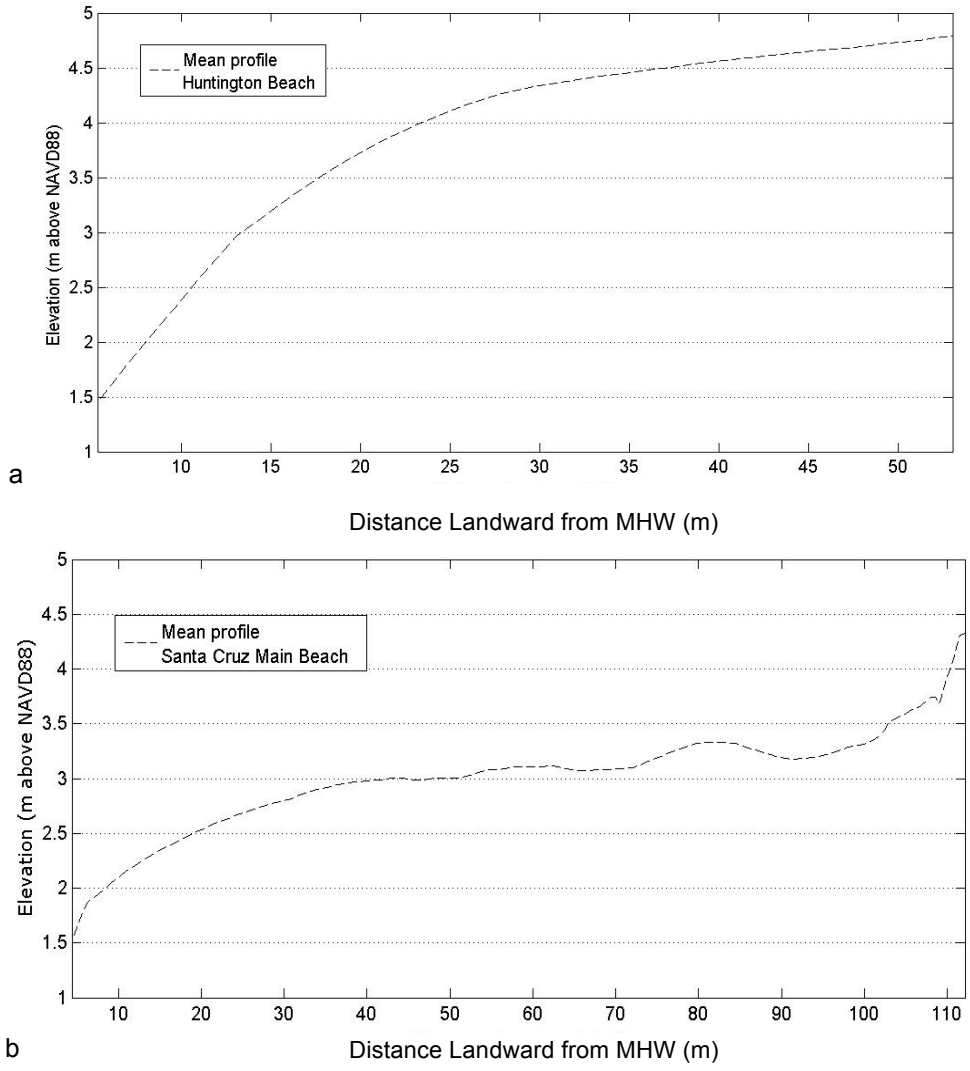

Fig. 2.58: (a) Average beach profile, Huntington Beach (b) Average beach profile, Santa Cruz Main Beach

A high back-beach barrier with physical height, such as a seawall, might act as a barrier controlling the maximum landward extent of extreme high water level inundation, but once the entire beach is inundated and the water level continues to rise, the potential for beach erosion will significantly increase as the swash depth and degree of beach saturation

increases. Deeper swash has a greater velocity on the uprush and backrush, and thus can suspend and transport a greater amount of sediment. In cases where the back-beach barrier is a parking lot or roadway, extreme high water levels have the potential to flood inland regions. For example, the Santa Barbara analysis shows that the beach would almost certainly be inundated annually when 2% exceedance run-up is included in water level calculations with a 140 cm sea-level rise, and thus any extreme water level at the 1-99% exceedance level has the potential to cause backshore flooding. Since the back-beach barriers for the region of Santa Barbara East Beach analyzed—parking lots, roadways—do not have significant elevation, the extreme high water plus run-up levels with less than 100% exceedance probabilities have the potential to threaten the backshore parking lots, and even Cabrillo Boulevard. In cases where there is not seawall or sea cliff, but a low-sloping, flat beach, extensive flooding of backshore infrastructure could result. Whether a back-beach barrier has significant elevation or not, it will act as a wall to landward beach migration that will have to occur with increasing sea level (given no increases in sediment supply) for beaches to survive elevated water levels. Given current policies and practices, it is likely that where there is an important highway backing the beach, coastal engineering measures will be initially preferred over retreat alternatives when the highway becomes threatened by rising seas or coastal erosion.

2.6. Conclusions

Beaches are some of the most dynamic environments on the planet, as they are subject to both marine and terrestrial processes, which vary on multiple time scales and can be constant or episodic, cyclical or stochastic. It is difficult to make predictions of beach morphology in 25, 50, or 100 years due to a change in sea level, as there is significant uncertainty surrounding the future rate of sea-level rise, future changes in wave climates, timing and frequency of episodic storm and El Niño events, potential changes in beach sand

supply, and anthropogenic impacts. Although sea level is currently rising at only a few mm per year, future cumulative sea-level rise plus extreme elevated water levels due to intense storm events could significantly change the shape of California's beaches.

While the results from this study are not yet recommended for direct application in coastal policy decisions, in general studies such as this are valuable for several important reasons. Public awareness of the concerns that coastal regions are facing and could face in the future is the first step in adopting pre-emptive coastal policies and practices rather than reactive, and almost certainly more costly, actions. For the sake of the protection of coastal development and infrastructure, the durability and lifespan of coastal engineering projects, and the preservation of coastal habitats such as beaches and wetlands, it is necessary that informed projections for the future be inherent in the design of coastal structures and setback lines, any armor or beach nourishment efforts, and in the management and protection of sensitive coastal ecosystems. Studies such as this also provide baseline datasets to which future analyses can be compared and upon which predictions can be formulated, tested, and improved.

CHAPTER 3

Seasonal Berm Morphodynamics and Alongshore Variability on a Coastal Lagoon Pocket Beach

3.1 Introduction and Background

Beach morphology varies in time and space as a result of complex interactions between and among marine and terrestrial forcings. Beaches serve as ecological habitats, buffers against wave attack to the coastline, and economically important environments for recreation and tourism. Understanding broad and site-specific processes and feedbacks involved in beach morphodynamics is important, especially in the face of future climate change and sea-level rise.

3.1.1 Wave Climate and Seasonal Beach Morphology

The most fundamental parameter influencing seasonal beach morphodynamics is the offshore wave steepness, or ratio of wave height to wavelength. The energy density of a particular sea state of deep-water gravity waves is defined by linear wave theory as being proportional to the square of the wave height. Since waves propagate energy, the deep-water wave energy flux, or wave power, is likewise proportional to the square of the wave height. As deep-water waves transform into shallow water waves in the nearshore, some of the energy is dissipated due to wave breaking, but much of it is transported to the shoreline to do work on the beachface. Thus, higher waves have the potential to cause greater sediment transport in the foreshore, not only because of increased wave energy, but also because higher and longer period waves can produce greater run-up levels on the beachface, thus increasing the horizontal swash extent and area of potential sediment transport.

Seasonal variations in beach morphology in California have been well observed since the 1940s (La Fond, 1940; Grant and Shepard, 1940; Grant, 1943), and were attributed to variations in wave height. La Fond (1940) observed in his study of a beach near La Jolla, California, that waves between 2.1-3.7 m (7-12 ft) high caused removal of sand from the beachface and subtidal sea floor to depths of 3.0-5.5 m (10-18 ft). Conversely, waves between 0.8-0.9 m (2-3 ft) high removed sand from 3.7-4.3 m (12-14 ft) below mean sea level and transported it onto the beachface 0.9-1.2 m (3-4 ft) above sea level. Changes in wave height along the California coast are associated with seasonal variations in cyclonic activity in the Pacific Ocean—high energy waves are typically generated by storms in the North Pacific during the northern hemisphere winter, while more gentle swell is generated by southern hemisphere Pacific cyclones during the northern hemisphere summer (e.g., Wingfield and Storlazzi, 2007); thus, the two end member beach profiles described by La Fond have become known as the 'summer,' or 'non-barred' profile, and the 'winter,' or 'storm/barred' profile. In general, a wide beach with a well-developed berm and steep foreshore slope characterizes the summer profile, whereas the winter profile is characterized by a narrower beach with a less steep foreshore and a low-to-nonexistent berm (Fig. 3.1).

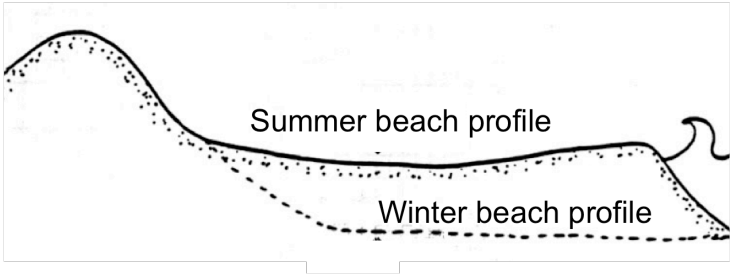

Fig. 3. 1: General idealized 'summer' and 'winter' beach profiles. The summer beach profile is characterized by a wide beachface, berm, and steep foreshore while the winter profile is characterized by a flatter shoreface where the berm has been temporarily eroded

Berms are morphologic features (sand bodies) on the upper beachface parallel to the shoreline, which separate a flat or landward-sloping backshore from a more steeply seaward-sloping foreshore. As berms are accretional features ascribed to the net onshore movement of sand by swash, they typically form at or just above the landward run-up extent, resulting in vertical and horizontally seaward growth of the beachface (Weir et al., 2006; Jensen et al., 2009). Swash run-up elevations have been shown to be function not only of wave height, but wavelength (period) as well (Stockdon et al., 2006; Ruggiero et al., 2004). This dependence of berm height on wave run-up has been coined the 'berm-height paradox,' which describes the phenomenon that increasing wave heights result in increased run-up elevations, and thus an increase in the berm height, while ultimately the highest waves serve to erode the beachface and reduce the berm height (Komar, 1998; Weir et al., 2006).

3.1.2 Beach Groundwater Table and Sediment Transport

Foreshore morphology is additionally controlled by the elevation of the groundwater table, or where subsurface pore water pressure is equal to atmospheric pressure. At the shoreline, the mean water surface is the water-level elevation averaged over a time interval much greater than infragravity wave periods (>30 s) but less than tidal periods (<12 hours; Nielsen, 1988).

The beach water-table elevation fluctuates at multiple frequencies in response to changing marine and climatological factors. At higher frequencies, changes in radiation stress (momentum flux) in the surf and swash zones due to breaking waves initiates an increase or decrease in the mean water surface. Reduced radiation stress in the surf zone as a result of the dissipation of wave energy and the landward propagation of momentum is balanced by an increase in, and a seaward sloping of, the mean water surface, or set-up (Bowen et al., 1968; Hanslow and Nielsen, 1993), which acts to raise the mean water surface at the shoreline. Uprush and backrush in the swash zone is essentially an oscillation around the maximum wave set-up.

Water table oscillations with the swash cycle (Waddell, 1976; Hegge and Masselink, 1991; Li et al., 1997) are superimposed onto a lower frequency oscillation associated with the semidiurnal tides, which is superimposed on the spring-neap tidal cycle (Lanyon et al., 1982).

3.1.3 Foreshore Dynamics

Cross-shore and alongshore sediment transport in the foreshore shapes foreshore morphology. In the case of no net sediment movement on/offshore or in/out of the beach system over a specified period of time, the beach should theoretically sustain a dynamic equilibrium shape that is a function of the local wave regime. Net sediment movement offshore by waves or alongshore by longshore transport out of the beach system would result in erosion of the beachface. Understanding sediment transport in the foreshore is therefore crucial to predicting foreshore morphodynamic evolution through time; however, surf and swash zone dynamics are difficult to measure, model, or predict due to the turbulent nature of the flow, swash interactions, and high spatial and temporal variability.

One of the most important hydrodynamic factors controlling sediment transport is the near-bed shear stress (force per unit area), which depends on the flow velocity. There are various empirical and theoretical sediment transport formulas used to calculate bedload and bedload plus suspended load transport by swash uprush that are generally functions of uprush duration, beach slope, sediment friction angle, and flow velocity (e.g., Bagnold 1963, 1966; Hardisty et al, 1984). Field surveys of swash dynamics show that on the uprush, swash almost instantaneously accelerates to its maximum velocity, and then more gradually decreases to zero (Hughes et al., 1997). In contrast to this, flow velocity on the backrush increases gradually and reaches a maximum at its seaward extent. As sediment movement is directly related to bed shear stress (~fluid velocity), swash uprush has greater potential for mobilizing sediment at the point of instantaneous acceleration, and gradually deposits sediment of decreasing grain size upslope as the flow velocity decreases. The net sediment movement up or down slope is dependent on swash asymmetry, which is controlled by wave

height and period, grain size, and therefore beachface infiltration and exfiltration, and foreshore slope.

The foreshore slope, which controls the cross-shore width of the intertidal zone, is a function of grain size and wave energy (~wave height). Larger grains support a higher angle of repose relative to smaller grains, and thus a steeper beach slope. Low wave energy should theoretically promote berm deposition at the landward extent of high water swash and thus support a steeper foreshore slope, while higher wave energy should tend to erode the berm and flatten out the foreshore. Sediment transport in the foreshore, however, is influenced by more than just wave energy.

A simple model describes cross-shore sediment transport in the foreshore as a function of the relationship between swash zone dynamics and the beach groundwater-table exit point (Grant, 1948; Duncan, 1964). As discussed earlier, the position of the groundwater-table exit point with respect to the extent of swash run-up at any point during the tidal cycle determines if there will be infiltration or exfiltration of water through the beachface. For the case when the groundwater-table exit point is at a higher elevation than, and thus decoupled from, the maximum extent of swash run-up, the hydraulic gradient below the exit point will promote the exfiltration of water out of the beach face. The subsequent increase in swash depth will result in greater swash velocity and turbulent flow on the backrush, which acts to transport sediment seaward. Conversely, when the elevation of the groundwater-table exit point is below the maximum extent of swash run-up, such as during high tide, water will infiltrate into the beach face, and thus the swash backrush will have a decreased depth and velocity. The sediment that was transported upslope on the initial uprush will be deposited at or near the extent of the uprush, and therefore net sediment transport will be landward, driving berm and thus subaerial beach growth.

3.1.4 Bar-Built and Coastal Lagoon Beaches

Deviations from expected seasonal berm behavior on barrier islands, sand spits and bar-built pocket beaches (Fig. 3.2) have been related to tidally driven and storm surge run-up variability and berm overtopping (Hine, 1979; Weir et al., 2006; Jensen et al., 2009). Both Hine (1979) and Weir et al. (2006) identified 3-4 different modes of berm behavior and cross-shore sediment transport corresponding primarily to the spring-neap tidal cycle: (1) Following a period of high beach erosion and/or lagoon breaching that decreases both the berm crest height and foreshore slope, (2) berm growth occurs both vertically and horizontally, moving up and seaward as the rising and falling tide delivers sediment from the surf and lower swash zones. Although high wave energy serves ultimately to move sediment down slope, during spring tide and with sufficient wave conditions, swash overtopping of the berm induces vertical berm growth and seaward progradation as sand that is transported upslope with run-up is quickly deposited where swash velocity is essentially zero or at a minimum at the berm crest; (3) During neap tide, lower run-up elevations induce the growth of a 'neap berm' lower on the beachface, (4) which migrates up onto the main berm on the subsequent spring tide.

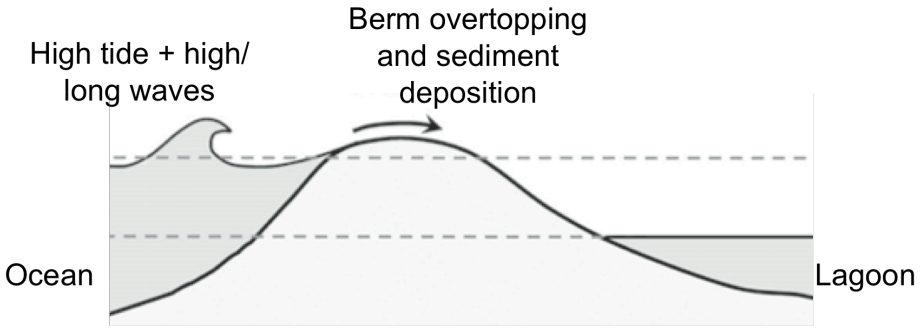

3.2: Typical profile of a bar-built or barrier island beach. Vertical growth and maintenance of the beach berm can result from run-up overtopping and subsequent sediment deposition during high wave and/or high tide events.

3.2 Objectives

The objective of this study is to assess seasonal changes in beach morphology on a coastal lagoon pocket beach, Younger Lagoon Reserve beach in Santa Cruz, California, and the processes and parameters that control the morphodynamics. More specifically, this study aims to characterize alongshore variations in morphology in terms of significant wave height, run-up, tide levels and water-table elevation, and subsequent foreshore hydrodynamics and sediment transport. As Younger Lagoon beach varies alongshore between a lagoon-backed beachface and a dune-backed beachface over a relatively short distance, comparing and contrasting the behaviors of these different zones will test if the processes that have been attributed to foreshore and berm variability on bar-built beaches, such as overtopping, have unique control on these environments.

As waves are the dominant force shaping much of the California coastline, it is expected that beachface parameters (e.g., foreshore slope) will vary primarily with changes in significant wave height and secondarily with factors such as the lagoon level and antecedent topography. Increasing significant wave heights in conjunction with increased North Pacific storm activity during the Northern Hemisphere winter months should cause erosion of the beachface unless berm overtopping occurs at a rate that supplies enough sediment to the berm and backshore system to sustain berm height.

3.3 Case Study: Younger Lagoon Beach, Santa Cruz, California

3.3.1 Background and Setting

Younger Lagoon Reserve is a generally undisturbed coastal lagoon and embayed pocket beach system located on the northern coast of the Monterey Bay (Fig. 3.3) and is part of the University of California Natural Reserve System. Since the uplifting of the 10-15 m high Miocene mudstone bluffs that bound the lagoon ~65,000 years ago (Perg et al., 2001),

in conjunction with the Holocene transgression over the last 5,000-10,000 years, wave action has pushed sand up into the relict drainage channel forming a coastal lagoon pocket beach. The modern beach is primarily maintained by alongshore transport of sand from the north within the Santa Cruz littoral cell, which extends from Point San Pedro north of Half Moon Bay south to the Monterey Submarine Canyon and is supplied primarily by a few small rivers and numerous streams flowing out of the Coast Ranges (Best and Griggs, 1991; Limber et al., 2008).

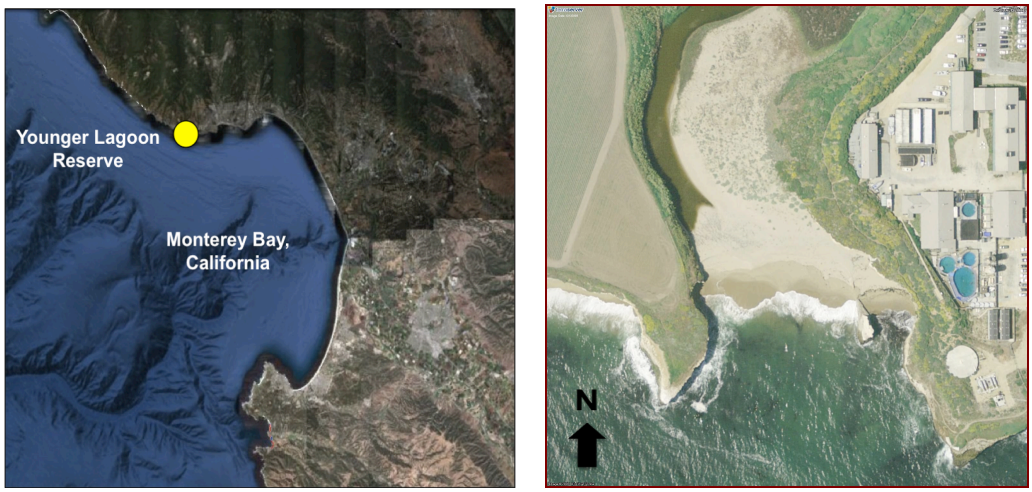

Fig. 3. 3: Study site Younger Lagoon Reserve (right), a lagoon and pocket beach system located in northern Monterey Bay, California (left).

Two sea stacks on eastern end of the beach—a larger stack in the intertidal zone equivalent in height to the surrounding bluffs and a smaller stack about one meter high landward of the large stack—create a small sub-pocket beach system on the eastern end of the beach (Fig. 3.4). On the western flank of the beach running perpendicular to the shoreline is a narrow lagoon channel that feeds water from the back-beach towards the ocean. During the summer months when the wave climate is dominated by long period and low energy Southern Hemisphere swell (e.g., Wingfield and Storlazzi), a berm forms at the mouth of the lagoon channel, and the channel becomes decoupled from the ocean. During

the winter months, the lagoon mouth may breach or break through the berm and connect with the ocean. This is a result either of increased wave energy due to a shift in the seasonal wave climate to higher energy Northern Hemisphere storm waves, elevated lagoon water levels due to increased precipitation and inland water recharge, or both, although the modest size of the drainage basin limits the extent and volume of recharge. Seasonal opening and closing of tidal inlets and lagoon channels that helps maintain important ecosystems for many anadromous species is a global coastal phenomenon and is particularly common along the Central Coast (Elwany et al., 1998; Ranasinghe and Pattiaratchi, 1999).

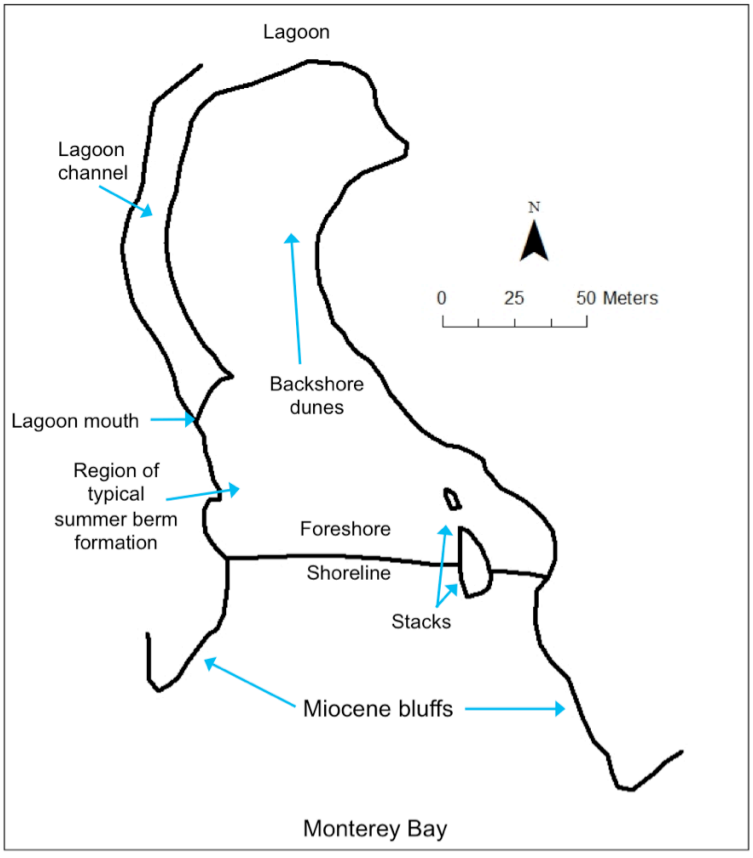

Fig. 3. 4: Plan view diagram of Younger Lagoon beach features

3.3.2 Methods: Total Station GPS Field Surveys

Six Global Positioning System (GPS)-equipped total station (laser theodolite) surveys were conducted at Younger Lagoon Beach between August 2010 and April 2011. GPS, in combination with a total station, allows for high resolution positioning of points on the ground with associated elevation values based on signal reflection line of sight between the total station instrument and a prism reflector, usually mounted on a rod of known height. Once a total station has been triangulated, it is azimuth-aware and able to measure the altitude of and distance to a prism reflector via infrared laser. Resulting X, Y, Z data points are immediately stored in the internal memory of the total station.

The system used in this study is the Trimble Geodimeter 640 Total Station. Prior to surveying, five fixed ground control points (Fig. 3.5) were established at the field site: three on the eastern cliff edge (CP0, CP2, CP3), one on a low stack located at the eastern end of the beach (CP1), and one low on the western cliff face (CP4). At the onset of each survey, level rods with total station reflector prisms were set up on level-rod support tripods directly over each control point, and a minimum of two control points were shot with the total station to establish the position of the instrument in space and to verify the accuracy and precision of the instrument operator.

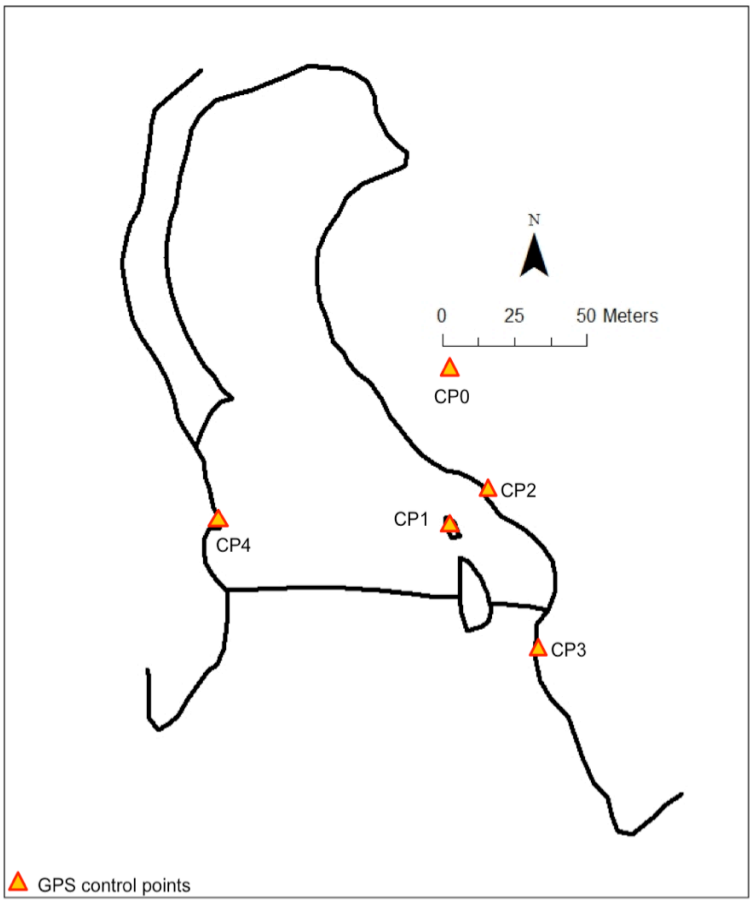

Fig. 3.5: Location of GPS control points (CP). CP0, 2, and 3 are located on the eastern bluff, CP1 is located on the low sea stack, and CP4 is located near the base of the western bluff.

Spacing and distribution of points for each survey were variable and determined by the position of topographic highs and lows and breaks in slope. More densely spaced data points were collected over regions of highly varying topography. For each survey, elevation data were collected from the maximum dune height in the backshore seaward into the swash zone. The seaward extent of swash data collected was constrained by the strength of the swash and water depth.

Sediment grab samples were collected coincident with the total station surveys for grain-size analysis. At least three samples about 1 m apart horizontally and between the

surface and about 10 cm depth within the sediment column were collected for the back beach, berm crest, foreshore, and swash zones in the region fronting the lagoon mouth as well as to the east of the lagoon mouth. Grain-size statistics were determined through sieve analysis (Sahu, 1965).

3.3.3 Data Processing and GIS Interpolation

The total station data points for each survey were downloaded directly from the total station memory and converted to ASCII point files. The files contained the easting, northing, and elevation positions of the data points in UTM Zone 10 coordinates, referenced to the NAVD88 vertical datum. The ASCII point files were subsequently converted to ArcGIS point-vector shapefiles. Continuous raster surfaces were interpolated from the point data using a natural neighbor interpolation algorithm (Sibson, 1981) with grid cell sizes ranging between 0.34 x 0.34 m and 0.40 x 0.40 m for the six surveys. Features unrelated to morphological changes due to sediment erosion or accretion—the two bedrock sea stacks on the eastern side of the beach, as well as an interpolated lagoon water surface were masked out of the raster surfaces in ArcMap. Natural neighbor interpolation is one of the most conservative interpolation methods in that it honors the original data points, being a weighted-average interpolation method that assumes that all minimum and maximum elevation points have been sampled, and as a result does not create artifacts. However, as it is a deterministic interpolation method that incorporates no additional information about the system other than the measured data points, it is difficult to determine interpolation uncertainty.

3.3.4 Transect Extraction and Volumetric Changes

Twenty-two shore-normal transects spaced at 10-m intervals were cast from the Mean High Water (MHW) shoreline to the landward extent of surveying using the Digital Shoreline Analysis System (DSAS) extension for ArcGIS (Thieler et al., 2009; Fig. 3.6). Beach profiles along nineteen of the transects (transects intersecting the sea stacks were

excluded) were extracted for all surveys from the respective raster datasets and processed in Matlab (The Mathworks, Inc.) to calculate individual profile parameters including the foreshore slope and berm crest elevation in reference to the MHW shoreline.

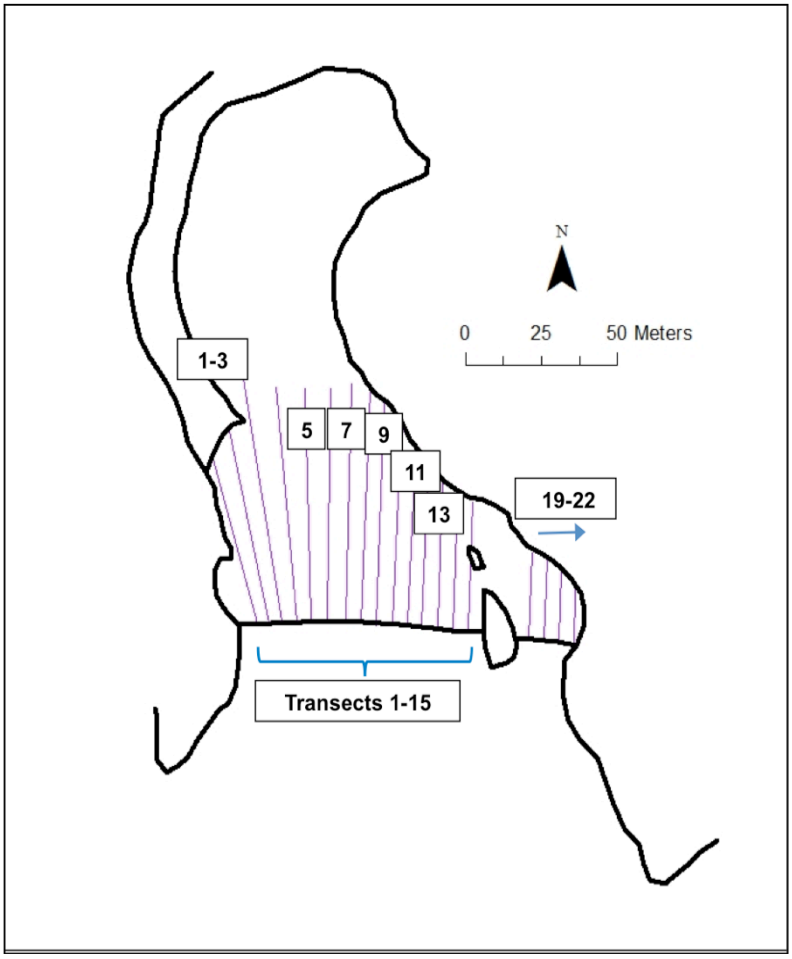

Fig. 3. 6: Shore-normal transects cast using the Digital Shoreline Analysis System (DSAS) extension for ArcGIS and from which beach profiles were extracted for each survey

Beach-volumetric changes between successive surveys were calculated using raster subtraction in ArcGIS. Successive survey rasters were differenced by subtracting the first survey in the temporal sequence from the second survey on a cell-by-cell basis, resulting in a matrix equal in size to the raster of coarsest grid cell resolution containing values of changes

in grid cell elevation between surveys with negative values for erosion and positive for accretion. Net volume change is the sum of total erosion and total accretion.

3.3.5 Run-Up Distributions

Seasonal variations in beach parameters were compared to deep-water spectral wave density and direction data from the NOAA National Buoy Data Center (NDBC) Monterey Bay Buoy (station 46042), located approximately 40 km southwest of Younger Lagoon Reserve in a water depth of 2098 m, and tide level data from the NOAA National Ocean Service Center for Operational Oceanographic Products and Services (NOS/CO-OPS) tide gauge for Monterey, CA. Swash run-up distributions based on beach slope, significant wave height and average wave period data at hourly intervals for the month prior to each survey were determined using the empirical methodology of Stockdon et al. (2006). Run-up distributions in conjunction with tide levels were then used to calculate inundation ranges at specific shore-normal transects and assess berm overtopping potential.

3.4 Results

3.4.1 Oceanographic Data

Approximately monthly Younger Lagoon beach morphology surveys began in August 2010 and were concluded in April 2011. The mean significant wave height of the month prior to each survey increased by over a meter between August 2010 and November 2010 from 1.4±0.3 m to 2.7±0.9 m. They decreased by less than half a meter between November 2010 and March 2011, and increased again to an average height of 2.9±0.9 m in April 2011 due to late season storms (Fig.3.7). The maximum significant wave height over the month prior to each survey increased between all surveys except between January 2011 and March 2011, and was 70-170% higher than the mean significant wave heights. Dominant wave directions were primarily from the northwest, with a small proportions of 1 to 2 m southwesterly waves

characterizing the August 2010 and October 2010 surveys (Fig. 3.8), reflecting low-energy Southern Hemisphere swell that is typical of summer and late fall wave conditions along the California coast.

The lagoon water level increased from 2.25-3 m (above NAVD88) between August 2010 and March 2011 and decreased to 2.6 m between March 2011 and April 2011 (Fig. 3.9). In this study, variations in the lagoon level are assumed to reflect relative variations in the beach water-table elevation.

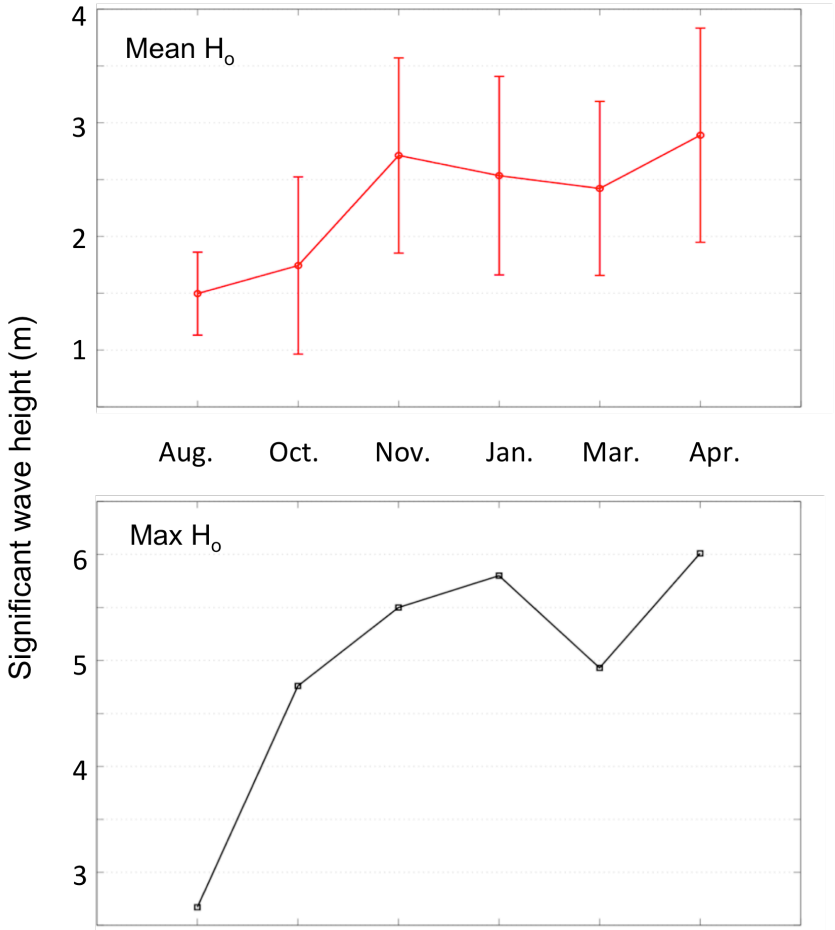

Fig. 3. 7: Monthly averaged (one month prior to each survey) deep-water significant wave heights (H_o) from NDBC buoy 46042 plus or minus one standard deviation (top); Maximum monthly wave heights from NDBC buoy 46042 (bottom)

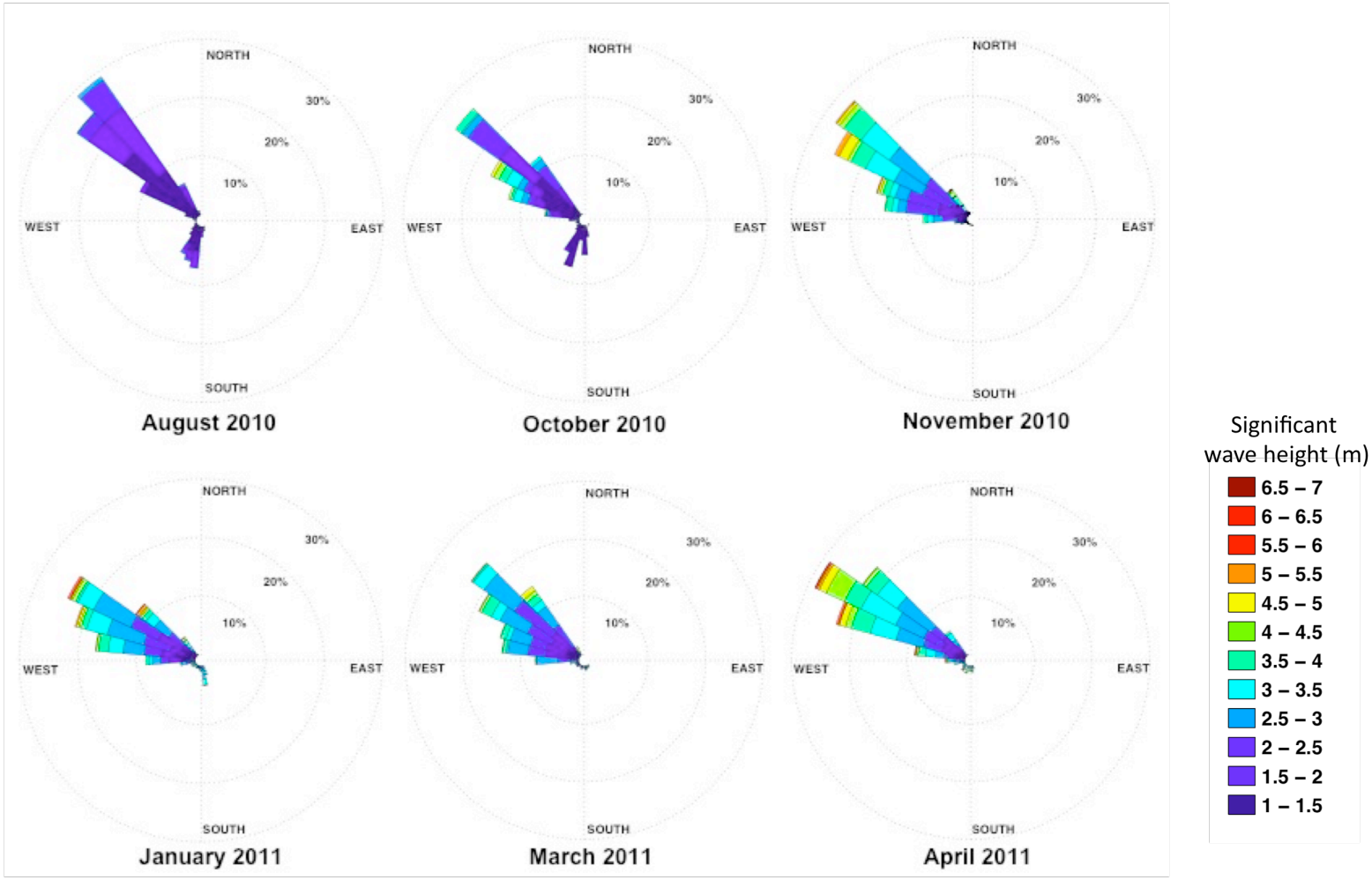

Fig. 3. 8: Dominant wave direction and significant wave heights for all frequency bins for the month prior to each survey

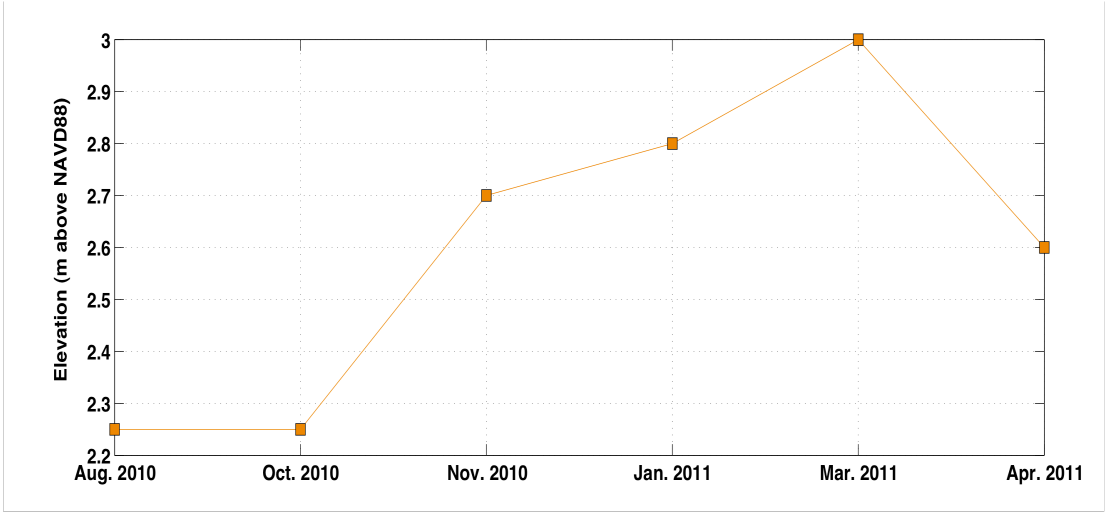

Fig. 3. 9: Lagoon water level in meters above the NAVD88 vertical datum measured for each survey

The six surveys were conducted at various phases within the spring-neap tidal cycle. The November 2010 survey was conducted at peak spring tide, while the January 2011 survey was conducted at neap tide. The August 2010, October 2010, March 2011, and April 2011 surveys were conducted during the transition between neap and spring tides (Fig. 3.10).

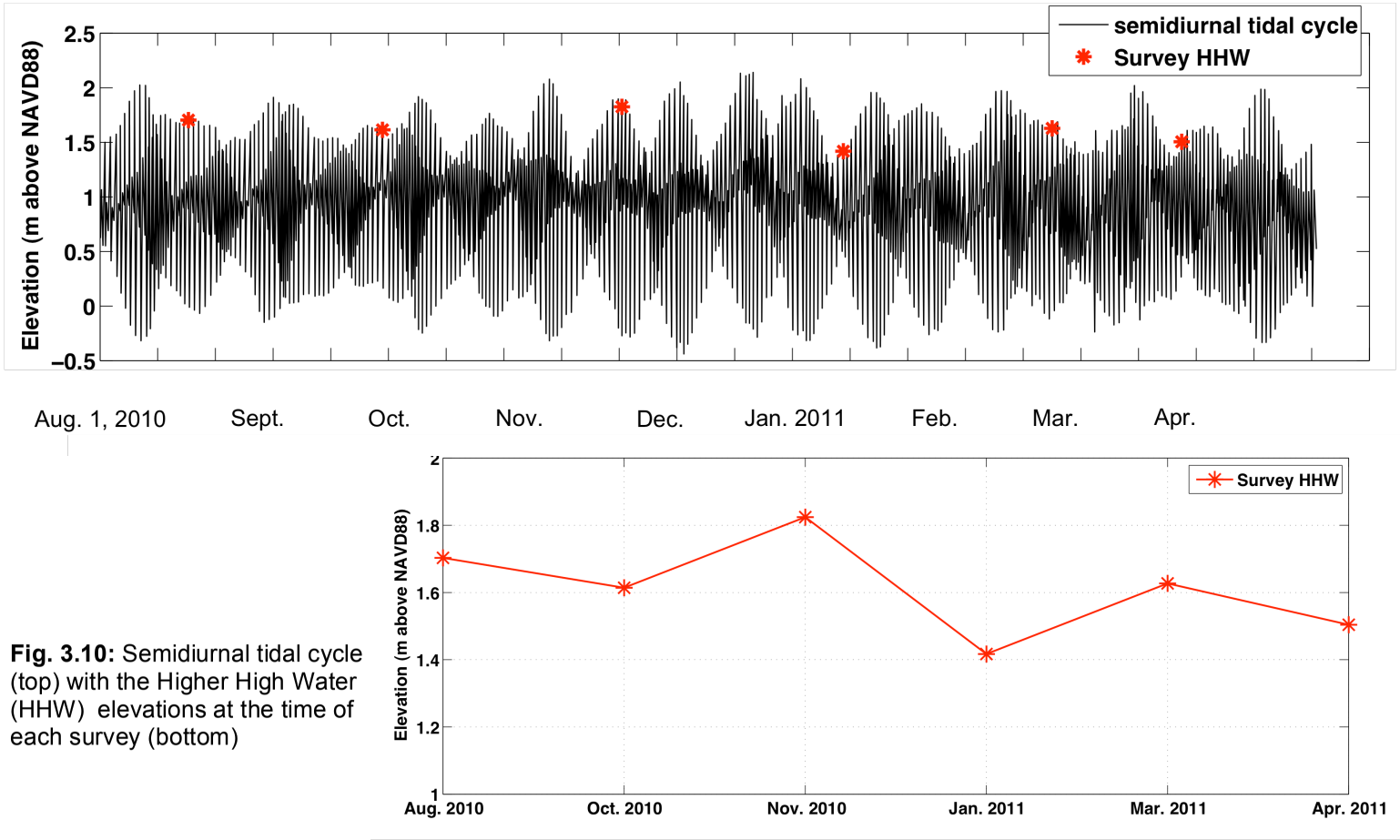

Fig. 3.10: Semidiurnal tidal cycle (top) with the Higher High Water (HHW) elevations at the time of each survey (bottom)

3.4.2 Error and Uncertainty

The error and uncertainty associated with elevation and volumetric change calculations are primarily due to the total station point reading uncertainty, which is a function of both the total station accuracy and precision and error associated with manual positioning of the prism rod. The maximum root mean square error (RMSE) in total station elevation readings calculated from repeat measurements of known fixed control points from all combined survey data is ±0.03 m, while the maximum horizontal uncertainty is 0.1 m. A prism rod that is not positioned exactly vertically will have an apparent height (H_A) equal to the known height of the rod (H) multiplied by the cosine of the angle (α) offset from the vertical (Fig. 3.11):

$$H_A = H\cos(\alpha)$$

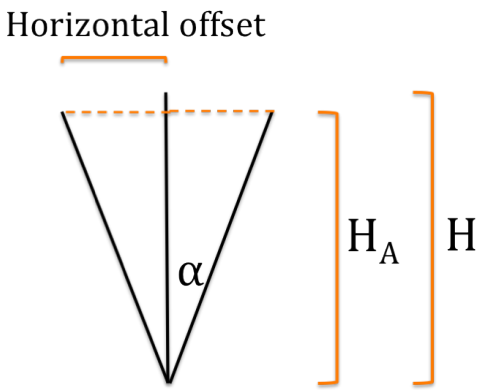

Fig. 3. 11: Horizontal and vertical uncertainties associated with a survey rod held at an angle, α, to the vertical

Thus, the magnitude of the vertical uncertainty is the difference between the true and apparent height of the rod, and the magnitude of the horizontal error is the sine of the angle offset multiplied by the true height:

$$\text{Vertical uncertainty} = H - H_A$$

$$\text{Horizontal uncertainty} = H\sin(\alpha)$$

The error in elevation associated with manual positioning of a 1.457 m high prism rod is -0.02 m. However, the maximum error in the horizontal associated with the manual rod positioning was estimated to be ~0.3 m. The manual positions errors were estimated by assuming a maximum angle offset of the prism rod from the vertical of no more than 10º at any particular point.

The surveying methodology at Younger Lagoon Reserve Beach was designed to accurately and precisely capture the variability in beach morphology; however, it is likely that additional uncertainty was introduced into the final raster surfaces due to interpolation. As the deterministic nature of natural neighbor interpolation method makes it difficult to calculated interpolation uncertainties, a conservative vertical uncertainty estimate of 2% of the maximum elevation above MHW, or ±0.2 m was used. The total horizontal error in the final raster surfaces is 0.3 m, and the elevation error is ± 0.1 m.

3.4.3 Beach Elevation and Volumetric Changes

Between August 2010 and October 2010 (Fig. 3.12), a significant amount of erosion (-0.1 to -1.8 m of vertical change) occurred in the foreshore across most of the beachface with the highest erosion (-1.5 to -1.8 m) occurring on the western side of the beachface in the foreshore fronting the lagoon mouth. Moderate accretion (+0.1 to +0.4 m) occurred the central berm and backshore regions. The cross-shore position of the lagoon mouth and lagoon water level did not change significantly. The changes in beach elevation that occurred between August 2010 and October 2010 equate to approximately 390 m^3 of net erosion of sediment from the beach (Table 3.1).

Between October 2010 and November 2010, approximately 0.1 to 1.2 m of vertical erosion occurred over the central foreshore, whereas approximately 0.1 to 1.2 m of vertical accretion directly surrounding the stack (Fig. 3.13). The changes in beach elevation that

occurred between October 2010 and November 2010 equate to approximately 230 m^3 of erosion, which is the smallest volumetric change between any two successive surveys.

Significant erosion over the beach occurred between November 2010 and January 2011 (Fig. 3.14). The region surrounding the sea stacks and backshore and berm in front of the lagoon mouth decreased in elevation during this period, with only a few areas in the foreshore and dunes showing low-to-moderate (+0.1 to +0.4 m) accretion. The leading edge of the lagoon mouth also migrated approximately 10 m seaward during this period. The regions of highest erosion—the backshore fronting and just east of the lagoon mouth and the area surrounding the sea stacks—were accretionary between October 2010 and November 2010. The net volumetric change between surveys November 2010 and January 2011 was 1120 m^3 of erosion.

The only net accretionary period occurred between January 2011 and March 2011 (Fig. 3.15). The foreshore and berm fronting the lagoon mouth increased in elevation between 0.1 and greater than 1 m. The lagoon mouth also migrated approximately 20 m seaward during this period. With only approximately 190 m^3 of erosion, primarily in front of the lagoon mouth and over the dunes, the net volumetric change between January and March was about +800 m^3.

The beach underwent the greatest net volumetric change between March 2011 and April 2011 (Fig. 3.16). Erosion of up to 1 m occurred over almost the entire swash and foreshore, including the region to the east of the sea stacks. The change in beach elevation that occurred between March and April equated to almost 1280 m^3 of erosion.

Table 3.1: Summary of accretion, erosion, and net volumetric change between consecutive surveys with 5% uncertainties in net volumetric change

Survey	Total Accretion (m^3)	Total Erosion (m^3)	Net volumetric change (m^3)	Uncertainty (m^3)
Aug.-Oct. 2010	+250	-640	-390	± 20
Oct.-Nov. 2010	+310	-540	-230	± 10
Nov. 2010-Jan.2011	+190	-1310	-1120	± 60
Jan.-Mar. 2011	+940	-140	+800	± 40
Mar.-Apr. 2011	+110	-1280	-1170	± 60
NET	**+1800**	**-3900**	**-2100**	**± 100**

Aug. 2010-Oct. 2010

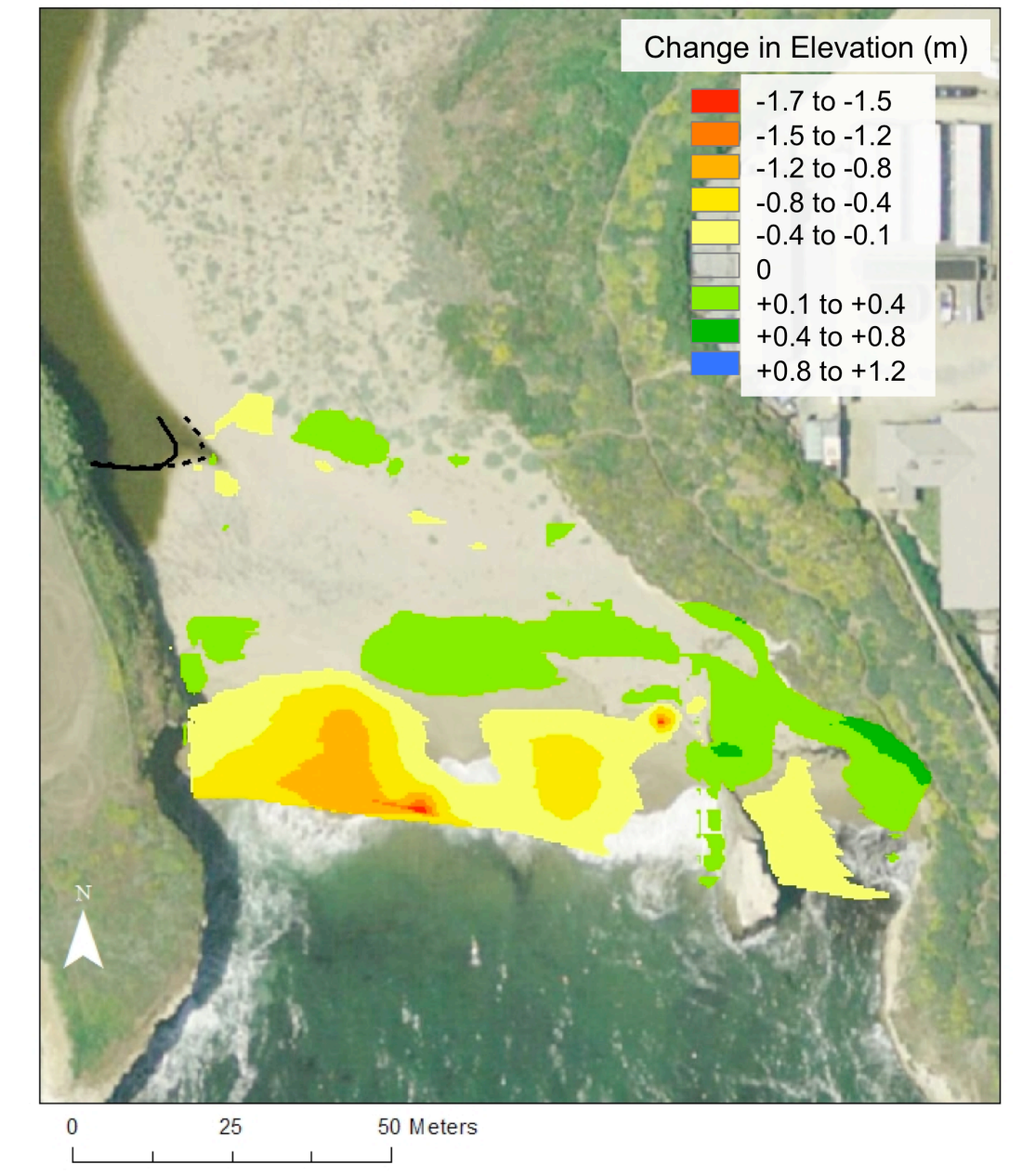

Fig. 3.12: Elevation changes between August 2010 and October 2010. The solid black line represents the position of the lagoon mouth in August, while the dashed black line represents the position of the lagoon mouth in October.

Oct. 2010-Nov. 2010

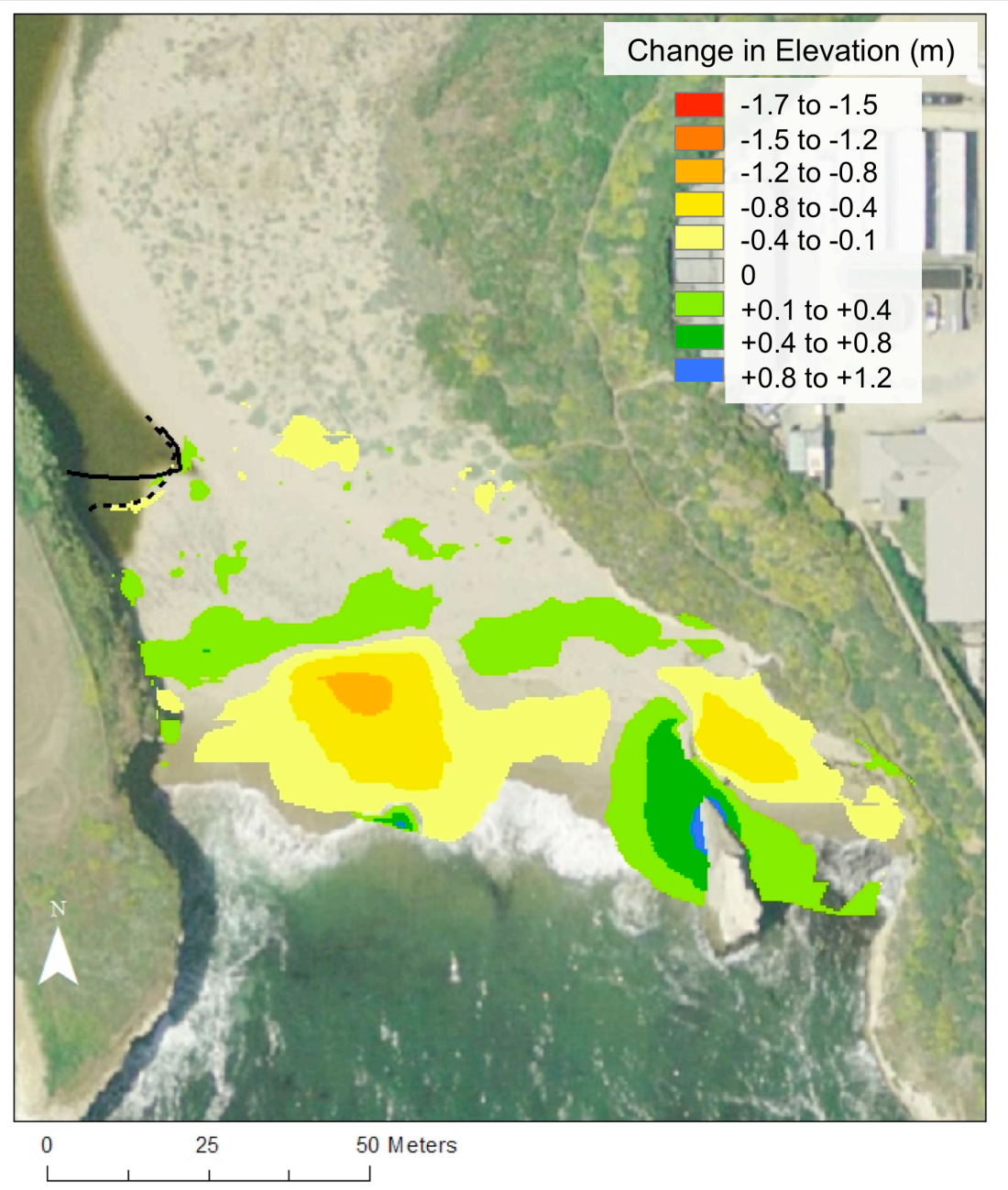

Fig. 3.13: Elevation changes between October 2010 and November 2010. The solid black line represents the position of the lagoon mouth in October, while the dashed black line represents the position of the lagoon mouth in November.

Nov. 2010-Jan. 2011

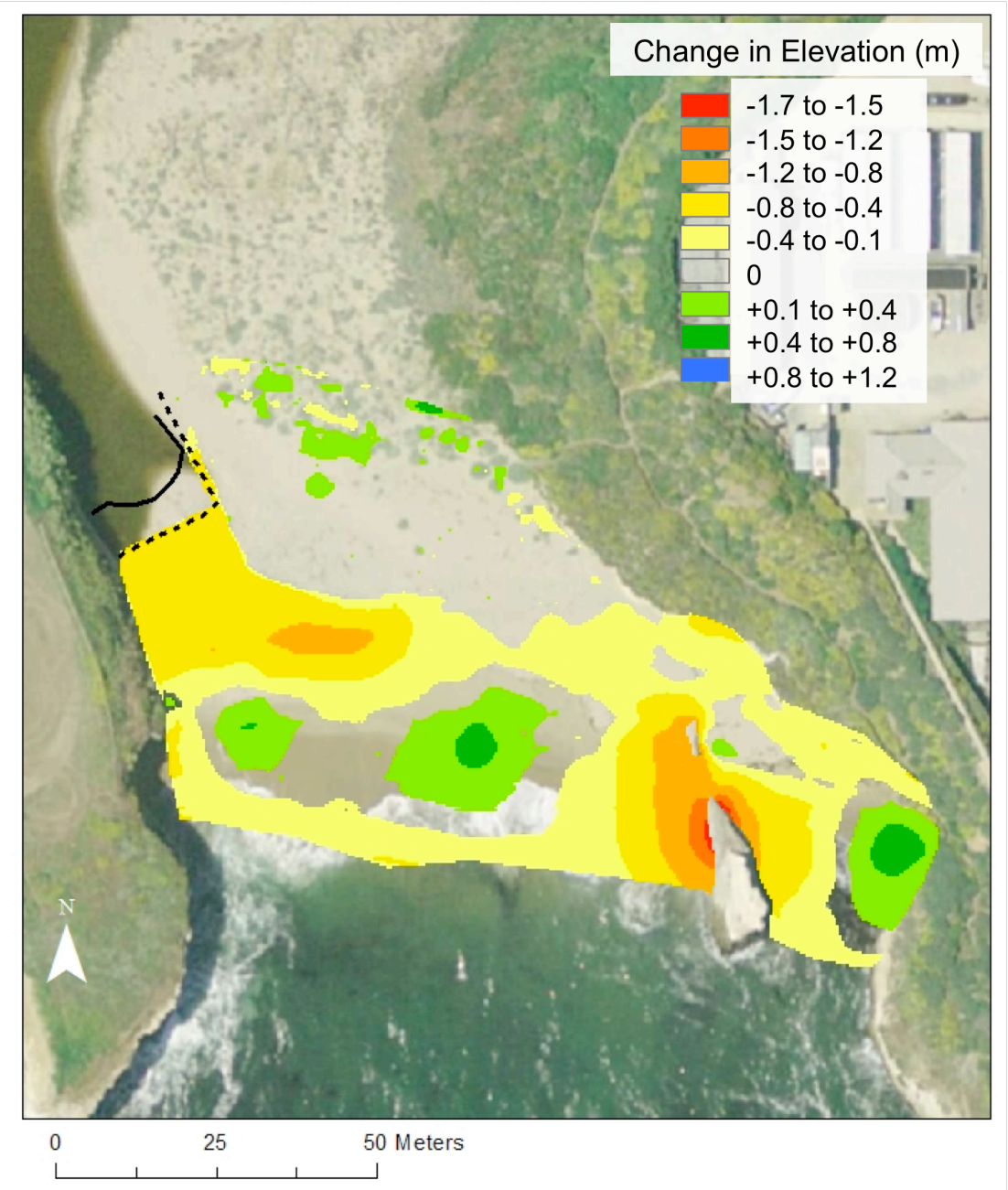

Fig. 3.14: Elevation changes between November 2010 and January 2011. The solid black line represents the position of the lagoon mouth in November, while the dashed black line represents the position of the lagoon mouth in January.

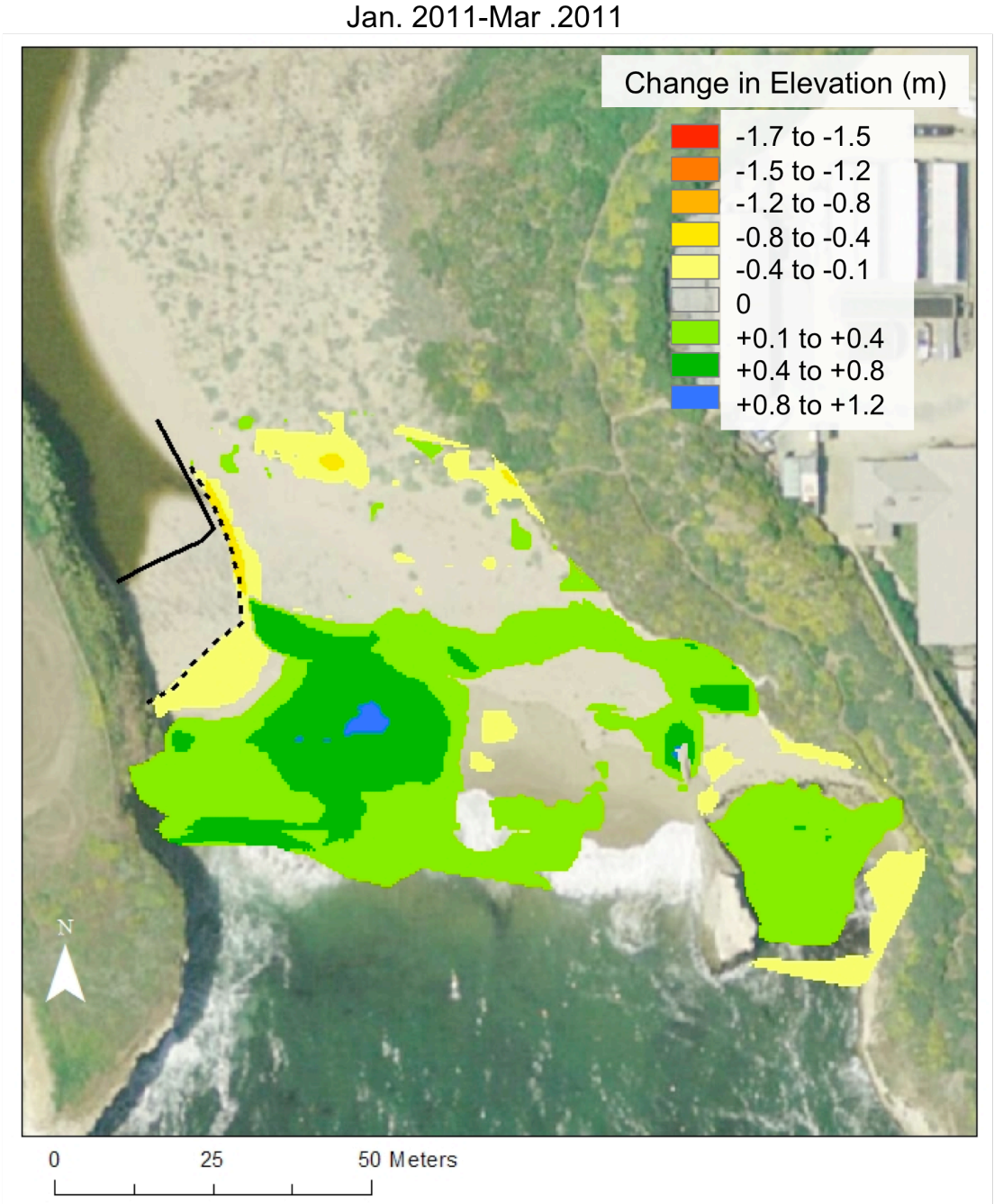

Fig. 3.15: Elevation changes between January 2011 and March 2011. The solid black line represents the position of the lagoon mouth in January, while the dashed black line represents the position of the lagoon mouth in March.

Mar. 2011-Apr. 2011

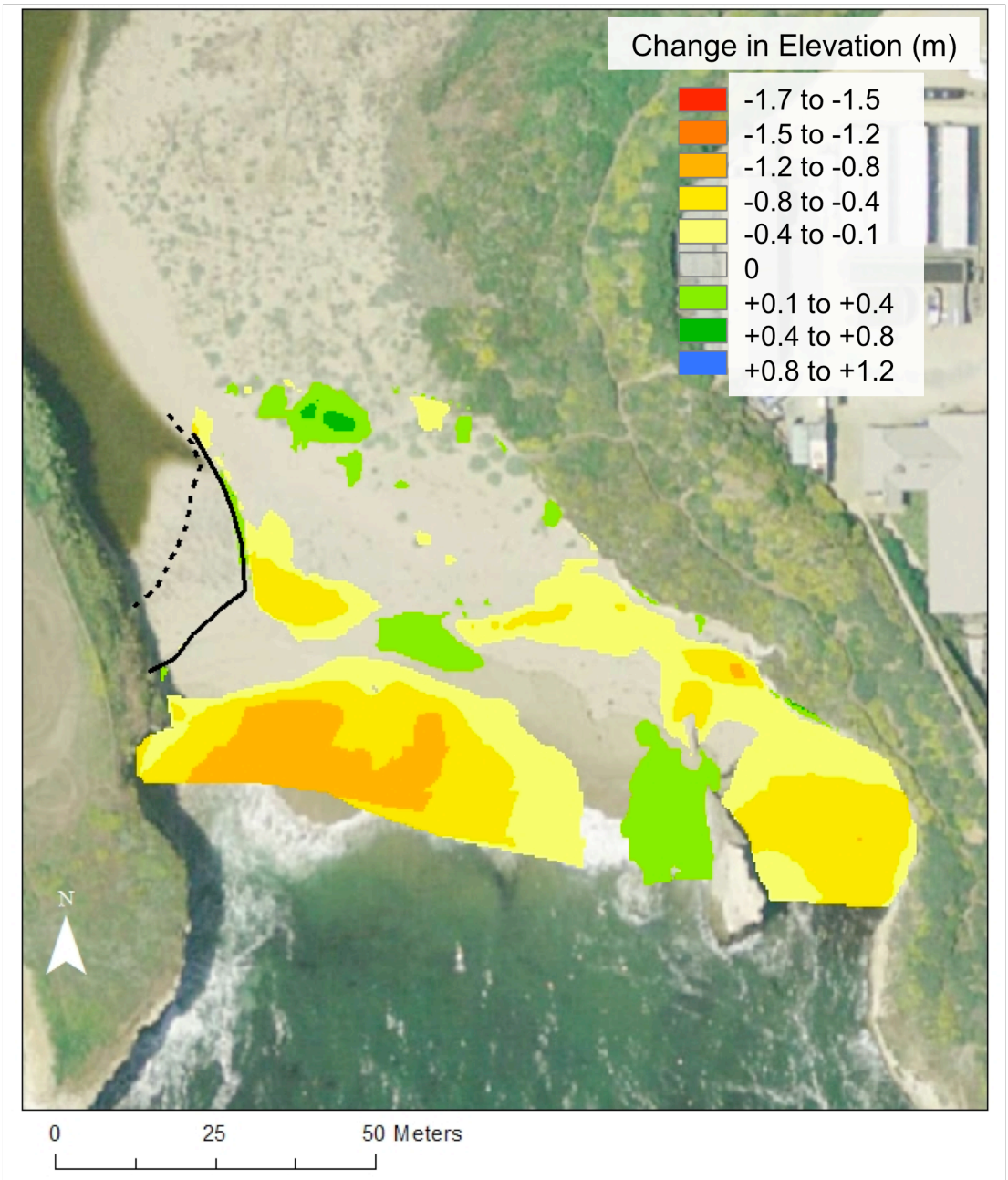

Fig. 3.16: Elevation changes between March 2011 and April 2011. The solid black line represents the position of the lagoon mouth in March, while the dashed black line represents the position of the lagoon mouth in April.

3.4.4 Transect Profiles

Analysis of the shore-normal transects shows significant spatial and temporal variability in the beach profile (Table 3.2). The berm crest at transect 1 (see Fig. 3.6) in front of the lagoon stayed more or less at an equilibrium position both horizontally along the profile and vertically throughout the survey period, with only a slight seaward migration between August 2010 and October 2010 (Fig. 3.17). The berm crest was basically a null point about which the profile swelled and contracted. During the fall and early winter months of the survey period (August-November), the backshore was high and broad, varying only slightly between 3.2-3.8 m in elevation. Between November 2010 and January 2011, the backshore had decreased significantly in elevation to less than or equal to 3 m and sloped landward . The foreshore at transect 1 steepened by about 5% between the first and second surveys, and then did not show significant change until January 2011 when the slope remained constant but the entire foreshore decreased in elevation by approximately 0.5 m. The foreshore regained this elevation between January and March 2011, and then between March 2011 and April 2011, steepened by about 6% to the greatest slope observed for transect 1 over the entire survey period. Transects 2 (Fig. 3.18) and 3 (Fig. 3.19) showed similar behavior to transect 1, although with more variability in the cross-shore berm position and berm height.

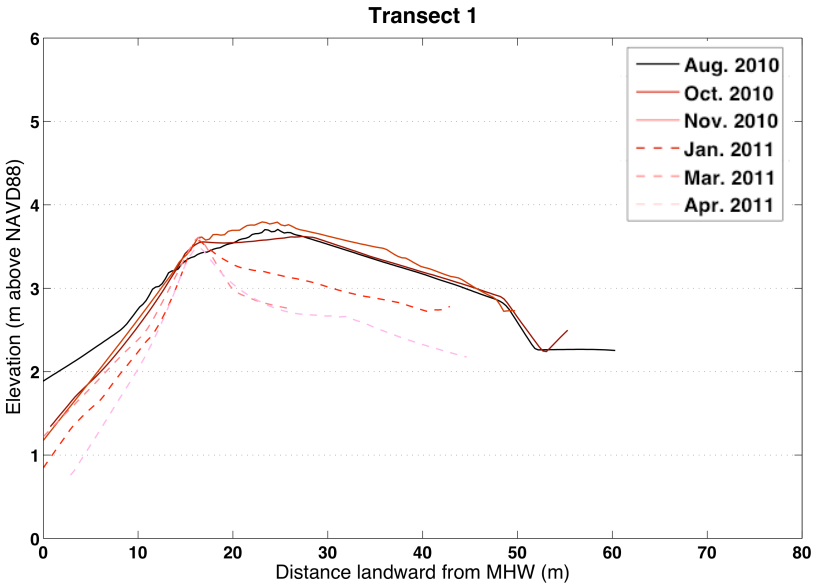

Fig. 3.17: Beach profiles associated with transect 1 for all survey periods

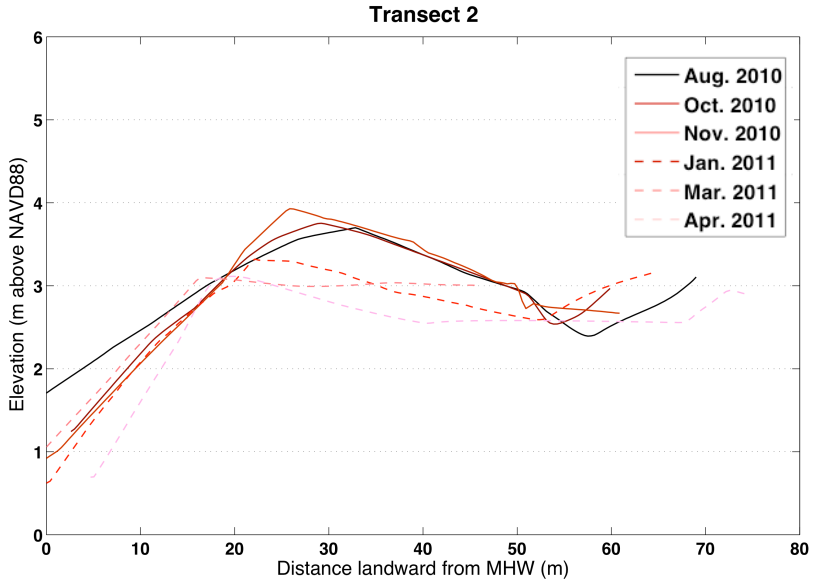

Fig. 3.18: Beach profiles associated with transect 2 for all survey periods

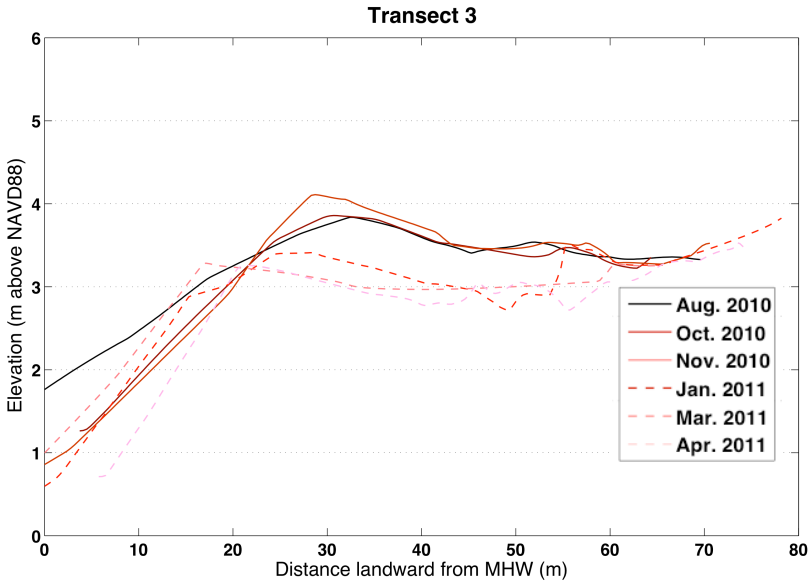

Fig. 3.19: Beach profile associated with transect 3 for all survey periods

Transects 5, 7, and 9, which lay to the east of the lagoon mouth, had distinctly different profile shapes compared with transects 1, 2, and 3. Between August 2010 and November 2010, the profile at transect 5 (Fig. 3.20) developed a steep foreshore and scarp, and the backshore flattened out between the berm and dunes. Farther east at transects 7 (Fig. 3.21) and 9 (Fig. 3.22), the berm became less prominent feature in the profile both spatially and temporally, and the backshore was predominantly seaward sloping. At transects 11 and 13 (Figs. 3.23 and 3.24), the berm was effectively undetectable after the first survey in August 2010, and the profile was relatively planar and entirely seaward sloping.

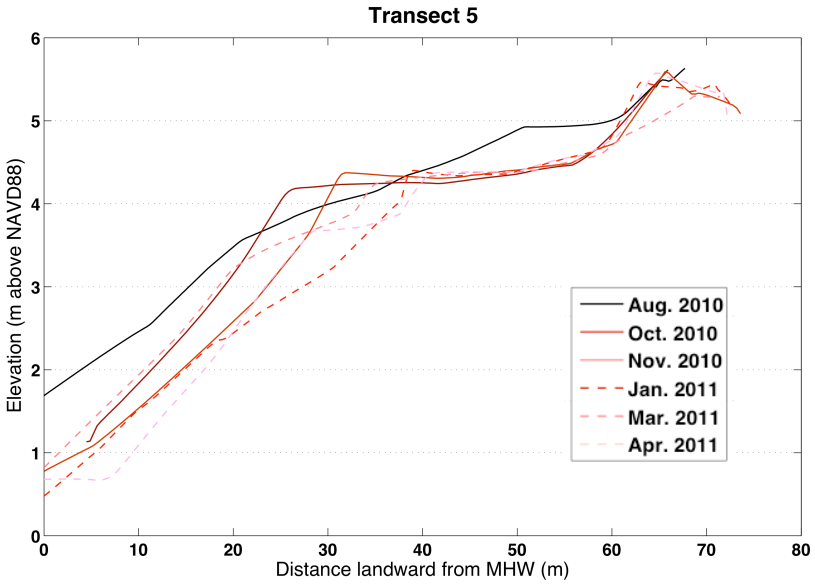

Fig. 3.20: Beach profiles associated with transect 5 for all survey periods

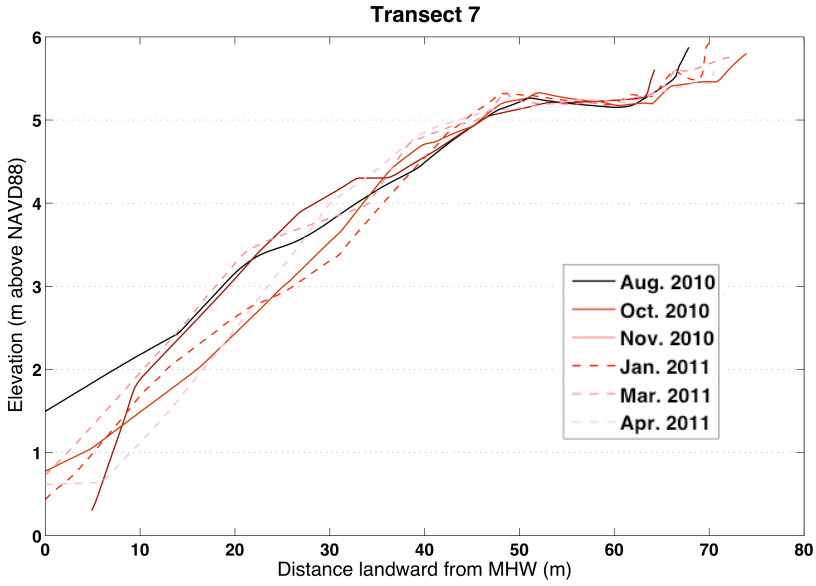

Fig. 3.21: Beach profiles associated with transect 7 for all survey periods

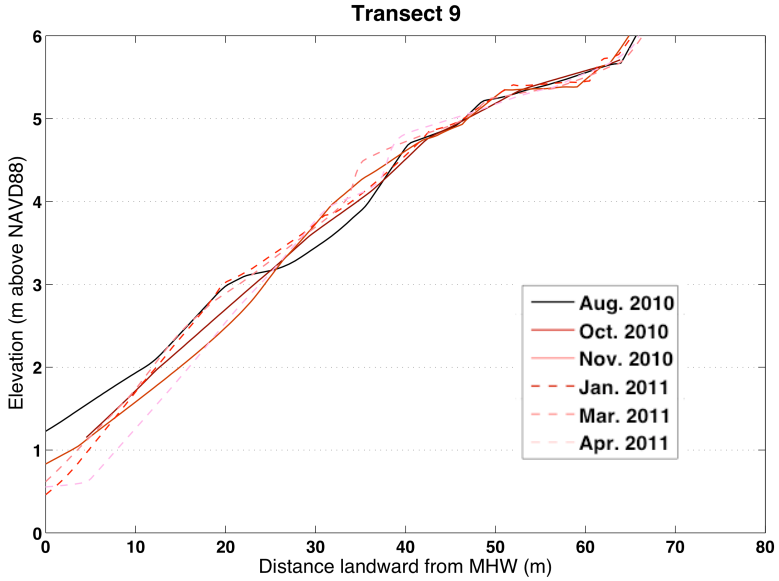

Fig. 3.22: Beach profiles associated with transect 9 for all survey periods

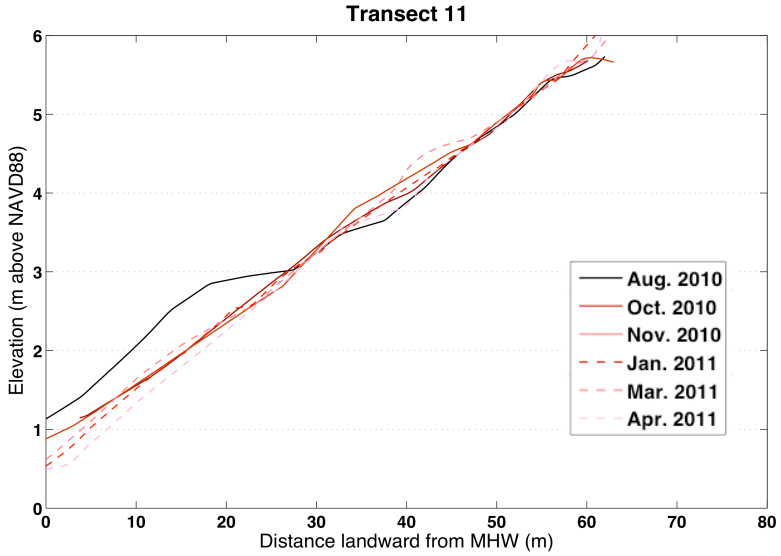

Fig. 3.23: Beach profiles associated with transect 11 for all survey periods

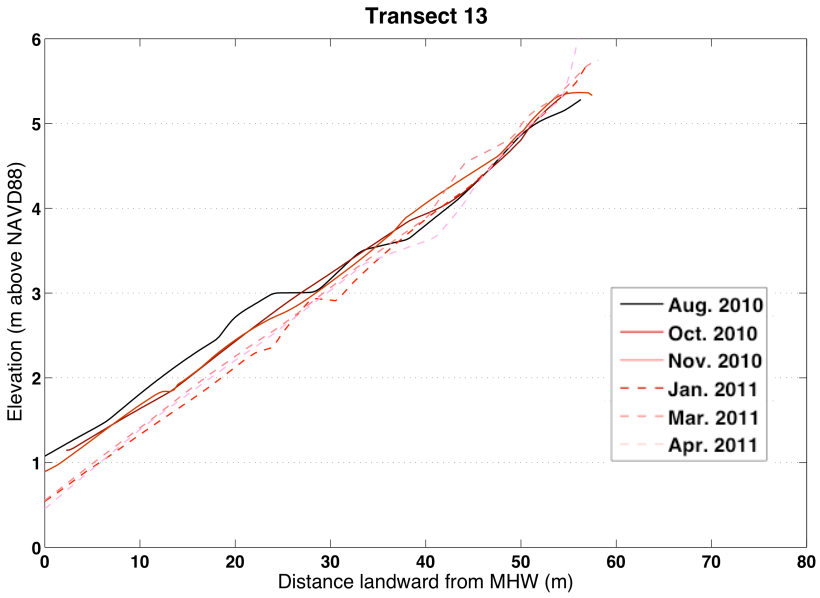

Fig. 3.24: Beach profiles associated with transect 13 for all survey periods

Table 3.2: Summary of beach parameters for transects 1-3, 5, 7, 8, 11, and 13 for all surveys

Transect	*1	*2	*3	5	7	9	11	13
Foreshore Slope								
Aug. 2010	8.5%	7.6%	7.2%	15.6%	14.7%	14.2%	15.3%	12.0%
Oct. 2010	13.6%	11.3%	11.7%	15.9%	12.7%	11.1%	10.4%	10.1%
Nov. 2010	14.8%	11.7%	11.3%	9.8%	9.1%	9.6%	7.4%	7.7%
Jan. 2011	14.9%	13.6%	15.0%	10.3%	11.2%	13.0%	9.8%	7.8%
Mar. 2011	13.0%	12.6%	13.3%	11.3%	12.7%	11.0%	8.8%	8.3%
Apr. 2011	18.5%	18.2%	17.4%	13.2%	13.6%	12.3%	9.7%	8.7%
Berm Crest Height (m above NAVD88)								
Aug. 2010	3.7	3.7	3.8	4.1	3.4	3.1	2.9	3.0
Oct. 2010	3.6	3.8	3.9	4.2	4.3	NDB	NDB	NDB
Nov. 2010	3.8	3.9	4.1	4.4	4.7	NDB	NDB	NDB
Jan. 2011	3.6	3.3	3.4	2.4	2.8	3.0	2.5	2.9
Mar. 2011	3.6	3.1	3.3	3.4	3.6	4.5	NDB	NDB
Apr. 2011	3.5	3.1	3.3	3.7	4.0	3.9	3.6	3.4
Cross-Shore Berm Position from MHW line (m)								
Aug. 2010	24.7	32.8	32.4	26.4	23.1	21.9	18.8	25.1
Oct. 2010	16.8	29.2	30.7	26.4	33.8	NDB	NDB	NDB
Nov. 2010	23.2	26.0	28.8	31.6	40.3	NDB	NDB	NDB
Jan. 2011	16.2	22.0	24.4	18.3	22.6	19.8	21.0	27.7
Mar. 2011	16.3	16.4	17.2	22.8	23.5	35.3	NDB	NDB
Apr. 2011	16.2	19.1	21.5	23.9	28.7	31.3	34.4	34.1

* Denotes transects fronting lagoon mouth
NDB= No distinguishable berm

3.4.5 Alongshore Comparisons: Transects 1-3 vs. 10-12

Alongshore variability in beach parameters, specifically the influence of the lagoon on foreshore morphology, was examined by comparing three transects in front of the lagoon mouth (T1-3) and three transects ~40 m east of the lagoon mouth (T10-12) backed by dunes and a 10-m high bluff (Figs. 3.25, 3.26).

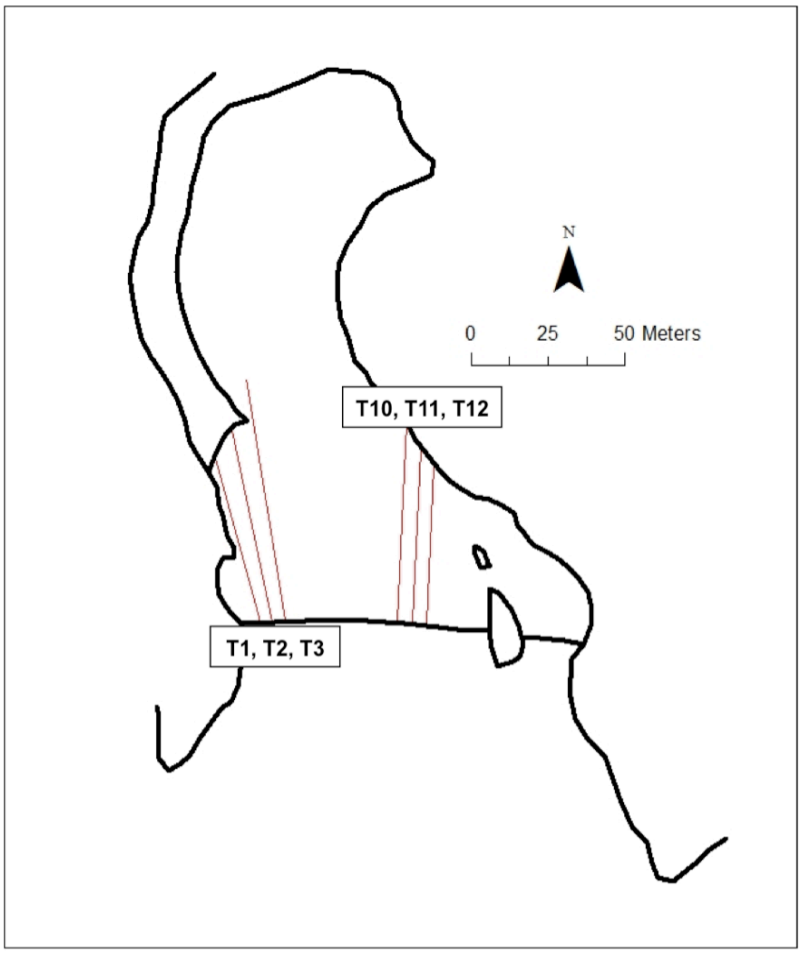

3.25: Location of transects (T) 1, 2, 3, and 10, 11, 12.

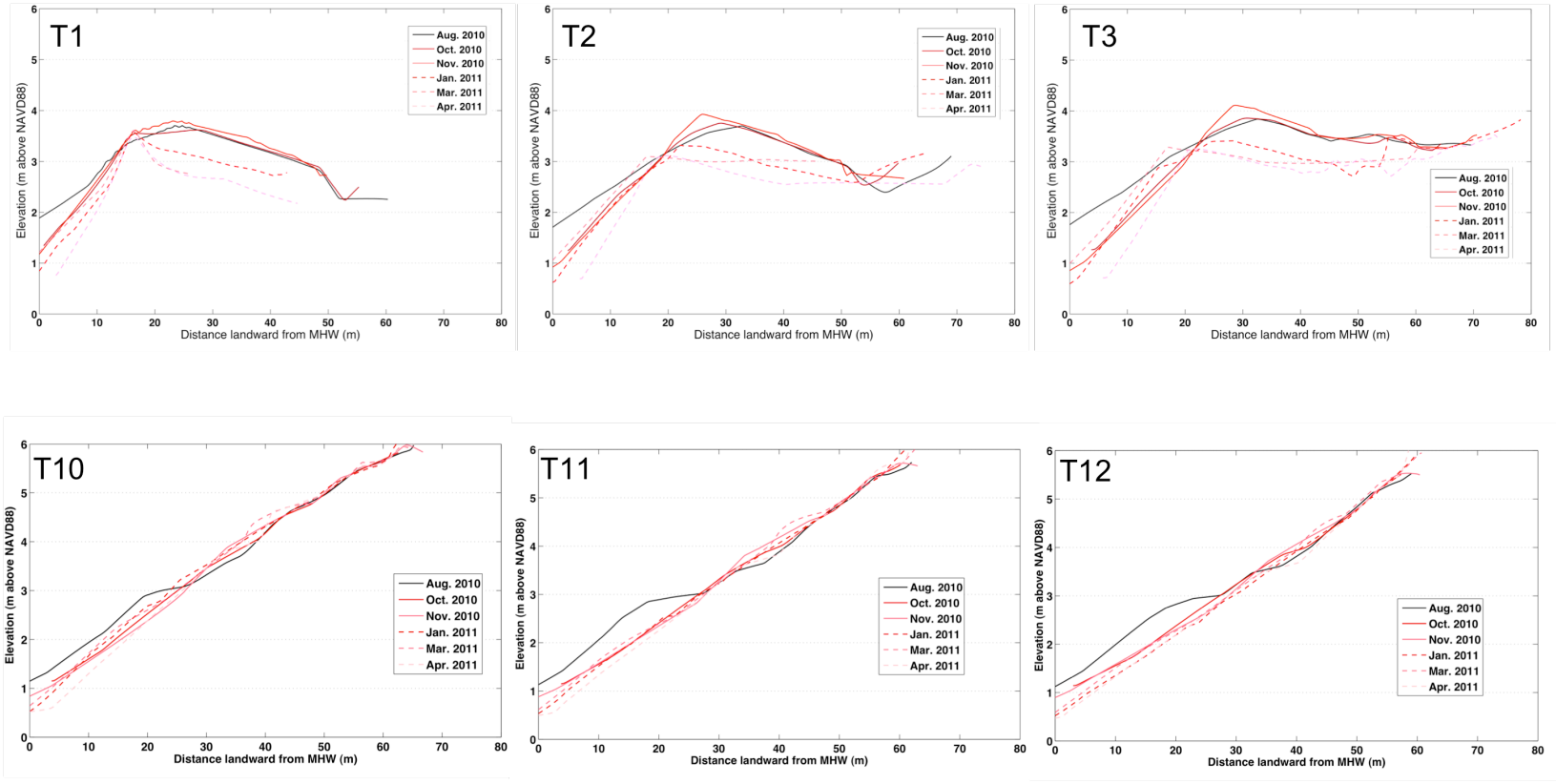

3.26: Profiles of transects (T) 1, 2, 3, and 10, 11, 12 over all surveys

3.4.6 Grain-Size Results

All of the grain-size surveys yielded moderately well- to well-sorted quartz sediment ranging from medium-grained sand (0.25-0.50 mm) to coarse-grained sand (0.50-1.00 mm). The swash zone fronting the lagoon mouth (T1 to 3) consisted of mainly medium-grained sand throughout all surveys, except for the April 2011 survey, which was characterized by a coarse-grained swash zone (Fig. 3.27). The swash zone at transects 10-12 was composed of similar size sand with transects 1-3 and exhibited similar trends in grain size variation through all surveys, except between March 2011 and April 2011, when the mean grain size decreased. There is an excursion in the mean grain size for both sets of transects from about 0.4 mm to 0.25 mm and then back up to about 0.45 mm between October 2010 and January 2011.

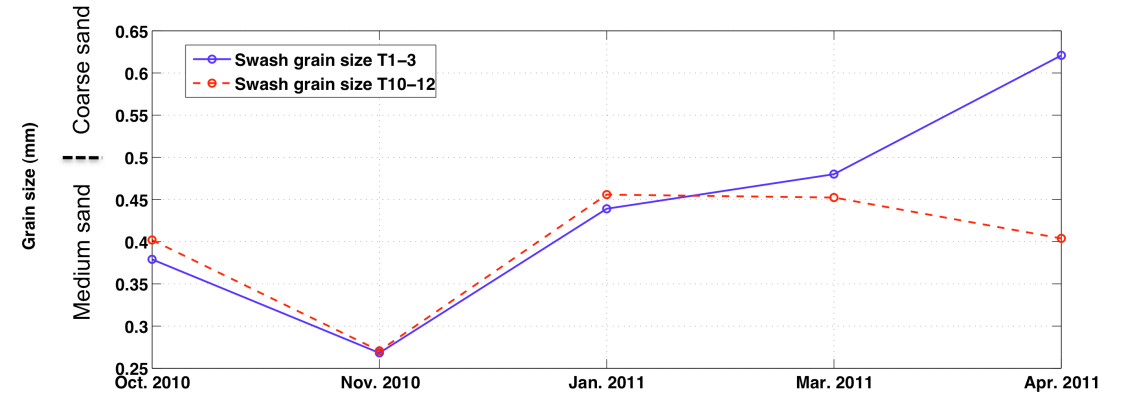

3.27: Swash zone mean grain size over all surveys for transects 1-3 (blue) and 10-12 (red)

The foreshore at transects 1-3 consisted primarily of medium-grained sand throughout the entire survey period with a narrow range in mean grain size (Fig. 3.28). The foreshore at transects 10-12 consisted primarily of medium-grained sand for the October and November 2010 and January 2011 surveys, and coarse sand during the August 2010 and March and April 2011 surveys.

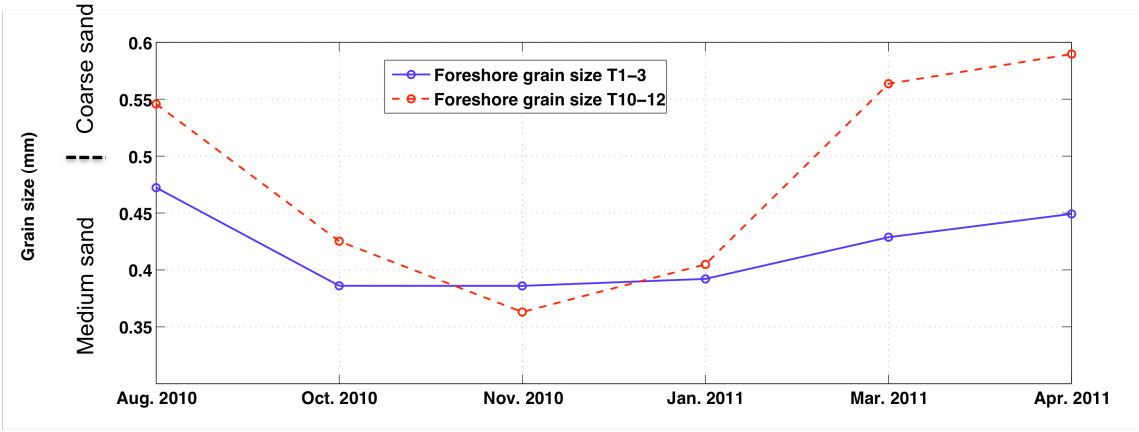

3.28: Foreshore mean grain size over all surveys for transects 1-3 (blue) and 10-12 (red)

The berms at transects 1-3 and transects 10-12 were composed of medium-grained sand for all surveys (Fig. 3.29). For transects 10-12, the berm grain size represents the mean grain size of the region between the high water line and dunes during surveys when a berm was not present. The mean berm grain size for both sets of transects also show a general increasing trend through time.

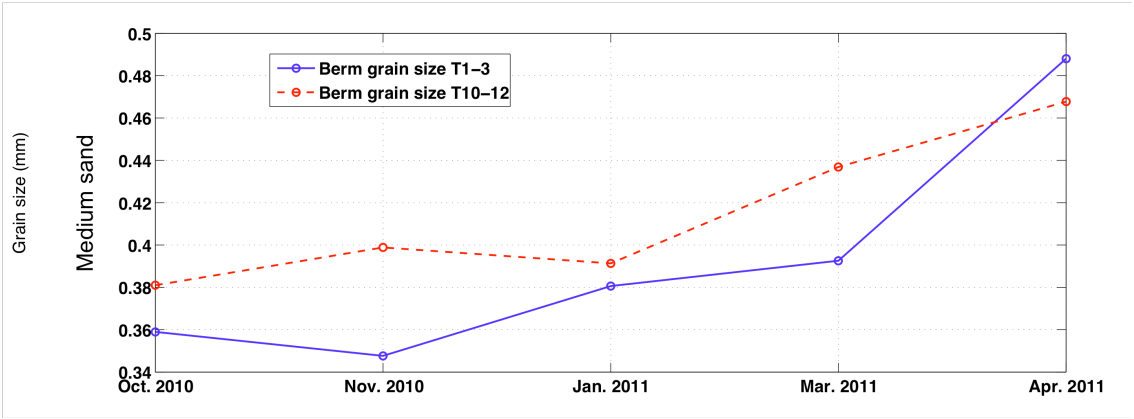

3.29: Berm (or region between the foreshore and backshore) mean grain size over all surveys for transects 1-3 (blue) and 10-12 (red)

3.4.7 Foreshore Slope Variability

The foreshore slopes associated with transects 1, 2, and 3 ranged between 0.06 and 0.2 and show a general increase between August 2010 and April 2011 (Fig. 3.30). In contrast, the foreshore slopes of transects 10, 11, and 12 ranged between 0.08 and 0.12 and did not show any obvious trends over time.

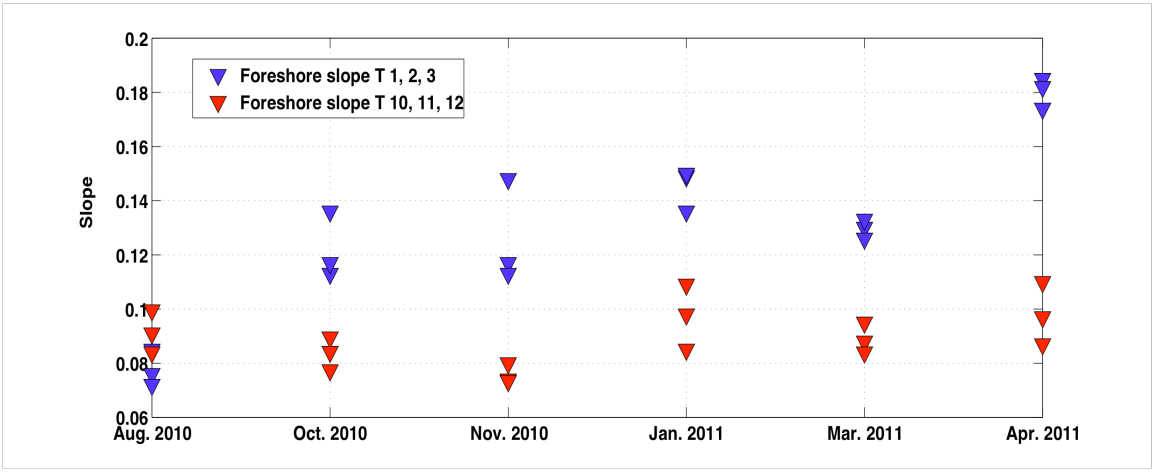

Fig. 3.30: Foreshore slopes of transects 1, 2, 3 (blue) and 10, 11, 12 (red) for all surveys

It is generally expected that the foreshore slope of a beach should decrease with increasing significant wave height as the higher-energy waves erode sand from the upper beachface and berm and transport it seaward or offshore. There is positive correlation at the 0.01 significance level between the foreshore slopes of transects 1, 2, and 3 and the mean significant wave height for the month prior to each survey (Fig. 3.31). There is no correlation between mean significant wave height and foreshore slopes for transects 10, 11, and 12.

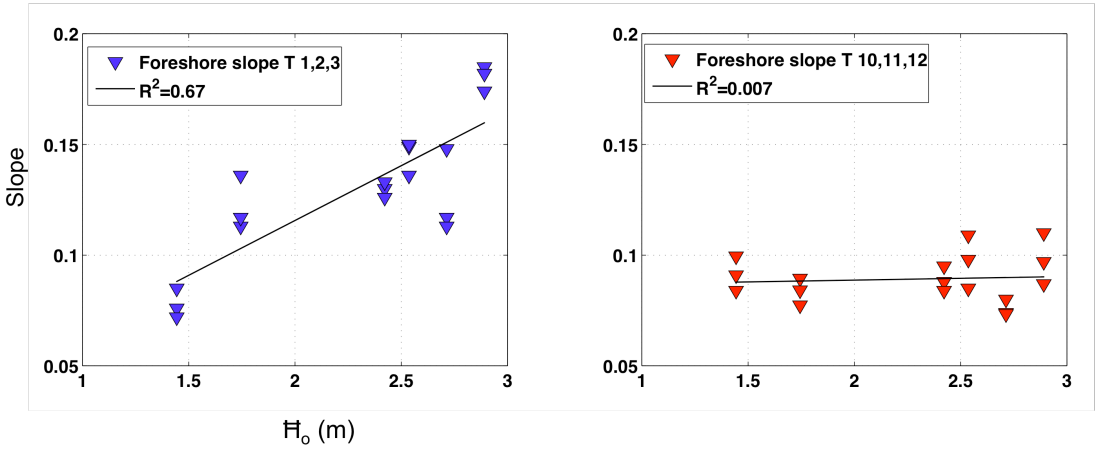

Fig. 3.31: Linear regressions of foreshore slope vs. mean significant wave height ($H_o$bar) for transects 1, 2, 3 (blue, left) and 10, 11, 12 (red, right)

In developing an empirical model to simulate variations in cross-shore hydrodynamic processes during the tidal cycle, Masselink and Short (1993) developed a parameter, the 'relative tide range' (RTR), for quantifying the tidal effects, where RTR is the ratio of the tide range (TR) to the wave height (H):

$$RTR = \frac{TR}{H} \qquad (3.1)$$

This parameter is a measure of the relative effects or importance of tides versus waves. The greater the RTR, the more influence the tidal range has on foreshore hydrodynamics and morphology relative to waves (and vice versa when the RTR is low). The results of Masselink's simulations actually suggested that on beaches with a relative tide range greater than 2 m, the beach profile was essentially insensitive to changes in wave height.

A similar parameter was developed for this study, the lagoon-wave height ratio (LWR), which is the ratio of the lagoon level (LL, referenced to NAVD88) to the mean significant wave height ($H_o$bar), and thus indicates the relative influences of the lagoon level and wave height on foreshore hydrodynamics:

$$LWR = \frac{LL}{\overline{H}_o} \qquad (3.2)$$

A relatively high LWR would indicate a comparatively high lagoon level relative to the mean significant wave height, while a relatively low LWR would indicate that waves dominate foreshore hydrodynamics. The lagoon level serves as a proxy for the relative water-table elevation, while the significant wave height and shallow-water wave transformation control wave set-up and run-up at the coast, which increases the mean water level at the shoreline.

While a significant correlation between mean significant wave height and foreshore slope fronting the lagoon mouth (transects 1-3) has already been demonstrated, when the slopes are plotted as a function of the LWR, the magnitude of the correlation increases slightly from R=0.82 (slope as a function of wave height only) to R=-0.86, which is significant at less than the 0.01 significance level (Fig. 3.32). Whether or not the increase is significant is questionable, but a small increase in the correlation would be expected based on the fact that waves are the primary dynamic force doing work on the foreshore, while the position of the water-table elevation is a secondary relatively static feature that controls the position of the groundwater exit point on the foreshore in relation to the extent of swash run-up.

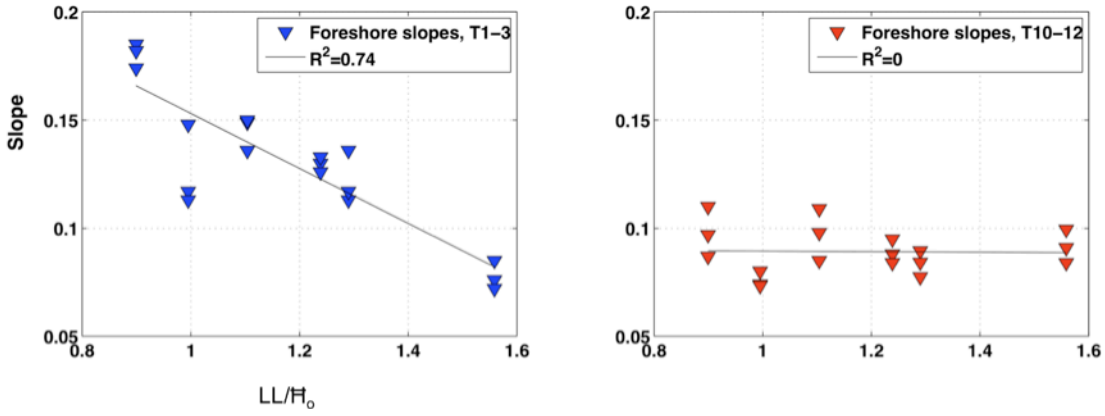

3.32: Linear regressions of foreshore slope vs. the lagoon-wave height ratio (LWR) for transects 1, 2, 3 (blue, left) and 10, 11, 12 (red, right)

3.4.8 Run-up and Berm Overtopping

The second characteristic difference between transects 1-3 and transects 10-12 is the stable versus ephemeral nature of the berm. The berm is a ubiquitous feature in transects 1-3, but is only a distinguishable feature in transects 10-12 in August 2010 and less distinguishable in January 2011 and April 2011. The beach profile characteristic of transects 10-12 is essentially planar for all surveys after August 2010. Berm overtopping has been shown to be an important process for building up and maintaining berm height (e.g., Weir et al., 2006). Berm overtopping can only be achieved if the swash run-up elevation above a defined reference datum is greater than the berm height, and if there is enough of a decrease in the beach slope landward of the berm to significantly decrease subsequent downrush depth and energy.

Distributions of run-up elevations above Mean High Water (MHW) compared with the average berm height for the survey *prior* to the month of wave observations utilized to calculate run-up show that only a small proportion (0.007-0.02) of run-up at high tide could have resulted in berm overtopping between August 2010 and October 2010 and January 2011-March 2011 (Figs. 3.33, 3.34).

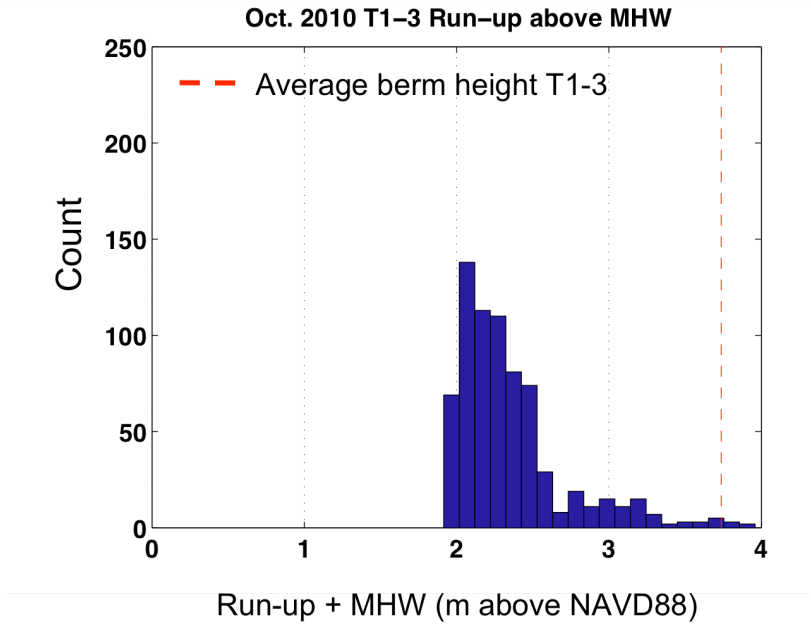

3.33: Distribution of run-up elevations above MHW determined using the empirical methods of Stockdon et al. (2006) between Sept. 2010 and Oct. 2010. The dashed red line indicates the mean berm height of transects 1-3 in Aug. 2010. Data points in the distribution greater than the mean berm height would have induced overtopping.

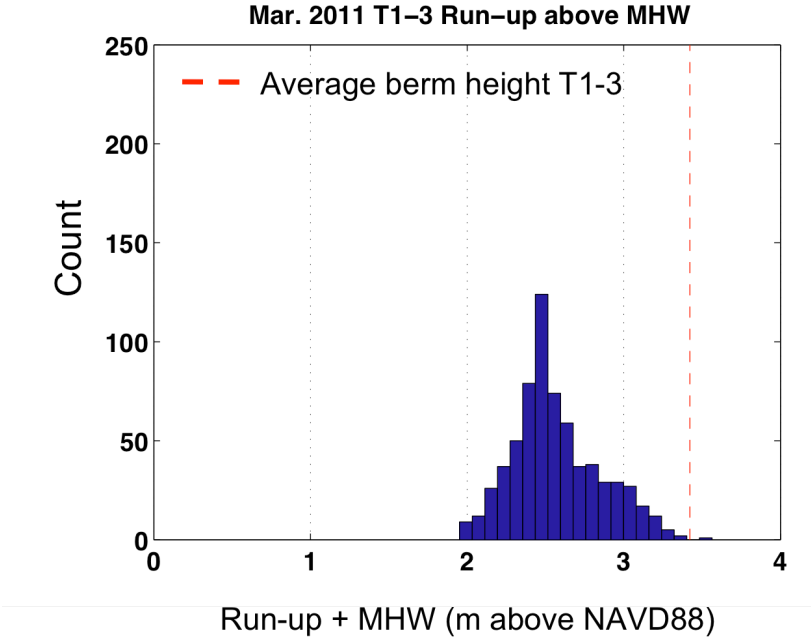

3.34: Distribution of run-up elevations above MHW determined using the empirical methods of Stockdon et al. (2006) between Feb. 2011 and Mar. 2011. The dashed red line indicates the mean berm height of transects 1-3 in Jan. 2011.

Between about 4-6% of the calculated run-up distribution was high enough to overtop the berm during high tide between October 2010 and November 2010 (Fig. 3.35), and between 12-22% of run-up was high enough between March 2011 and April 2011 (Fig. 3.36).

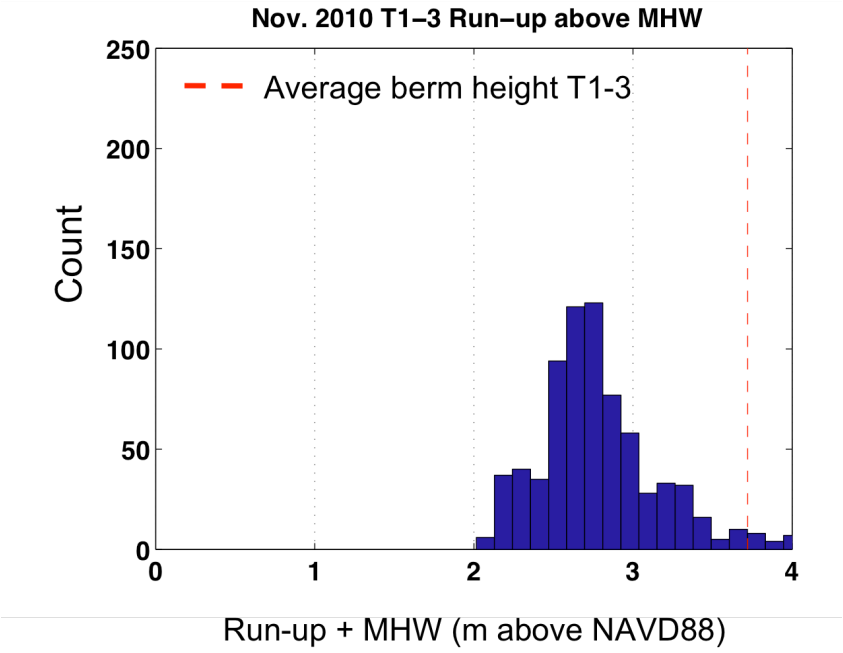

3.35: Distribution of run-up elevations above MHW determined using the empirical methods of Stockdon et al. (2006) between Oct. 2010 and Nov. 2010. The dashed red line indicates the mean berm height of transects 1-3 in Oct. 2010.

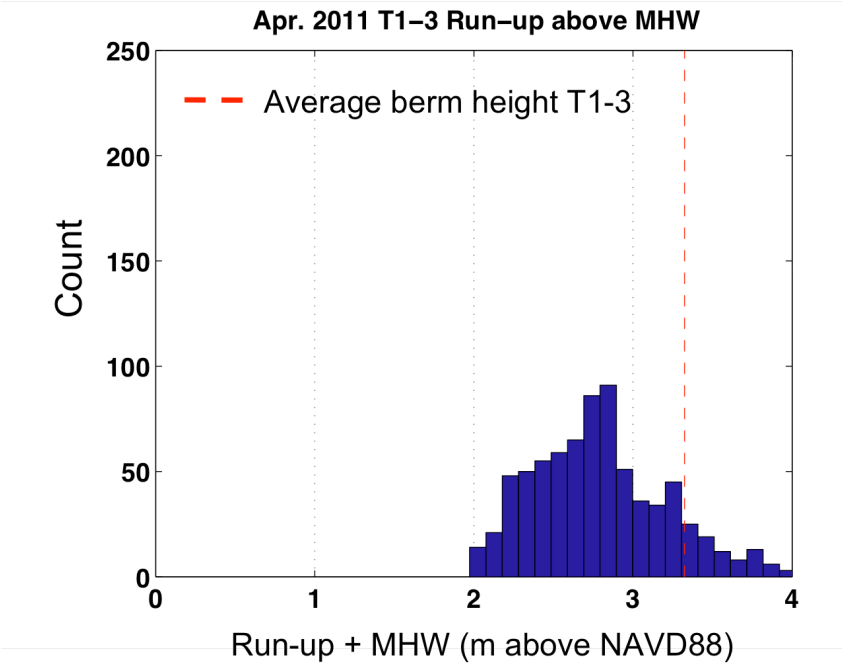

3.36: Distribution of run-up elevations above MHW determined using the empirical methods of Stockdon et al. (2006) between Mar. 2011 and Apr. 2011. The dashed red line indicates the mean berm height of transects 1-3 in Mar. 2011.

The change in berm height between surveys when overtopping was predicted relative to MHW is correlated at the 0.05 significance level with the logarithm of the proportion of run-up that produces overtopping (P_{ovetop}) when P_{ovetop} is between 0.002 and 0.04 (Fig. 3.37). The same correlation exists at the 0.10 significance level relative to MHHW when P_{ovetop} is between 0.01 and 0.06. Although the median run-up elevations were greater for transects 10-12 compared with transects 1-3, there is no prominent and ubiquitous berm present for overtopping to occur.

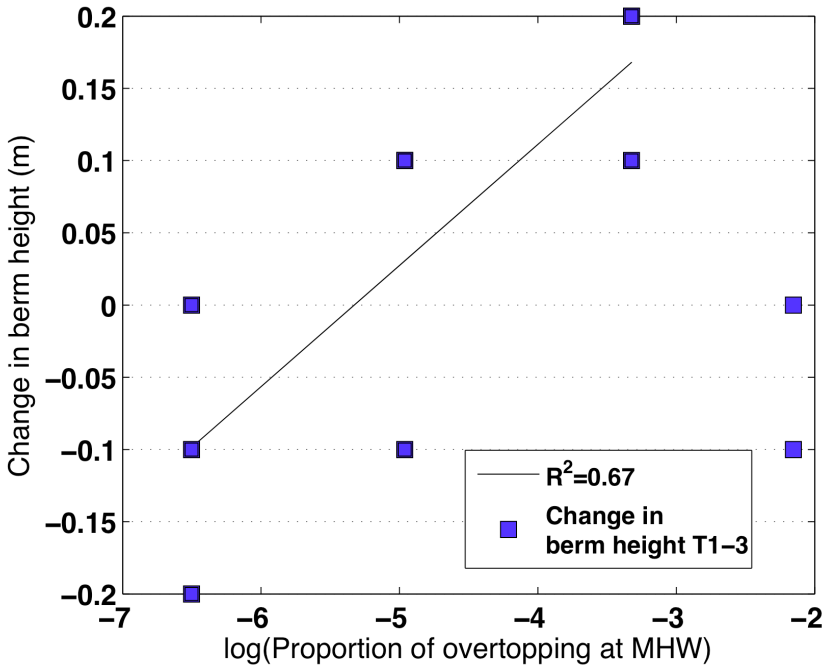

3.37: Change in berm height vs. log($P_{overtop}$) relative to MHW showing correlation when 0.002< $P_{overtop}$ <0.04 (-7<log($P_{overtop}$)<-3). Log($P_{overtop}$)>-3 data not included in regression.

3.5 Discussion

The morphological changes observed at Younger Lagoon Reserve beach do not conform to the commonly predicted progression of seasonal beach profile variability due to alongshore variability in the backshore. Observations and conceptual models of the physical forces and feedbacks acting on the shoreline show that many beaches in California should, and do, become flat and narrow as a result of higher energy waves during the winter months. Bar-built beaches, however, have demonstrated uniquely different seasonal behaviors that result in changes to the beachface that are contrary to what would be expected. Younger Lagoon beach is a wave-dominated reflective embayed beach, meaning that wave energy minimally dissipated as waves approach the shoreline. Changes in beach morphology are highly correlated with wave height, while secondary parameters such as the water table

elevation and tidal range influence the cross-shore position and extent of surf and swash zone processes induced by breaking waves.

3.5.1 Alongshore Variability in Morphology

The results of this study indicate that the presence of the lagoon mouth on the western flank of Younger Lagoon beach is the primary factor controlling alongshore variability in the foreshore and berm behaviors. Significant wave height is the dominant forcing that leads to and enhances this variability.

The transects fronting the lagoon mouth (transects 1-3) showed a general increase in foreshore slope between August 2010 and April 2011, and the corresponding berm crests either showed little change both in cross-shore position and elevation (in the case of transect 1) or migrated seaward as the foreshore slope increased (transects 2-3). With increasing distance alongshore from the lagoon mouth, the beach profile flattened out and the berm became virtually nonexistent during any of the surveys.

The berm fronting the lagoon mouth was a prominent profile feature throughout all surveys. The lagoon never permanently breached and connected with the ocean except during some high tide and wave events when the run-up elevation was high enough to overtop the berm. Even in this case, the breaching was from the marine side of the berm, indicating that the lagoon water height never reached a sufficient level to induce breaching from the terrestrial side, which is likely due to the modest drainage size and lack of large stream flow into the basin. As changes in the lagoon level in this study were treated as a proxy to the relative change in water-table elevation, this would suggest that a significantly high water-table elevation is required in conjunction with wave overtopping to permanently breach the berm and induce lagoon-ocean coupling. Positive feedbacks due to overtopping (e.g. decreased sediment stability and greater mobility) would result in a rapid erosion of the berm.

3.5.2 Berm Overtopping and Run-up Potential

What was observed in general between August 2010 and April 2011 in the beach profile fronting the lagoon (transects 1-3) were positive feedbacks related to antecedent topography that maintained the berm rather than eroded it. The positive correlation between foreshore slope and significant wave height, and negative correlation between the foreshore slope and LWR at transects 1-3 compared with no correlation at transects 10-12 supports the hypothesis that overtopping as a physical mechanism for maintaining berm height is a process unique to bar-built beaches, barrier islands, and similar beach environments where there is a landward-sloping or flat backshore. Berm overtopping transports and deposits sediment upslope, increasing the foreshore slope. Sediments that are transported down slope and deposited in the lower foreshore or swash zone can be moved swiftly back upslope with the following berm overtopping,

The correlation between the logarithm of $P_{overtop}$ and berm height fronting the lagoon additionally supports the concept that overtopping is an important process for building and maintaining the berm; however, the breakdown of the correlation beyond a certain value of $P_{overtop}$ suggests that there is a threshold frequency of overtopping, and thus a threshold magnitude of significant wave heights, which separates constructive overtopping from destructive overtopping. This is the 'berm-height paradox', where waves of increasing height serve to build up and maintain the berm on a bar-built beach, while the highest and most energetic waves will ultimately erode the berm. Although the median run-up elevations were greater for transects 10-12 compared with transects 1-3 due to comparatively lower foreshore slopes, the lack of a prominent and ubiquitous berm and a comparatively steep seaward-sloping backshore inhibit overtopping.

The grain size surveys reflect similarities in swash zone processes between transects 1-2 and 10-12, but differences in foreshore and berm processes. The mean berm grain sizes varied conversely throughout the survey period: when the berm grain size increased between surveys at transects 1-3, the mean grain size of the region between the foreshore and

backshore where a berm would form (if at all) decreased at transects 10-12, and vice versa. This supports the conclusion that the beach profile in front of the lagoon was in a more static and stable equilibrium throughout the surveys, while the profile at transects 10-12 was in a more dynamic equilibrium with greater sediment exchange across-shore. As sediment movement is directly related to bed shear stress (~fluid velocity), swash uprush has greater potential for mobilizing sediment at the point of instantaneous acceleration, and gradually deposits sediment of decreasing grain size upslope as the flow velocity A comparison of all grain sizes with the LWR shows that for mid-range values of the ratio, this relationship is true in front of the lagoon mouth (swash grain size > foreshore grain size > berm grain size (Fig. 3.38). However, for transects 10-12, this relationship is generally not true. With increased sediment transport on both the uprush and downrush due to a higher ratio of downrush velocity to uprush velocity, absence of any distinguishable berm, and potential for swash reflection off of the back-beach bluff, the lack of a landward decrease in grain size would be expected.

T1-3 **T10-12**

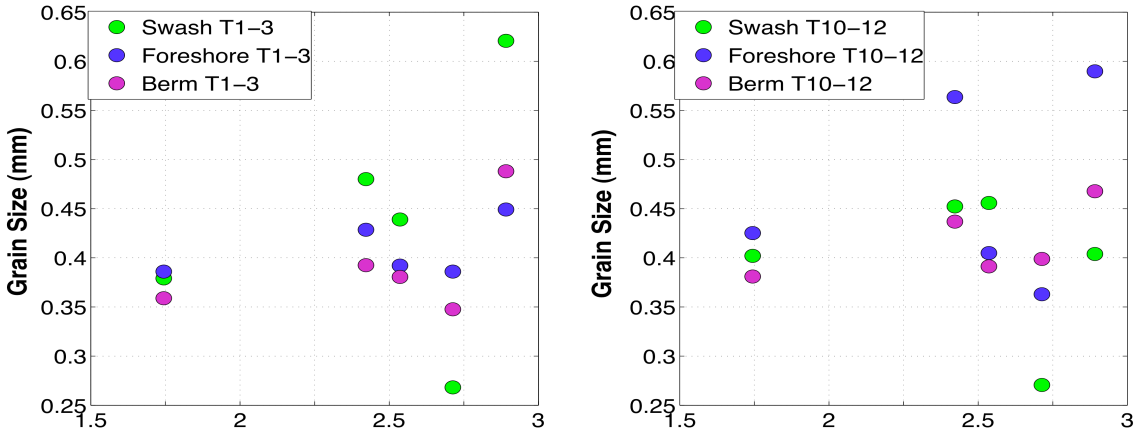

3.38: Mean grain sizes for the swash (green), foreshore (blue), and berm (purple) regions for transects 1-3 (left) and transects 10-12 (right)

The negative correlation between the ratio of lagoon level to significant wave height (LWR) and the foreshore slope suggests that the water-table elevation and fluid exchange through the berm could be an important factor at Younger Lagoon in foreshore sediment transport. A high LWR would indicate a relatively high water level compared with wave height, a conditions which favors exfiltration of water out of the beachface and sediment transport down slope, decreasing the slope (Fig. 3.39). A low LWR would thus promote beachface infiltration and sediment deposition upslope, with an increase in slope. This is indeed what is observed at Younger Lagoon; however, as morphology at Younger Lagoon is controlled primarily by waves, it is difficult to determine the foreshore slope effects due to secondary and more static variables like wave-table elevation. One way to potentially resolve this in future studies is to survey the beach at frequencies high enough to capture oscillations in the water-table elevation in conjunction with direct water- table observations and perform a

principle components analysis to analyze the variance in the data that can be explained by processes other than wave height.

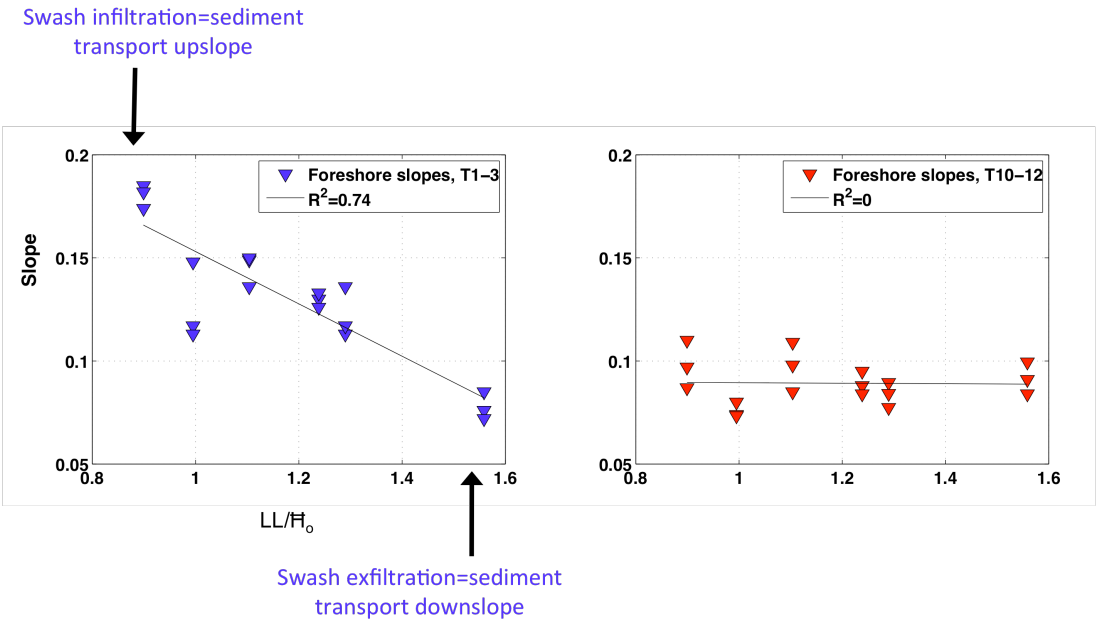

3.39: Linear regressions of foreshore slope vs. LWR for transects 1, 2, 3 (blue, left) and 10, 11, 12 (red, right). High values of LWR suggest a relatively higher water-table elevation vs. run-up, which would promote sediment mobility and down slope transport due to exfiltration of water out of the beachface. Lower values of LWR suggest relatively higher run-up levels compared with the water table, which would promote upslope transport and deposition of sediment due to infiltration into the beachface, and thus a higher foreshore slope.

The system of beach groundwater and swash zone processes is complex, and many of the predictions and conclusions regarding sediment erosion and deposition in the foreshore exist due to extensive mathematical and conceptual modeling and, to a lesser extent, field observations. Despite these models and observations, there is still much uncertainty surrounding the dynamics of swash zone sediment transport in relation to the water table.

3.6 Conclusions

The alongshore variability in beach morphodynamics at Younger Lagoon Reserve is ultimately controlled by differences in back beach morphology and feedbacks that arise within the system. The position of the lagoon mouth on the western flank of the beach created a seaward-sloping or flat backshore when a berm was present. Swash overtopping and thus maintenance of the berm elevation would are dependent on run-up overtopping of the berm at frequencies lower than a threshold frequency. East of the lagoon mouth, the beach profile is entirely seaward sloping and backed by a 10-m high bluff, and the swash processes and feedbacks in this region create a planar profile with no berm.

While the general forces and processes that shape beaches—waves, tides, and sediment supply— are recognized and globally applicable, the interactions of these processes and feedbacks that exist within the coastal system are ultimately complex, and thus lead to a wide array of morphologies both spatially and temporally. The case study of seasonal beach and berm morphology at Younger Lagoon Reserve Beach highlights the importance of process interactions and site-specific variables that influence beach behavior. The results of this study have important implications for understanding how long or short-term changes in natural forcings as well as anthropogenic modifications to the coastal zone—coastal engineering structures on the back beach that can affect the coastal water table—can lead to changes in beach geometry and response to forcing.

References

Bagnold, R.A. (1963) Mechanics of marine sedimentation, In: The Sea-Ideas and Observations, Ed. M.N. Hill, Wiley, New York, pp. 507-528.

Bagnold, R.A. (1966) An approach to the sediment transport problem from general physics, U.S. Geological Survey Prof. Pap. 422-1, 37 pp.

Barnard, P.L., Eshleman, J.L., Erikson, L.H. and Hanes, D.M. (2007) Coastal processes study at Ocean Beach, San Francisco, CA: Summary of data collection 2004-2006, U.S. Geological Survey Open-File Report 2007-1217.

Barnard, P.L. and Hanes, D.M. (2005) Integrating field research, modeling and remote sensing to quantify morphodynamics in a high-energy coastal setting, Ocean Beach, San Francisco, California, 5th International Conference on Coastal Dynamics, 14 pp.

Best, T.C. and Griggs, G.B. (1991) A sediment budget for the Santa Cruz littoral cell, California: In Osborne, R. H., ed., From shoreline to abyss: SEPM (Society for Sedimentary Geology) Special Publication 46, pp. 35-50.

Boehm, A.B., Sanders, B.F. and Winant, C.D. (2002) Cross-shelf transport at Huntington Beach: Implications for the fate of sewage discharged through an offshore ocean outfall, Environ. Sci. Technol. 36(9):1899–1906.

Boruff, B.J., Emrich, C. and Cutter, S.L. (2005) Erosion hazard vulnerability of US coastal counties, Journal of Coastal Research 21(5):932-942.

Bowen, A.J., Inman, D.L. and Simmons, V.P. (1968) Wave 'set-down' and set-up, Journal of Geophysical Research 73(8):2569-2577.

Brinks, M.V., Dwight, R.H., Osgood, N.D., Sharavanakumar, G., Turbow, D.J., El-Gohary, M., Caplan, J.S. and Semenza, J.C. (2008) Health risk of bathing in Southern California coastal waters, Archives of Environmental & Occupational Health 63(3):123-135.

Bromirski, P.D., Miller, A.J., Flick, R.E. and Auad, G. (2011) Dynamical suppression of sea-level rise along the Pacific coast of North America: Indications for imminent acceleration, Journal of Geophysical Research 116:1-13.

Bruun, P. (1954) Coast erosion and the development of beach profiles, U. S. Army Corps of Engineers, Beach Erosion Board, Technical Memo 44, Washington, D.C., 79 pp. + Appen.

Bruun, P. (1962) Sea level rise as a cause of shoreline erosion, Proceedings of the American Society of Civil Engineers, Journal of the Waterways and Harbors Division 88: 117-130.

Butler, D. (2006) Mashups mix data into global service, Nature 439:6-7.

California Natural Resources Agency (2009) California Climate Adaptation Strategy: A Response to the Governor of the State of California in Response to Executive Order S-13-2008, 197 pp.

California Coastal Records Project: An Aerial Survey of the California Coastline. <www.californiacoastline.org>

Cayan, D., Bromirski, P., Hayhoe, K., Tyree, M., Dettinger, M. and Flick, R. (2006) Projecting Future Sea Level, California Climate Change Center White Paper CEC-500-2005-202-SF, 64 pp.

Cayan, D.R., Bromirski, P.D., Hayhoe, K., Tyree, M., Dettinger, M.D. and Flick, R.E. (2008) Climate change projections along the California coast, Climatic Change 87(S1):57-73.

Cayan, D., Tyree, M., Dettinger, M., Hidalgo, H., Das, T., Maurer, E., Bromirski, P., Graham, N. and Flick, R. (2009) Climate change scenarios and sea-level rise estimates for the California 2009 Climate Change Scenarios Assessment, California Climate Change Center Report CEC-500-2009-014-F, 64 pp.

Chapman, D.J. and Hanemann, W.M. (2001) Environmental Damages in Court: The American Trader Case, Department of Agricultural & Resource Economics, UCB CUDARE Working Paper 913, 43 pp.

Church J.A., Gregory J.M., Huybrechts P., Kuhn M., Lambeck K., Nhuan M.T., Qin D. and Woodworth P.L. (2001) Changes in sea level, Chapter 11 of the Intergovernmental Panel on Climate Change Third Assessment Report, Cambridge University Press, Cambridge, pp. 639–694.

Church, J.A., White, N.J., Hunter, J.R. and Lambeck, K. (2008) Briefing: a post-IPCC AR4 update on sea-level rise, Antarctic Climate and Ecosystems Cooperative Research Centre, pp. 1-12.

Clayton, T.D. (1991) Beach replenishment activities on the U.S. Continental Pacific Coast, Journal of Coastal Research 7(4): 1195-1210.

Coastal Sediment Management Workgroup (CSMW) Results from CSMW Task 3: Beach Nourishment Projects – Performance and Sediment Characteristics, California Department of Boating and Waterways, pp. 1-16.

Cooper, J.A.G. and Pilkey, O.H. (2004) Sea-level rise and shoreline retreat: time to abandon the Bruun Rule, Global and Planetary Change 43(3-4): 157-171.

Crossett, K. M., Culliton, T.J., Wiley, P.C. and Goodspeed, T.R. (2004) Population trends along the coastal United States: 1980-2008, NOAA/National Ocean Service.

Dare, J. (2005) Coastal armoring and bluff erosion geographic information system, California Coastal Commission.

Domingues, C.M., Church, J.A., White, N.J., Gleckler, P.J., Wijffels, S.E., Barker, P.M. and Dunn, J.R. (2008) Improved estimates of upper-ocean warming and multi-decadal sea-level rise, Nature 453:1090-1093.

Duncan, J.R. (1964) The effects of water table and tide cycle on swash-backwash sediment distribution and beach profile development, Marine Geology 2:186-197.

Dwight, R.H., Brinks, M.V., SharavanaKumar, G. and Semenza J.C. (2007) Beach attendance and bathing rates for Southern California beaches, Ocean & Coastal Management 50:847-858.

Elwany, M.H.S., Flick, R.E. and Aijaz, S. (1998) Opening and closing of a marginal Southern California lagoon inlet, Estuaries 21(2):246-254.

Fischer, D.W. and Arredondo, M.C. (1999) Municipal Coastal Hazard Planning: Los Angeles and Orange County City Responses, California, Journal of Coastal Research 15(4): 974-984.

Flick, R.E. (1993) The myth and reality of Southern California beaches, Shore and Beach 61(3):3-13.

Flick, R.E. (2005) Dana Point to the Mexican Border, In: Griggs. G., Patsch, K. and Savoy, L., Living with the Changing California Coast, University of California Press, pp.474-514.

Flick, R.E. and Cayan, D.C. (1984) Extreme sea levels on the coast of California, Proc., 19th Int. Conf. Coastal Eng., Amer. Soc. Civil Eng., pp. 886-898.

Google Earth Version 6.2 [Software]. <http://www.google.com/earth/index.html>

Grant, S.B., Sanders, B.F., Boehm, A.B., Redman, J.A., Kim, J.H., Mrse, R.D., Chu, A.K., Gouldin, M., McGee, C.D., Gardiner, N.A., Jones, B.H., Svejkovsky, J., Leipzig, G.V. and Brown, A. (2001) Generation of enterococci bacteria in a coastal saltwater marsh and its impact on surf zone water quality, Environ. Sci. Technol. 35(12): 2407-2416.

Grant, U.S. (1943) Waves as a sand-transporting agent, American Journal of Science 241(2):117-123.

Grant, U.S. and Shepard, F.P. (1940) Shallow-water sediment shifting processes along the Southern California Coast, Sixth Pac. Sci. Congr. Proc. 2:801-805.

Griggs, G.B., Patsch, K. and Savoy, L.E. (2005) Living with the Changing California Coast, Univ. of California Press, Berkeley, California, 540 pp.

Griggs, G.B. and Russell, N.L. (2012) City of Santa Barbara: Sea-Level Rise Vulnerability Study, California Energy Commission Public Interest Energy Research Program, 87 pp.

Griggs, G.B. and Savoy, L.E. (1985) Living with the California Coast, Duke University Press, Durham, North Carolina, 393 pp.

Habel, J.S. and Armstrong, G.A. (1978) Assessment and atlas of shoreline erosion along the California coast, State of California Dept. of Boating and Waterways, Sacramento, 277 pp.

Hanak, E. and Moreno, G. (2008) California Coastal Management with a Changing Climate, Public Policy Institute of California, 40 pp.

Hanslow, D. and Nielsen, P. (1993) Shoreline setup on natural beaches, Journal of Coastal Research SI 15:1-11.

Hapke, C.J. and Reid, D. (2006) The National Assessment of Shoreline Change: A GIS Compilation of Vector Shorelines and Associated Shoreline Change Data for the Sandy Shorelines of the California Coast, U.S. Geological Survey Open-File Report 2006-1251.

Hapke, C.J., Reid, D., Richmond, B.M., Ruggiero, P. and List, J. (2006) National Assessment of Shoreline Change Part 3: Historical Shoreline Change and Associated Coastal Land Loss Along Sandy Shorelines of the California Coast, U.S. Geological Survey Open-File Report 2006-1219.

Hapke, C. and Richmond, B. (2000) Monitoring beach morphology changes using small-format aerial photography and digital softcopy photogrammetry, Environmental Geosciences 7(1):32-37.

Hardisty, J., Collier, J. and Hamilton, D. (1984) A calibration of the Bagnold beach equation, Marine Geology 61:95-101.

Heberger, M., Cooley, H., Herrera, P., Gleick, P.H. and Moore, E. (2009) The impacts of sea-level rise on the California coast, California Climate Change Center report CEC-500-2009-024-F, 101 pp.

Hegge, B.J. and Masselink, G. (1991) Groundwater-table responses to wave run-up: An experimental study from Western Australia, Journal of Coastal Research 7:623-634.

Hine, A.C. (1979) Mechanisms of berm development and resulting beach growth along a barrier spit complex, Sedimentology 26:333-351.

Holman, R.A. (1986) Extreme value statistics for wave runup on a natural beach, Coastal Engineering 9(6):527-544.

Hughes, M.G., Masselink, G. and Brander, R.W. (1997) Flow velocity and sediment transport in the swash zone of a steep beach, Marine Geology 138:91-103.

Hunt, I.A. (1959) Design of seawalls and breakwaters, Proc. Journal of Waterways and Harbors Division, ASCE 85(WW3):123-152.

Intergovernmental Panel on Climate Change (IPCC) (2007) Climate Change 2007: The Physical Science Basis, Contribution of Working Group 1 to the Fourth Assessment Report of the Intergovernmental Panel on Climate Change, Eds. Soloman et al., Cambridge Univ. Press, Cambridge, UK, and New York, 996 pp.

Jensen, S.G., Aagaard, T., Baldock, T.E., Kroon, A and Hughes, M. (2009) Berm formation and dynamics on a gently sloping beach; the effect of water level and swash overtopping, Earth Surf. Process. Landforms 34:1533-1546.

King, P. (1999) The Fiscal Impact of Beaches in California, Public Research Institute, San Francisco University, Report Commissioned by California Department of Boating and Waterways.

King, P. and Symes, D. (2003) The Potential Loss in Gross National Product and Gross State Product from a Failure to Maintain California's Beaches, In: A report commissioned by California Department of Boating and Waterways, San Francisco State University: Public Research Institute, pp. 1-43.

Kinsman, N. and Griggs, B. (2010) California coastal sand retention today: Attributes and influence of effective structures, Shore & Beach 78(4):64-74

Komar, P. (1998) The 1997-98 El Niño and erosion on the Oregon coast, J. Am. Shore Beach Preserv. Assoc. 66:33-41.

Kraus, N., Patsch, K. and Munger, S. (2008) Barrier beach breaching from the lagoon side, with reference to Northern California, Shore & Beach 76(2):33-43.

La Fond, E.C. (1940) Sand movement near the beach in relation to tides and waves, Sixth Pac. Sci. Congr. Proc. 2:795-799.

Lakshmanan, V., T. M. Smith, G. J. Stumpf, and K. D. Hondl (2007) The Warning Decision Support System—Integrated information, Wea. Forecasting 22:596–612.

Lanyon, J.A., Eliot, I.G. and Clarke, D.J. (1982) Groundwater-level variation during semidiurnal spring tidal cycles on a sandy beach, cycles on a sandy beach, Aust. J. Mar. Freshwater Res. 33:377-400.

Lew, D.K. and Larson, D.M. (2008) Valuing a beach day with a repeated nested logic model of participation, site choice, and stochastic time value, Marine Resource Economics 23(3): 233-252.

Li, L., Barry, D.A., Parlange, J.-Y. and Pattiaratchi, C.B. (1997) Beach water table fluctuations due to wave run-up: Capillarity effects, Water Resources Research 33(5):935-945.

Limber, P.W., Patsch, K.B. and Griggs, G.B. (2008) Coastal sediment budgets and the littoral cutoff diameter: A grain size threshold for quantifying active sediment inputs, Journal of Coastal Research 24(Sp2):122-133.

Mann, H. B. and Whitney,D. R. (1947) On a test of whether one of two random variables is stochastically larger than the other, Annals of Mathematical Statistics 18:50-60.

Mantua, N.J. (2002) Pacific-Decadal Oscillation (PDO): Volume 1, The Earth system: Physical and chemical dimensions of global environmental change; In: Encyclopedia of Global Environmental Change, Eds. MacCracken, M.C. and J.S. Perry, pp. 592-594.

Mantua, N.J. and Hare, S.R. (2002) The Pacific Decadal Oscillation, Journal of Oceanography 58:35-44.

Masselink G. and Short A.D. (1993) The effect of tide range on beach morphodynamics and morphology: a conceptual beach model, Journal of Coastal Research 9(3):785-800.

Masters, P.M. (2006) Holocene sand beaches of Southern California: ENSO forcing and coastal processes on millennial scales, Palaeogeography, Palaeoclimatology, and Palaeoecology 232:73-95.

Matthews, H.D. and Caldeira, K. (2008) Stabilizing climate requires near-zero emissions, Geophysical Research Letters 35:1-5.

Meier, M.F., Dyurgerov, M.B., Rick, U.K., O'Neel, S., Pfeffer, W.T., Anderson, R.S., Anderson, S.P. and Glazovsky, A.F. (2007) Glaciers dominate eustatic sea-level rise in the 21st century, Science 317(5841):1064-1067.

Merrifield, M.A. (2011) A shift in western tropical Pacific sea level trends during the 1990s, Journal of Climate 24:4126-4138.

Merritts, D.J. (1996) The Mendocino triple junction: active faults, episodic coastal emergence, and rapid uplift, Journal of Geophysical Research 101:6051-6070.

Morton, R. A., Gelfenbaum, G., Buckley, M. L., and Richmond, B. M. (2011) Geological effects and implications of the 2010 tsunami along the central coast of Chile, Sedimentary Geology 242:34-51.

Moser, S. (2007) Is California preparing for sea level rise? Calif. Coast Ocean (22):24-30.

Newman, M., Compo, G.P. and Alexander, M.A. (2003) ENSO-Forced Variability of the Pacific Decadal Oscillation, Journal of Climate 16(23):3853-3857.

Nielsen, P. (1988) Wave setup: A field study, Journal of Geophysical Research 93(15):643-652.

Nielsen, P. (1990) Tidal Dynamics of the Water Table in Beaches, Water Resources Research, 26(9):2127-2134.

NOAA Coastal Services Center (CSC) (1997), Airborne LIDAR assessment of coastal erosion (ALACE) project, National Oceanic and Atmospheric Administration Coastal Services Report, Charleston, SC. <http://www.csc.noaa.gov/digitalcoast/data/coastallidar/index.html>

NOAA National Data Buoy Center Online. < http://www.ndbc.noaa.gov/>

NOAA National Ocean Service Center for Oceanographic Products and Services (NOS/CO-OPS) Tides & Currents Online. <http://tidesandcurrents.noaa.gov/.

NOAA National Weather Service California Nevada River Forecast Center (CNRFC). <http://www.cnrfc.noaa.gov/rainfall_data.php>

Nourbakhsh, I., Sargent, R., Wright, A., Cramer, K., McClendon, B. and Jones, M. (2006) Mapping disaster zones, Nature 439:787-788.

Patrick, William H. Jr. and DeLaune, R.D. (1990) Subsidence, Accretion, and Sea Level Rise in south San Francisco Bay marshes, Limnology and Oceanography 35(6):1389-1395.

Patsch, K. and Griggs, G. (2006) Littoral cells, sand budgets, and beaches: Understanding California's shoreline, California Department of Boating and Waterways, California Coastal Sediment Management Workgroup, 35 pp.

Patsch, K. and Griggs, G. (2006) Littoral cells, sand budgets, and beaches: Understanding California's shoreline, California Department of Boating and Waterways, California Coastal Sediment Management Workgroup, 35 pp.

Patsch, K. and Griggs, G. (2007) Development of sand budgets for California's major littoral cells, Report to the California Coastal Sediment Management Working Group, 105 pp.

Pendleton, E.A., Thieler, E.R. and Williams, S. J. (2006) Coastal vulnerability assessment of Point Reyes National Seashore (PORE) to sea-level rise, U.S. Geological Survey Open-File Report 2005-1059.

Perg, L.A., Anderson, R.S. and Finkel, R.C. (2001) Use of new 10Be and 26Al inventory method to date marine terraces, Santa Cruz, CA, USA, Geology 29(10):879-882.

Pilkey, O.H. (1981) Geologists, engineers, and a rising sea level, Northeastern Geology 3:150-158.

Plant N.G. and Griggs, G.B. (1992) Nearshore processes and beach morphology near a seawall, Journal of Coastal Research 8(1):183-200.

Ranasinghe, R. and Pattiaratchi, C. (1999) The seasonal closure of tidal inlets : Wilson Inlet — a case study, Coastal Engineering, 37:37-56.

Ruggiero, P., Holman, R.A. and Beach, R.A. (2004) Wave run-up on a high-energy dissipative beach, Journal of Geophysical Research, 109(C6):1-12.

Ruggiero P., Kaminsky, G.A., Gelfenbaum, G. and Voigt, B. (2005) Seasonal to inter-annual morphodynamics along a high-energy dissipative littoral cell, Journal of Coastal Research 21(3):553-578.

Ruggiero, P. Komar, P.D., McDougal, W.G., Marra, J.J. and Beach, R.A. (2001) Wave run-up, extreme water levels and the erosion of properties backing beaches, Journal of Coastal Research 17(2):407-419.

Runyan, K. and Griggs, G.B. (2003) The effects of armoring seacliffs on the natural sand supply to the beaches of California, Journal of Coastal Research 19(2):336-347.

Ryan, H.F. and Noble, M. (2002) Sea level response to ENSO along the central California coast: how the 1997-1998 even compared with the historic record, Progress in Oceanography 54:149-169.

Sahu, B.K. (1965) Theory of sieving, Jour. Sed. Petrology 35:750-753.

Scharl, A. (2007) Towards the Geospatial Web: Media Platforms for Managing Geotagged Knowledge Repositories, The Geospatial Web - How Geo-Browsers, Social Software and the Web 2.0 are Shaping the Network Society, Eds. A. Scharl, K. Tochtermann, London, Springer pp. 3-14.

Sea level rise task force of the Coastal Ocean Working Group of the California Climate Action Team (CO-CAT) (2010) State of California sea-level rise task force interim guidance document, State of California Ocean Protection Council, pp.1-10.

Sherman, D.J., Barron, K.M. and Ellis, J.T. (2002) Retention of beach sands by dams and debris basins in Southern California, Journal of Coastal Research SI 36:662-674.

Sibson, R. (1981) A brief description of natural neighbor interpolation, In: Vic Barnet, ed., Interpreting Multivariate Data, John Wiley & Sons, Chichester, pp. 21-36.

Slagel, M.J. and Griggs, G.B. (2008) Cumulative losses of sand to the California coast by dam impoundment, Journal of Coastal Research 24(3):571-584.

Stockdon, H.F., Holman, R.A., Howd, P.A. and Sallenger Jr., A.H. (2006) Empirical parameterization of setup, swash, and runup, Coastal Engineering 53:573-588.

Storlazzi, C.D. and Griggs, G.B. (1998) The 1997-98 El Nino and erosion processes along the Central Coast of California, Shore & Beach 66(3):12-17.

Storlazzi, C.D. and Griggs, G.B. (2000) Influence of El Niño−Southern Oscillation (ENSO) events on the evolution of central California's shoreline, Geological Society of America Bulletin 112(2): 236-249.

Storlazzi, C.D., Willis, C.M. and Griggs, G.B. (2000) Comparative impacts of the 1982-83 and 1997-98 El Niño winters on the Central California coast, Journal of Coastal Research 16(4):1022-1036.

The Mathworks, Inc., Matlab and Simulink Student Version 7.8.0 (R2009a) [Software]. < http://www.mathworks.com/>

Thieler, E.R. and Hammar-Klose, E.S. (2000) National Assessment of Coastal Vulnerability to Future Sea-Level Rise: Preliminary Results for the U.S. Pacific Coast, U.S. Geological Survey Open-File Report 00-178.

Thieler, E.R., Himmelstoss, E.A., Zichichi, J.L. and Ergul, Ayhan (2009) Digital Shoreline Analysis System (DSAS) version 4.0—An ArcGIS extension for calculating shoreline change: U.S. Geological Survey Open-File Report 2008-1278.

Thieler, E.R., Pilkey, O.H., Young, R.S., Bush, D.M., and Fei Chai (2000) The use of mathematical models to predict beach behavior for U.S. coastal engineering: a critical review, Journal of Coastal Research 16:48-70.

Thompson, W. C. (1987) Seasonal orientation of California beaches, Shore & Beach 55(3-4):67-70.

Turner, I.L., Coates, B.P. and Acworth, R.I. (1996) The effects of tides and waves on water table elevations in coastal zones, Hydrogeology Journal, 4(2):51-69.

Turner, I.L. and Leatherman, S.P. (1997) Beach Dewatering as a ' Soft ' Engineering Solution to Coastal Erosion: A History and Critical Review, Journal of Coastal Research, 13(4):1050-1063.

U.S. Army Corps of Engineers (USACOE) (1971) National Shoreline Study: California Regional Inventory, San Francisco District.

U.S. Census Bureau: United States Census 2000 <http://www.census.gov/census2000/states/ca.html>

Vermeer, M. and Rahmstorf, S. (2009) Global sea level linked to global temperature, PNAS 106(51):21527-21532.

Waddell, E. (1976) Swash-groundwater-beach profile interactions, SEPM Spec. Publ., 24:115-125.

Watson, D.F. (1988) Natural neighbor sorting on the N-dimensional sphere, Pattern Recognition 21(1):63-67.

Weir, F.M., Hughes, M.G. and Baldock, T.E. (2006) Beach face and berm morphodynamics fronting a coastal lagoon, Geomorphology 82:331-346.

Wiegel, R.L. (1994) Ocean beach nourishment on the USA Pacific Coast, Shore & Beach 62(1):11-36.

Wiegel, R.L. (2002) Seawalls, seacliffs, beachrock: what beach effects? Part 2, Shore & Beach 70(2):13-22.

Wilcoxen, P.J. (1986) Coastal erosion and sea level rise: Implications for ocean beach and San Francisco's Westside transport project, Coastal Zone Management Journal 14(3):173-191.

Wingfield, D.K. and Storlazzi, C.D. (2007) Spatial and temporal variability in oceanographic and meteorologic forcing along Central California and its implications on nearshore processes, Journal of Marine Systems 68(3-4):457-472.

Young, A.P. and Ashford, S.A. (2006) Application of airborne Lidar for seacliff volumetric change and beach-sediment budget contributions, Journal of Coastal Research 22(2):307-318.